

University of Alberta

RAB32 FAMILY PROTEINS AND THEIR INTERACTORS

by

CAROLINA GUADALUPE ORTIZ SANDOVAL

A thesis submitted to the Faculty of Graduate Studies and Research
in partial fulfillment of the requirements for the degree of

MASTER OF SCIENCE

CELL BIOLOGY

©CAROLINA GUADALUPE ORTIZ SANDOVAL

FALL 2013

EDMONTON, ALBERTA

Permission is hereby granted to the University of Alberta Libraries to reproduce single copies of this thesis and to lend or sell such copies for private, scholarly or scientific research purposes only. Where the thesis is converted to, or otherwise made available in digital form, the University of Alberta will advise potential users of the thesis of these terms.

The author reserves all other publication and other rights in association with the copyright in the thesis and, except as herein before provided, neither the thesis nor any substantial portion thereof may be printed or otherwise reproduced in any material form whatsoever without the author's prior written permission.

ABSTRACT

The ER mitochondria-associated membrane (MAM) is a hub for many calcium-mediated processes required for cell survival, including apoptosis, autophagy, and ATP production. In this thesis, we identified and characterized the interaction between MAM-enriched Rab32 and its effector Drp1, a master regulator of mitochondrial fission. Evolutionary studies of Rab32 suggest that it forms a family with Rab38 and Rab29. While only Rab32 and Rab38 participate in melanosome trafficking, all family members interact with Drp1 to influence the mitochondria phenotype, Rab32 being the stronger interactor, followed by Rab38 and Rab29. Moreover, I was also able to determine that Rab32 interacts with syntaxin-17, a MAM-enriched SNARE protein which, like Rab32, participates in autophagy; Rab29 showed a weaker interaction with this SNARE, while this interaction was not seen with Rab38. Lastly, phylogenetic studies indicate that Rab29 and Rab38 are both a result of Holozoan expansion of Rab32, and that Rab29 diverged earlier in evolution from Rab32 than Rab38.

TABLE OF CONTENTS

CHAPTER 1. Introduction.....	1
1.1 Specialized subdomains of the endoplasmic reticulum.....	2
1.1.1. Overview.....	2
1.1.2. ER mitochondria-associated membrane (MAM).....	3
1.1.2.1. Lipid metabolism.....	3
1.1.2.2. Calcium signalling and apoptosis.....	4
1.1.2.3. Tether complexes and other proteins that aid in MAM formation and stabilization.....	5
1.2. Membrane trafficking.....	7
1.2.1. Rab proteins.....	7
1.2.1.1. Rab protein structure.....	9
1.2.2. Rab cycle.....	10
1.2.3. Cellular localization and function of Rabs.....	13
1.2.3.1. Rabs in vesicle formation and cargo selection.....	13
1.2.3.2. Rabs in vesicle motility.....	14
1.2.3.3. Rabs in vesicle tethering.....	14
1.2.3.4. Rabs in vesicle fusion.....	15
1.3. Rab32 family proteins.....	16
1.3.1. Rab32.....	16
1.3.1.1. Overview.....	16
1.3.1.2. Rab32 and the MAM.....	19
1.3.1.3. Rab32 and autophagy.....	20
1.3.2. Rab38.....	20
1.3.3. Rab29.....	21

1.4. ER-shaping proteins.....	22
1.4.1. Reticulons/DP1 and atlastins.....	22
1.4.1.1. Reticulon/DP1 families.....	23
1.4.1.2. Atlastins.....	24
1.5. Mitochondrial membrane dynamics.....	25
1.5.1. Fusion machinery.....	25
1.5.2. Fission machinery.....	26
1.6. Comparative genomics and phylogenetics.....	28
1.7. Goal of this thesis.....	30
CHAPTER 2. Materials and Methods.....	31
2.1. Materials and reagents.....	32
2.1.1. Common buffers and solutions.....	35
2.1.2. Plasmids and primers.....	36
2.1.3. Software and equipment.....	41
2.2. Methods.....	42
2.2.1. Mammalian cell culture techniques.....	42
2.2.1.1. Maintenance of cell lines.....	42
2.2.1.2. Experiment set up.....	43
2.2.1.3. Transient transfection of cell lines.....	43
2.2.2. Basic biochemical techniques.....	43
2.2.2.1. Preparation of whole cell lysates.....	43
2.2.2.2. Phosphorylation assays.....	43
2.2.2.3. Protein precipitation.....	44
2.2.2.4. Sodium Dodecyl Sulfate-Polyacrylamide Gel Electrophoresis (SDS-PAGE)....	44
2.2.2.5. Western blot.....	44

2.2.3. Cell fractionation technique.....	45
2.2.4. Immunoprecipitation experiments.....	45
2.2.4.1. Immunoprecipitation of Flag- or HA-tagged proteins.....	45
2.2.4.2. Protein crosslinking.....	46
2.2.5. Immunofluorescence experiments.....	46
2.2.5.1. Preparation of slides and data acquisition.....	46
2.2.5.1. Image quantification.....	47
2.2.6. Molecular biology techniques.....	47
2.2.6.1. Simple Polymerase Chain Reaction (PCR).....	47
2.2.6.2. PCR-based splicing by overlap extension.....	48
2.2.6.3. Separation of DNA fragments by agarose gel electrophoresis.....	48
2.2.6.4. DNA extraction from agarose gel.....	48
2.2.6.5. Restriction digest.....	49
2.2.6.6. DNA ligation.....	49
2.2.6.7. Bacterial transformation.....	49
2.2.6.8. Bacterial culture.....	49
2.2.6.9. Isolation of plasmid DNA from bacteria.....	50
2.2.6.9.1. Midiprep protocol.....	50
2.2.6.9.2. Miniprep protocol.....	50
2.2.6.10. DNA sequencing.....	50
2.2.7. Comparative genomics and phylogenetic studies.....	51
2.2.7.1. Homology searching.....	51
2.2.7.2. Homology visualization.....	51
2.2.7.3. Phylogenetic analysis.....	52

CHAPTER 3. Rab32 family interactors alter mitochondrial membrane dynamics.....	53
3.1. Rationale.....	54
3.2. Results.....	54
3.2.1. Drp1 as a Rab32 effector.....	54
3.2.1.1. Endogenous and active Drp1 bind to Rab32.....	55
3.2.1.2. Knockout of Drp1 and inactivation of Rab32 by its GAP protein confirms that Drp1 acts as a Rab32 effector.....	57
3.2.2. Other Rab32 interactors.....	60
3.2.2.1. Rab32 interacts with reticulons and atlastins.....	63
3.2.3. Rab32 family proteins.....	66
3.2.3.1. Subcellular distribution of the Rab32 family proteins.....	66
3.2.3.2. Rab32 family proteins alter mitochondria morphology.....	68
3.2.3.3. Rab38 and Rab29 also interact with Drp1.....	71
3.2.3.4. Absence of Drp1 alters the distribution of the Rab32 family proteins.....	75
3.2.3.5. Rab32 family proteins interact with dynamin-2.....	75
3.2.4. Rab32 interacts with the SNARE syntaxin-17.....	78
CHAPTER 4: Rab32 family evolution.....	81
4.1. Rationale.....	82
4.2. Results.....	83
4.2.1. Rab32A and Rab32B are the most ancient members of the family.....	83
4.2.2. Rab38 and Rab29 are descendants of Rab32A.....	83
CHAPTER 5: Discussion and Future Perspectives.....	89
5.1. Rab32 family proteins' interactors modulate both ER and mitochondrial membrane dynamics.....	90

5.2. Rab32 family proteins in autophagy.....	93
5.3. Rab32 family evolution.....	94
5.4. Rab32 expression and function across eukaryotes.....	96
5.5. Rab32 family in disease.....	97
5.6. Conclusions.....	98
CHAPTER 6: References.....	100
6.1. References.....	101
CHAPTER 7: Appendix.....	116
7.1. Appendix.....	117

LIST OF TABLES

Table 2.1 Chemicals and reagents.....	32
Table 2.2. Primary antibodies.....	33
Table 2.3. Secondary antibodies.....	34
Table 2.4. Cell lines.....	35
Table 2.5. Molecular size standards.....	35
Table 2.6. Multicomponent systems.....	35
Table 2.7. Enzymes.....	35
Table 2.8 Buffers and solutions.....	35
Table 2.9. Plasmids.....	36
Table 2.10. Primer combinations for the generation of DNA constructs.....	38
Table 2.11. Primer sequences.....	39
Table 2.12. siRNAs and shRNAs.....	40
Table 2.13. Detection and analysis software.....	41
Table 2.14. Software used for comparative genomics and phylogenetic studies.....	42
Table 2.15. Equipment.....	42
Table 7.1. List of eukaryotic organisms used in this study.....	117
Table 7.2. List of protein sequences used for the phylogenetic studies of this thesis, identified through comparative genomics.....	119

LIST OF FIGURES

Figure 1.1. Membrane trafficking.....	8
Figure 1.2. Rab cycle at the ER.....	11
Figure 3.1. Endogenous Drp1 interacts with WT Rab32.....	56
Figure 3.2. Rab32 preferentially interacts with active Drp1.....	58
Figure 3.3. Active Drp1 preferentially interacts with active Rab32.....	59
Figure 3.4. Drp1 knockout MEF's resemble dominant-negative Rab32's mitochondrial phenotype.....	61
Figure 3.5. Rab32's GAP, RUTBC1, decreases its interaction with Drp1.....	62
Figure 3.6. Rab32 interacts with atlastin-2.....	64
Figure 3.7. Rab32 WT interacts with reticulon-4.....	65
Figure 3.8. Subcellular distribution of the Rab32 family proteins.....	67
Figure 3.9. Inactive Rab32 family proteins disrupt the mitochondrial network.....	69
Figure 3.10. Inactive Rab32 family proteins alter the mitochondrial network.....	70
Figure 3.11. Rab38 and Rab29 preferentially interact with active Drp1.....	72
Figure 3.12. Rab38 and Rab29 preferentially interact with active Drp1.....	73
Figure 3.13. Rab32 is the strongest Drp1 interactor of the Rab32 family proteins.....	74
Figure 3.14. Drp1 knockout alters the distribution of the Rab32 family proteins.....	76
Figure 3.15. Rab29 interacts stronger with dynamin-2.....	77
Figure 3.16. Rab32 interacts with syntaxin-17.....	79
Figure 4.1. Distribution of the Rab32 family proteins across eukaryotic taxa.....	84
Figure 4.2. Phylogenetic evolution of Rab32 family proteins.....	86
Figure 4.3. Holozoan evolution of Rab32 family proteins.....	87

LIST OF ABBREVIATIONS

AKAP	A kinase-anchoring protein
AP-1	Adaptor protein-1
Atg	Autophagy-related genes
Bap31	B-cell receptor associated protein of 31kDa
BLOC-2	Biogenesis of lysosome-related organelles complex-2
Drp1	Dynamin-related protein 1
ER	Endoplasmic reticulum
ERAD	ER-associated degradation
ERES	ER exit sites
ERGIC	ER-Golgi intermediate compartment
ERMES	ER-mitochondria encounter structure
ERQC	ER-derived quality control compartment
FACL4	Long-chain fatty acid-CoA ligase type 4
GAP	GTP-hydrolysis activating protein
GEF	Guanine-nucleotide exchange factor
GDF	GDI-displacement factor
GDI	GDP-dissociation inhibitor
GRP75	Glucose-regulated protein of 75kDa
GRP78	Glucose-regulated protein of 78kDa
IMM	Inner mitochondrial membrane
IP3	Inositol-1,4,5-triphosphate
IP3R	IP3-receptor
LRO	Lysosome-related organelle
MAM	Mitochondria-associated membrane

mtDNA	mitochondrial DNA
OMM	Outer mitochondrial membrane
PACS-2	Phosphofurin-acidic cluster sorting protein-2
PAM	Plasma membrane-associated ER
PD	Parkinson's disease
PDI	Protein disulfide isomerase
PKA	Protein kinase A
PSS-1	Phosphatidylserine synthase-1
RER	Rough endoplasmic reticulum
REP	Rab escort protein
RGGT	Rab geranyl-geranyl transferase
SER	Smooth endoplasmic reticulum
SERCA	Sarco-endoplasmic reticulum calcium ATPase
Sig-1R	Sigma-1 receptor
SNARE	Soluble N-ethylmaleimide-sensitive fusion protein-attachment protein receptor
TBC	Tre-2/Bub2/Cdc16
TGN	Trans-Golgi network
TMD	Transmembrane domain
Tyrp1	Tyrosine-related protein-1
VDAC	Voltage-dependent anion channel

CHAPTER 1:

Introduction

1. INTRODUCTION

1.1. Specialized subdomains of the endoplasmic reticulum

1.1.1. Overview

The eukaryotic cell is composed of many membrane-defined compartments, or organelles, that allow the cell to carry out a great variety of functions. For example: the nucleus, which contains the cell's genetic material; the Golgi apparatus, which participates in the packaging of proteins to be sent to different subcellular destinations; endosomes, which transport cargo from the plasma membrane to the lysosome, another organelle that contains acid hydrolases to degrade waste materials and non-essential cellular components. One such organelle is the endoplasmic reticulum (ER), a continuous-membrane organelle that stretches from the nuclear envelope to the cell periphery, comprising more than 50% of the cell's membranes (Croze and Morr , 1984). It fills the cell forming different subdomains that allow it to carry out a great variety of functions including protein and lipid synthesis, protein folding, translocation of secretory and transmembrane proteins, and very importantly, calcium storage (Lynes and Simmen, 2011).

ER domains were first recognized in the 1940-50's: the rough ER (RER), which is made of perinuclear sheet-like structures covered with ribosomes, and the smooth ER (SER), which comprises a tubular network devoid of ribosomes stretching out into the cell periphery (Lin et al., 2012; Sitia and Meldolesi, 1992). After these, many other subdomains within the SER have been discovered, basing the classification on function rather than structure, including ER exit sites (ERES), the plasma membrane-associated ER or PAM (also known as cortical ER), the ER-derived quality control compartment (or ERQC), and the mitochondria-associated membrane (MAM) (Lynes and Simmen, 2011).

ERES were discovered in 1975 to be the site for budding vesicles containing secretory proteins from the ER (Palade, 1975; Saraste and Svensson, 1991), and were later characterized as COPII-coated vesicles that ultimately fuse with the ER-Golgi intermediate compartment or ERGIC and follow along the secretory pathway (Bannykh et al., 1996; Budnik and Stephens, 2009; Watson and Stephens, 2005). The PAM was first described in 2001 as a portion of the ER that is in close contact with the plasma membrane. This domain is enriched in lipid-synthetizing enzymes (Pichler et al., 2001), and serves as a hub for biosynthetic sterol transport (Baumann et al., 2005). Another subdomain of the ER is the ERQC; it plays a role in accommodating chaperones (mainly

calnexin and calreticulin) along with misfolded proteins that are subject for degradation by the ER-associated degradation (ERAD) machinery (Kamhi-Nesher et al., 2001; Leitman et al., 2013). Finally, the MAM is another SER subdomain that has been a major subject of study in the past 20 years. Since the focus of this project is related to this subdomain, it will be described rather extensively below.

1.1.2. ER mitochondria-associated membrane (MAM)

Physical interactions between the ER and mitochondria were first discovered more than 50 years ago in teleost fish (COPELAND and DALTON, 1959), and similar observations were later made in frog brain (Lieberman, 1971), mouse spinal cord (Bird, 1978), rat brain and liver (McGraw et al., 1980; Meier et al., 1981; Shore and Tata, 1977), among others, but they were initially thought to be artifacts of the imaging technique. Many years later, biochemical fractionation assays were able to separate the portion of the ER that associates with mitochondria and this intracellular structure was named the MAM, or mitochondria-associated membrane (Vance, 1990), and since then the MAM continues to be a hot topic of research worldwide.

Although the ER-mitochondria apposition was known for many years, its structure was not well understood. Today we know that out of the total surface of mitochondria, at least 20% is in close contact with the ER (Rizzuto et al., 1998), as demonstrated by high-resolution 3D imaging. Also, electron tomography studies have shown that these organelles can come in close contact of up to 15nm (Perkins et al., 1997) and are linked by protein tethers (Csordás et al., 2006). The MAM's functions, protein composition, and formation will be described in the following sections.

1.1.2.1. Lipid metabolism

At the beginning of the 1990s, the first function of the MAM was identified, in the form of phospholipid exchange and synthesis (Vance, 1990; Voelker, 1989). The machinery involved in the formation and trafficking of the main phospholipid components of biological membranes (phosphatidylcholine, phosphatidylserine, and phosphatidylethanolamine) is found on both organelles of the contact sites, including long-chain fatty acid-CoA ligase type 4 (FACL4), which ligates fatty acids to coenzyme A, and phosphatidylserine synthase-1 (PSS-1) (Lewin et al., 2001; Lewin et al., 2002; Stone and Vance, 2000), as well as enzymes required for the biosynthesis of cholesterol,

cholesterol esters and triacylglycerols (Rusiñol et al., 1994). This suggested that the MAM is a lipid exchange and transport hub that gives this specific subdomain singular properties that ultimately affect various cellular organelles, including mitochondria, peroxisomes and lipid droplets (Raturi and Simmen, 2013).

1.1.2.2. Calcium signalling and apoptosis

Besides supporting lipid transfer, the MAM has also been shown to be extremely important for calcium signalling between these two organelles. As soon as it was discovered that the ER is the cell's major Ca^{+2} storage entity by electron-probe x-ray microanalysis (Somlyo, 1984), major studies aimed to elucidate how calcium release, uptake, and storage is regulated in this organelle and how it affects the cell overall. Not only do various ER and mitochondrial enzymes require Ca^{+2} for their proper functioning, but Ca^{+2} itself can trigger MAM formation when released from the ER. For instance, small amounts of Ca^{+2} ions, or Ca^{+2} puffs, released from the ER have been shown to attract mitochondria, which come to a complete stop as soon as they encounter these calcium puffs (Yi et al., 2004), thus increasing its apposition with this organelle.

In this regard, one of the first proteins identified to be involved in ER-mitochondria Ca^{+2} signalling was the inositol-1,4,5-triphosphate (IP3) receptor (IP3R), a non-selective cation channel enriched in the ER membrane (Boehning et al., 2001). The IP3R is mainly responsible for releasing Ca^{+2} puffs upon activation by IP3, which ultimately leads to mitochondrial calcium uptake by the mitochondrial calcium uniporter (Baughman et al., 2011; De Stefani et al., 2011; Rizzuto et al., 1993). Moreover, a sustained activation of the IP3R and a massive release of calcium from the ER causes a loss of membrane potential and a permeability transition of mitochondria, resulting in cytochrome c release (Choe and Ehrlich, 2006; Rizzuto et al., 1998). Cytochrome c has been shown to also bind the IP3R, creating a positive feed-forward loop that eventually leads to apoptosis (Parys and De Smedt, 2012). Furthermore, the IP3R was found to be regulated by the sigma-1 receptor (Sig-1R) at the MAM, where they co-localize (Hayashi and Su, 2007). In this study, the authors stated that under normal conditions, Sig-1Rs are normally interacting with the chaperone glucose-regulated protein 78 (GRP78, or BiP), but upon IP3R's activation and a subsequent decrease in ER Ca^{+2} concentration, Sig-1R dissociates from GRP78 and inhibits IP3Rs, thus maintaining a proper Ca^{+2} signalling at

the MAM which would otherwise result in proteasome degradation of IP3Rs (Hayashi et al., 2009).

Besides the IP3R, there is another calcium channel in the ER membrane, the sarco-endoplasmic reticulum calcium ATPase (SERCA), that functions as a calcium pump by transferring Ca^{+2} from the cytosol to the lumen of the ER by means of ATP hydrolysis (Møller et al., 2010). This calcium pump is regulated by the ER-resident Ca^{+2} -binding chaperones calnexin and calreticulin, which thus determine the internal store of calcium in the ER (John et al., 1998; Roderick et al., 2000). All in all, past, present, and ongoing evidence suggests that Ca^{+2} signalling between these two organelles is very important for cellular survival.

1.1.2.3. Tether complexes and other proteins that aid in MAM formation and stabilization

In order for all of these functions to be carried out efficiently, the ER and mitochondria must be close enough to each other and in at least temporary physical association. Using electron micrographs and tomographs, Csordás and colleagues very accurately showed in rat cells that indeed these organelles are linked together by tethers that are 6-15nm in distance and that can be weakened by proteases (Csordás et al., 2006).

Subsequent studies have showed that indeed, ER-mitochondria contacts are maintained by physical interactions or protein complexes. One of these complexes includes the voltage-dependent anion channel or VDAC, the IP3R, and the glucose-regulated protein 75 or GRP75 (Szabadkai et al., 2006). VDAC is a protein that localizes to the outer mitochondrial membrane (OMM) and acts as a pore or channel through which anionic compounds can be transported in and out of mitochondria, depending on its membrane potential and its interaction with different types of modulating molecules, including NADH, chaperones, metabolic enzymes, among others (Colombini, 2012; Giorgi et al., 2009; Shoshan-Barmatz et al., 2004). The second member of the complex, the ER-resident IP3R, is linked to the mitochondrial VDAC by the third member GRP75, a cytosolic chaperone that regulates cell proliferation and antigen processing, dependent on cell stress (Ran et al., 2000; Wadhwa et al., 2002). This ternary complex enhances Ca^{+2} release from the ER and its uptake by mitochondria, playing an important role in cell physiology and apoptosis (Szabadkai et al., 2006).

Another complex tethering the ER and mitochondria was found in 2008 by the Scorrano group. In this study, the GTPase mitofusin-2 was identified not only to localize

in regions of juxtaposition between these two organelles, but also to alter ER morphology and reduce MAM contact sites when depleted; this was proven to be especially important for mitochondrial Ca^{+2} uptake and its release from the ER, hampering Ca^{+2} signalling and increasing apoptosis stimuli (de Brito and Scorrano, 2008).

Lastly, the B-cell receptor associated protein of 31 kDa (Bap31) was also discovered to be part of another ER-mitochondria tethering complex (Iwasawa et al., 2011). Bap31 is an integral protein of the ER membrane that interacts with the outer mitochondrial membrane fission protein Fis1 (Iwasawa et al., 2011). This complex constitutes a scaffold for subsequent procaspase-8 recruitment, which results in Bap31 cleavage by caspase-8 and stimulates Ca^{+2} and cytochrome c release from the ER and mitochondria, respectively, ultimately leading to enhanced apoptosis (Breckenridge et al., 2003; Iwasawa et al., 2011). This multi-protein complex reiterates that a stable crosstalk between the ER and mitochondria is crucial for efficient apoptosis signalling (Grimm, 2012).

Yeast, however, contain a different set of proteins that serve as MAM tethers as well and comprise the ER-mitochondria encounter structure (ERMES) (Kornmann et al., 2009). The members of the ERMES complex are the outer mitochondria membrane proteins Mdm10 and Mdm34, the peripheral protein Mdm12, and the ER-integral protein Mmm1; together they form a stable tether at the ER-mitochondria interface that allows for an efficient lipid exchange, regulation of the mitochondrial DNA (mtDNA) replication, and protein import (Michel and Kornmann, 2012). Even though the MAM functions identified for this protein complex are very similar to the ones described above, no ERMES-homologous proteins have yet been identified in mammals, although a few have been identified in other eukaryotic supergroups (Wideman et al., 2013).

Besides stabilizing and forming MAM contacts, there are other proteins that are involved in regulating MAM composition. One such protein is the cytosolic phosphofurin-acidic cluster sorting protein-2 (PACS-2). PACS-2 is a multifunctional sorting protein that was found to be necessary for the ER-mitochondria apposition in humans, since knockdown of this protein caused mitochondrial fragmentation and their separation from the ER (Simmen et al., 2005). Moreover, PACS-2 depletion was also found to play a role in maintaining ER homeostasis (as it resulted in an increase in the components of the ER-folding machinery), as well as apoptosis (by blocking cytochrome c release from mitochondria, thus hindering the cell death signalling pathway). Also,

overexpression of this sorting protein led to an increase of the presence of FACL4 and PSS-1 at the MAM, thus regulating the enrichment of proteins at the MAM (Simmen et al., 2005).

1.2. Membrane trafficking

All newly translated proteins, proteins that had just been internalized from the plasma membrane, and proteins that are destined either for recycling or for degradation, need to be transported to their final destination so that they can perform their function. This occurs through a highly regulated process known as membrane trafficking. This mechanism consists mainly of four stages. First cargo proteins are selected and the vesicles that transport them are formed; these vesicles are usually coated with clathrin or COPI/COPII for Golgi-to-plasma membrane and ER-to-Golgi cisternae protein transport, respectively. Then, cargo vesicles are transported towards their destination organelles by molecular motors through the actin or microtubule networks. Next, tethering or docking of this vesicle with the destination membrane occurs through the action of complementary SNAREs (soluble *N*-ethylmaleimide-sensitive fusion protein-attachment protein receptors) in both of these membranes. Finally, stable vesicle docking in the target compartment leads to the fusion of these two membranes, and thus completion of the process (Hutagalung and Novick, 2011).

This multi-stage process requires a large number of proteins to maintain an accurate and efficient delivery of proteins to their proper organelle. Among them, Rab proteins are known to act as the master regulators of membrane trafficking, because they are distributed to different subcellular compartments and ensure that appropriate cargo delivery is carried out, thus giving a high level of specificity to all the steps mentioned above (Hutagalung and Novick, 2011). The role of Rabs in membrane trafficking will be described in the following sections.

1.2.1. Rab proteins

Rab proteins, from Ras-related in *rat* brain, are a ubiquitously expressed family of proteins that belongs to the Ras superfamily of small GTPases, approximately 20-25kDa. They are known to localize to the cytosolic face of many organelles (Kahn et al., 1992; Touchot et al., 1987). Rabs have been identified in all eukaryotes investigated to date, including humans (66 Rabs), *Saccharomyces cerevisiae* (11 Rabs), *Drosophila*

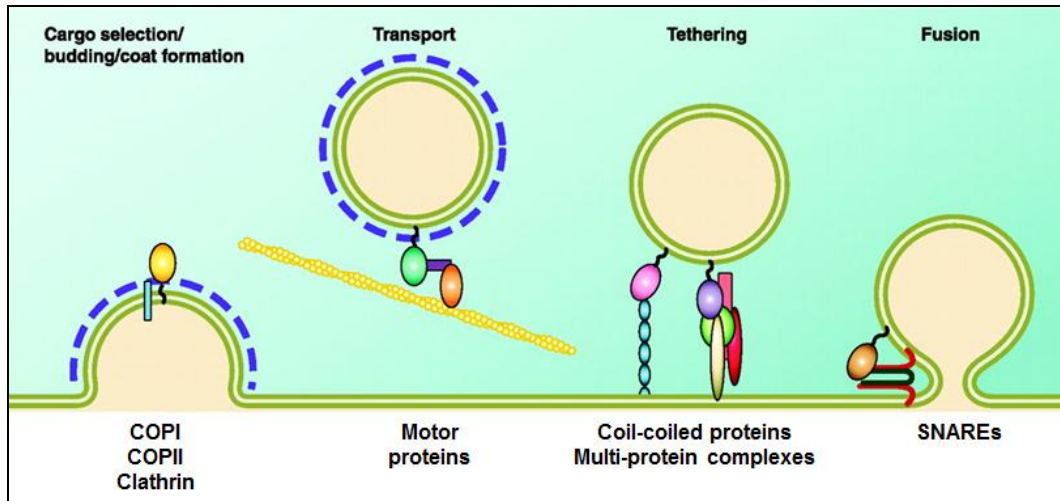


Figure 1.1. Membrane trafficking. Newly translated proteins and proteins destined for recycling or degradation are transported to their final destination through a process called membrane trafficking, which consists mainly of four stages: 1) first, cargo proteins are selected and the vesicles that transported are formed, mainly coated by COPI, COPII, and clathrin proteins; 2) next, these vesicles are transported to their destination organelle by molecular motors through the actin or microtubule networks; 3) then, coil-coiled proteins and multi-protein complexes mediate the stable docking and tethering of these vesicles with its destination membrane; 4) lastly, the fusion of the vesicle and destination organelle membranes is mediated by SNARE proteins, which results in the release of cargo in the final organelle, thus completing the process. Rabs are depicted as oval-shaped structures anchored to membranes by their prenyl (black) tails. Adapted from (Hutagalung and Novick, 2011).

melanogaster (29 Rabs), *Arabidopsis thaliana* (56 Rabs), *Trypanosoma cruzi* (23 Rabs), and *Toxoplasma gondii* (15 Rabs) (Elias et al., 2012). This wide distribution and the large number of Rabs per organism suggests they are very important in eukaryotic biology, but also that different organisms could have different levels of trafficking regulation.

1.2.1.1. Rab protein structure

Rab proteins, as all guanine nucleotide-binding proteins (or G-proteins), share a common fold structure composed of five parallel-, and one antiparallel-stranded β -sheets, bordered by five α -helices. These strands and helices are linked together by 5 loops containing the amino acid sequences required for binding of a Mg^{+2} cofactor, as well as for GTP binding and hydrolysis (Vetter and Wittinghofer, 2001). This multi-loop structure is also known as switch I and II regions, which are essential for the GDP/GTP-dependent Rab function, since both regions are in contact with the γ phosphate of GTP (Hutagalung and Novick, 2011). Switch regions in Rab proteins adopt a different conformation when they are in their active state (or GTP-bound) and when they are inactive (or GDP-bound). In their inactive state, these structures tend to be disordered, but adopt a stable state upon GTP-binding (Milburn et al., 1990; Schlichting et al., 1990; Stroupe and Brunger, 2000).

Besides this well-conserved domain, Rabs have a hypervariable region close to the C-terminus that contains the greatest amino acid heterogeneity between Rabs of different eukaryotic organisms; this region has been identified to be essential for the correct targeting of individual Rab proteins to their specific organelle membrane where they carry out their function (Chavier et al., 1991). Also, Rabs contain a cysteine motif at the very end of the C-terminus that is involved in prenylation, a post-translational modification that consists of the covalent addition of one or two C20 (geranylgeranyl in the case of Rabs) isoprenoid groups, which is essential for its anchoring to cellular membranes (Pereira-Leal et al., 2001; Stenmark and Olkkonen, 2001).

Furthermore, extensive sequence analysis identified a feature that distinguishes Rabs from other Ras-related GTPases, since they all share common domains. In this study, the researchers used various sequence alignment techniques using all the known mammalian Rab sequences to that date. They were able to identify five Rab-specific regions that they termed Rab family (RabF1-5) motifs. Also, they were able to distinguish “related” Rabs that shared specific clusters of amino acids, naming them Rab subfamily

(RabSF1-4) motifs; these regions had higher amino acid identity in Rabs within subfamilies (around 58%) than with Rabs in general (14%) (Pereira-Leal and Seabra, 2000). This study shed some light into the understanding of how different Rabs can have many different functions and be targeted to different cellular subdomains by means of the specificity given by their aminoacid sequence.

1.2.2. Rab cycle

Rab proteins act as molecular switches by cycling between the cytosol and their target organelle membrane in a nucleotide-dependent manner (Zerial and McBride, 2001). This is a highly regulated process mediated by the interaction of the Rab with various proteins that give them function and localization specificity. For the purpose of this thesis, this process will be illustrated with the ER example (Figure 1.2).

After being translated, a GDP-bound Rab is bound to a Rab escort protein (REP), which acts as a chaperone that escorts the unprenylated Rab and prevents it from aggregating in the cytosol (Anant et al., 1998; Andres et al., 1993). This Rab-REP complex then acts as a substrate of the enzyme Rab geranylgeranyl transferase (RGGT) (Anant et al., 1998). RGGT catalyses the covalent addition, via thioether bonds, of one or two geranylgeranyl moieties to cysteine residues in the C-terminus of the Rab that allows its association with membranes (Seabra et al., 1992). The prenylated Rab is then escorted and delivered by REP to its target membrane where it can perform its biological role (Alexandrov et al., 1994; Wilson et al., 1996).

Once the Rab protein is anchored to its target membrane, it needs to be activated in order for it to carry out its specific function. A guanine-nucleotide exchange factor, or GEF, is an enzyme specialized for this function, as it accelerates the change from GDP to GTP several orders of magnitude, and thus activates the Rab protein (Vetter and Wittinghofer, 2001). Very recently, a study revealed that this may not be the only function for GEFs, as Blümer and colleagues were able to determine that GEFs also display the minimal targeting machinery for recruiting Rabs to their specific subcellular membrane from the cytosol, and consequently are very important for the localized activation of the Rab protein only when its anchored to its target membrane (Blümer et al., 2013).

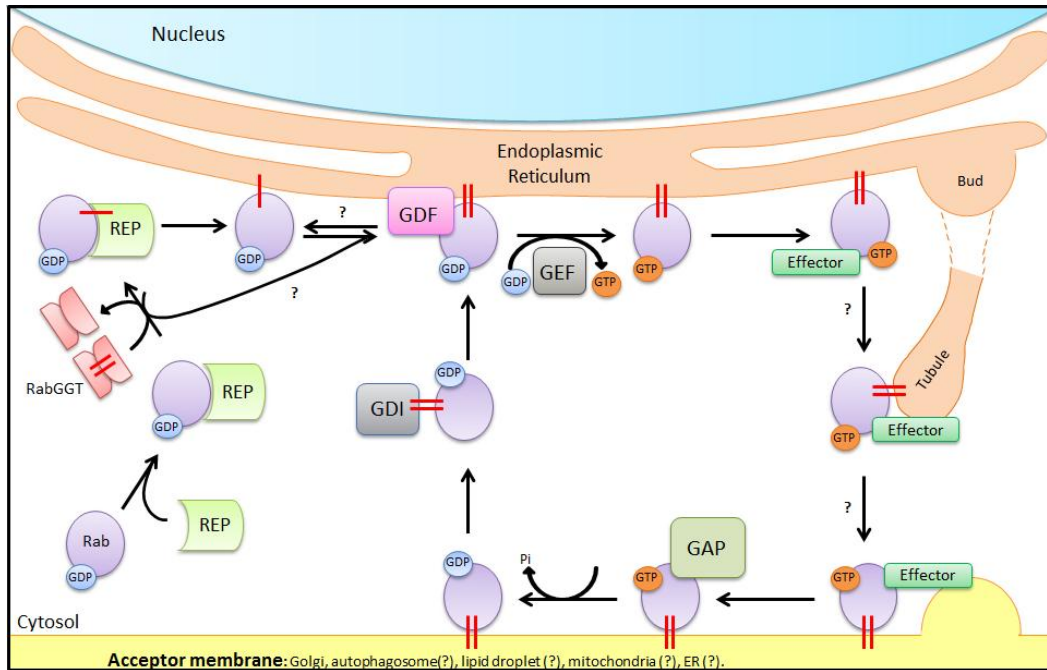


Figure 1.2. Rab cycle at the ER. Newly translated Rabs associate with Rab-escort protein (REP), which directs it to RabGGT for prenylation (prenyl groups are depicted by red bars). REP then delivers the prenylated Rab to its target membrane where it is activated by its GEF (guanine-nucleotide exchange factor). Proteins called effectors then associate with the active Rabs, to mediate the downstream steps of its trafficking pathway in the acceptor membrane. GAPs (GTP hydrolysis activating proteins) then regulate the activity of Rabs by inactivating the Rab through GTP hydrolysis. The inactive Rab is then extracted from the acceptor membrane by a protein called GDI, or GDP-dissociation inhibitor, which also stabilizes the Rab protein in the cytosol. Finally, GDI-displacement factor (GDF) reinserts the inactive Rab in its target membrane where it is ready to be reactivated and start the cycle again. Figure taken from (Sandoval and Simmen, 2012).

Activated, membrane-bound Rabs are able to perform various functions through proteins called effectors. Effector molecules comprise a very heterogeneous group of proteins that are known to bind specific Rabs preferentially in their GTP-bound state and mediate at least one of their downstream effects in the acceptor membrane (Grosshans et al., 2006). As mentioned above, Rabs are involved in many membrane trafficking steps, so it is expected that their effector molecules should be proteins of these machineries as well. Some effector proteins are involved in regulating protein motility, sorting, recruitment, and recycling; others stimulate vesicle transport, adherence, docking, and fusion of appropriate membranes together (Zerial and McBride, 2001). Specific examples of Rab-effector pairs and their functions are described in section 1.2.3.

After the Rab protein has completed its function, its activity is terminated by a GTP hydrolysis activating protein, or GAP (Barr and Lambright, 2010). The intrinsic rate of Rabs to hydrolyze GTP is very low, so they need the help of GAPs to accelerate this process and to be converted back to their inactive GDP-state (Bos et al., 2007). Most Rab GAPs have a conserved domain termed TBC (Tre-2/ Bub2/Cdc16) that has been shown to be responsible for its GAP activity (Richardson and Zon, 1995). To date, the TBC/Rab GAP family comprises 44 different potential members that share sequence homology in the TBC domain (Gabernet-Castello et al., 2013); this may suggest that a single GAP may inactivate more than one Rab participating in the same intracellular pathway, and that a Rab protein may be inactivated by more than one GAP. It is important to note, however, that some TBC/GAPs have been shown to have many different subcellular functions besides helping with GTP-hydrolysis, including melanosome transport, cilia formation, regulating neurite length, cytokinesis, and endocytic trafficking (Frasa et al., 2012), so future studies will uncover many more exciting ways how these proteins are involved in regulating a plethora of membrane trafficking pathways.

Continuing with the cycle, after a Rab protein has been inactivated, it must return to its original target membrane. GDP-dissociation inhibitor, or GDI, extracts GDP-bound Rabs from the acceptor membrane, by sequestering their isoprenyl tails, and thus solubilizing the proteins in the cytosol (Hutagalung and Novick, 2011). GDIs, very similar to REPs, have a strong affinity for GDP-bound Rabs; however, GDI's affinity for unprenylated Rabs is 1,000-fold lower than for mono- or di-prenylated Rabs, unlike REPs, which can bind relatively low both to prenylated and unprenylated Rabs

(Pylypenko et al., 2006; Wu et al., 2007), thus giving the cycle a little bit more of specificity.

The last step in the Rab cycle is the reinsertion of the cytosolic Rab in the target membrane (Figure 1) (Sandoval and Simmen, 2012). As mentioned before, the affinity of GDI to Rabs is very high, so GDI needs the activity of another protein to release the Rabs from this complex to be activated again (Collins, 2003; Sivars et al., 2003). In 1997, Dirac-Svejstrup and colleagues discovered this protein and named it GDI-displacement factor, or GDF. This study revealed that this membrane-bound protein was not acting as a GEF, as it did not have any effect on the GDP/GTP exchange rate; rather, GDF caused the release of Rabs from GDI, which allowed Rabs to be activated by GEFs in the target membrane (Dirac-Svejstrup et al., 1997), thus completing the cycle, as the newly activated Rab is ready to bind to its effectors again and carry out its physiological role.

1.2.3. Cellular localization and function of Rabs

As aforementioned, Rabs coordinate many membrane trafficking events by acting as molecular switches in many subcellular compartments, including the ER, Golgi, ERGIC, endosomes, and the plasma membrane (Hutagalung and Novick, 2011). The following paragraphs will briefly describe some of these events and the Rabs, as well as their interactors, involved.

1.2.3.1. Rabs in vesicle formation and cargo selection

Most membrane trafficking events require the formation of vesicles that carry specific cargo between organelles. Cargo proteins contain signals in their structure that are recognized by proteins that coat these vesicles, normally COPI, COPII, or clathrin proteins (Cai et al., 2007). Rab9 was shown to participate in vesicle formation from endosomes destined to fuse with the trans-Golgi network (TGN) (Lombardi et al., 1993; Riederer et al., 1994), with the help of its effector, TIP47 (Aivazian et al., 2006). Also, Rab5 has been reported to be involved in clathrin-coated vesicle formation from endosomes, confirmed by quantitative electron microscopy and in vitro endocytosis assays (McLauchlan et al., 1998). Besides vesicle formation, Rab5, as well as Rab7, have been implicated in the recruitment of the retromer complex, which mediates the retrograde transport of cargo (mainly transmembrane proteins), from endosomes to the TGN (Rojas et al., 2008).

1.2.3.2. Rabs in vesicle motility

Rab proteins interact with effectors that are involved in vesicle movement, often motor proteins from the microtubule and actin networks (Hutagalung and Novick, 2011). Confocal microscopy studies of frog retinal photoreceptors showed that Rab8 associates with actin microfilaments and attaches newly formed vesicles containing rhodopsin, a biological pigment involved in the perception of light (Deretic et al., 1995). Moreover, Rab6's effectors rabkinesin-6, a kinesin-like protein important for cytokinesis, and mitosis kinesin protein MKLP2, modulate transport of vesicles within the Golgi towards the plus end of microtubules (Jordens et al., 2005). Rab11 acts through its effector myo2, a type V myosin motor, to transport vesicles at secretion sites (Lipatova et al., 2008). Lastly, Rab7, which is implicated in transport of vesicles between late endosomes and lysosomes, interacts with a Rab-interacting lysosomal protein of 45kDa, or RILP, to recruit dynein motors for the transport of late endosomal and lysosomal vesicles towards the minus end of microtubules (Cantalupo et al., 2001; Jordens et al., 2001).

In addition to vesicle transport, Rabs have also been found to be involved in organelle movement. Studies in yeast have identified that Rab Ypt11p overexpression results in the increased migration of mitochondria and Golgi to the daughter cell, and in contrast, the deletion of Ypt11p causes the accumulation of these organelles in the mother cell; this is thought to be through their interaction with myo2, as described above (Arai et al., 2008; Boldogh et al., 2004; Itoh et al., 2002).

1.2.3.3. Rabs in vesicle tethering

After the vesicle is formed and transported, it needs some sort of signal to identify its destination organelle. These signals or “factors” are known as tethering proteins, as upon their recognition, the vesicle is stably attached to the acceptor membrane and membrane fusion follows (Cai et al., 2007). Tethering proteins can be divided into two categories: coiled-coil proteins and multi-protein complexes (Whyte and Munro, 2002). p115, a Rab1 effector, was one of the first coiled-coil proteins to be identified to be important for targeting ER-derived vesicles to the Golgi (Cao et al., 1998b); this process requires p115 binding to its receptor molecules, and two other coiled-coil proteins, giantin and GM130, in COPII and COPI-coated vesicles, respectively (Moyer et al., 2001; Sönnichsen et al., 1998). Another well studied tethering coiled-coil protein is the early endosome antigen 1 (EEA1), which mediates the docking

of endosomes leading to membrane fusion, and thus, acts as a Rab5 effector (Christoforidis et al., 1999).

Vesicle tethering can also be carried out by multi-protein complexes. Some of these complexes include: a) the transport protein particle (TRAPP) I and II, which acts as GEFs for Rab1 and regulate traffic from the ER to the Golgi network, but also within the Golgi and between early endosomes and the Golgi, respectively (Cai et al., 2007); b) the exocyst complex, which consists of eight subunits, binds to active Rab Sec4, and mediates the targeting of vesicles destined for exocytosis, as they fuse with the plasma membrane (Guo et al., 1999); c) the conserved oligomeric Golgi (COG) complex comprised of eight subunits, that regulates Golgi retrograde traffic through its effector interaction with the Rab Ypt1 (Suvorova et al., 2002; Ungar et al., 2006); d) the four subunit Golgi-associated retrograde protein (GARP) complex that is recruited by active Rab6 to the late Golgi and mediates the recycling of membrane proteins (Siniosoglou and Pelham, 2001); and finally e) the homotypic fusion and vacuole protein sorting (HOPS) complex and the class C core vacuole/endosome tethering (CORVET) complex that regulate endosome/lysosome traffic, since both of these complexes share subunits that interact with Rab7 and Rab5, respectively (Balderhaar and Ungermann, 2013).

1.2.3.4. Rabs in vesicle fusion

After being tethered to the correct membrane, the next essential step in membrane trafficking is the fusion of the cargo-containing vesicles with the ultimate organelle. The master regulators of membrane fusion are SNAREs (soluble N-ethylmaleimide-sensitive fusion protein-attachment protein receptors), a superfamily of proteins that share this function across eukaryotic cells (Lang and Jahn, 2008). SNAREs can be grouped via two main classification methods: 1) target or t-SNAREs, and vesicle or v-SNAREs, depending on the membrane where they are localized when performing its function; or 2) Q-SNAREs and R-SNAREs, depending on the amino acid contributed by the SNARE in the interaction, glutamine and arginine, respectively. Typically, membrane fusion requires the binding of one R or v-SNARE, and three Q (Qa, Qb, and Qc) or t-SNAREs (Pfeffer, 2007).

Rabs interact often only indirectly with SNAREs by binding to regulatory proteins of these membrane fusion proteins. For example, the yeast homolog of Rab8, Sec4, indirectly interacts with a t-SNARE, SNAP25, through its effector Sro7 to mediate

exocytosis (Novick et al., 2006). Also, the aforementioned interaction of Rab5 with its effector EEA1, requires the binding of a third element, the SNAREs syntaxin-6 and syntaxin-13 individually, for the fusion of early endosomes (McBride et al., 1999; Simonsen et al., 1999).

1.3. Rab32 family proteins

As mentioned before, related Rabs can be grouped together in subfamilies by means of their sequence similarity in the Rab subfamily motifs (RabSF1-4) (Pereira-Leal and Seabra, 2000). Using this method Rab32 is grouped together with Rab38 and a protein called Rab7L1, a human protein which was proposed to be called Rab29 because it had 93% sequence homology with rat Rab29 (Pereira-Leal and Seabra, 2000; Pereira-Leal and Seabra, 2001). This family of Rabs share an unusual characteristic in their aminoacid structure: instead of containing the conserved GTPase domain sequence WDTAGQE in their switch II region like most Rab proteins, they all have a WDIAGQE sequence instead (Bao et al., 2002), suggesting their GTP-binding properties might be different. This and other studies have shown that all other Rab32 homologues, that derive from a common ancestor, i.e. murine Rab32 (Bao et al., 2002), RabE from the slime mold *Dictyostelium discoideum* (Norian et al., 1999), rat Rab38 (Jäger et al., 2000), and human Rab29 (Shimizu et al., 1997), all share this unique sequence. This protein subfamily will be described below.

1.3.1. Rab32

1.3.1.1. Overview

Rab32 was first discovered in blood platelets, and a mRNA distribution profile reported it was highly expressed in heart, liver, and kidney cells. In contrast, placenta, pancreas, and lung cells showed lower expression of this protein. Even lower levels were found in brain and skeletal muscle tissues (Bao et al., 2002). This same study identified Rab32 as a 28kDa protein by Western Blot, and subcellular fractionation assays reported Rab32 to be enriched in the granule/mitochondria and membrane fractions.

Consistent with this, Alto and colleagues found by immunofluorescence that the Rab32 staining pattern overlapped with MitoTracker, that labels mitochondria, and this finding was confirmed by subcellular fractionation (Alto et al., 2002). Rab32 contains two cysteines in its C-terminus, which as mentioned in section 1.2.2., are essential for the

membrane association of Rabs. A Rab32 mutant lacking this pair of aminoacids (Rab32 Δ CC) could not associate with mitochondria, suggesting they indeed are required for anchoring this protein in the mitochondrial membrane (Alto et al., 2002).

Perhaps one of the most interesting findings of this study was the fact that Rab32 was also reported to contain a cyclic adenosine monophosphate or cAMP-dependent protein kinase A (or PKA)-binding domain (Alto et al., 2002). PKA contains two regulatory and two catalytic subunits. Binding of cAMP (a second messenger produced in response to hormones and neurotransmitters) to the regulatory subunits of PKA releases the activated catalytic subunits, which phosphorylate substrates locally due to their interaction with A-kinase anchoring proteins or AKAPs. These proteins recruit them to specific locations in the cell (Carlucci et al., 2008; Feliciello et al., 2001). Rab32 showed a 7-fold increased activity in a PKA activity assay, when compared to the Rab32 L188P, which disrupts the PKA-binding domain. Thus, Rab32 acts as an AKAP, recruiting PKA to mitochondria. Intriguingly, Rab32 seems to be the only Rab that acts as an AKAP, as it contains an alanine in the aminoacid position 185, which is a critical PKA-binding determinant. In contrast, most Rab proteins have a conserved phenylalanine in this position. Even the closely related Rab38 and Rab29, which instead have serine and methionine residues, respectively, cannot bind PKA as well (Alto et al., 2002).

The other exciting finding of this study was that overexpression of a GTP-binding deficient mutant of Rab32 (Rab32 T39N) caused mitochondria to aggregate in the perinuclear region. Moreover, expression of the double mutant Rab32 T39N Δ CC showed a minor collapse of mitochondria suggesting that its subcellular localization is essential to generate this phenotype. Low level expression of Rab32 T39N only displayed a mild phenotype, in which mitochondrial fusion was apparently enhanced, as seen by highly interconnected and elongated mitochondria. Conversely, overexpression of wild type (WT) Rab32, as well as a GTPase-inactive, or constitutively active, mutant (Rab32 Q85L), did not exhibit this mitochondrial phenotype (Alto et al., 2002).

Later studies showed that both human Rab32 and its mouse homologue localized to melanosomes in cells that contain these organelles, as seen by their co-localization with melanosomal markers Tyrp1 (for tyrosine-related protein-1) and DCT (dopachrome tautomerase, also known as tyrosine-related protein-2 or Tyrp2), proteins involved in the synthesis of melanin (Cohen-Solal et al., 2003). This was the first in a series of studies that tie Rab32 to melanosomes.

In 2006, Wasmeier and coworkers confirmed that Rab32, as well as Rab38, are expressed in mouse melanocytes and that their depletion using siRNA caused a loss in melanosome pigmentation, as well as an 87% decrease in melanin concentration in these cells. Furthermore, Rab32/38 depletion caused the redistribution of Tyrp1 and tyrosinase (enzymes required for melanin synthesis, as mentioned above) from peripheral vesicular structures to the perinuclear region, where they co-localized with a TGN marker (TGN38), suggesting that both Rab32 and 38 are involved in tyrosinase and Tyrp1 post-Golgi transport to melanosomes (Wasmeier et al., 2006). In addition, follow-up studies showed that the effector-type interaction between active Rab32 and Rab38 and vacuolar protein sorting 9 (VPS9)-ankyrin-repeat protein or VARP, is essential for Tyrp1 localization at melanosomes, since the depletion of both Rab proteins resulted in a massive reduction of Tyrp1 in these organelles (Tamura et al., 2009; Wang et al., 2008).

At this point, it was suggested that Rab32 and 38 had redundant functions in cells that contain melanosomes or lysosome-related organelles (LROs), as exogenous expression of either Rab restored melanosome pigmentation when the other was depleted. This idea was challenged in a recent study that reported an interaction between these two Rabs and three protein complexes involved in the packaging of tyrosinase into transport vesicles: biogenesis of lysosome-related organelles complex (BLOC)-2, adaptor protein complex (AP) -1 and -3 (Bultema et al., 2012). Although they interacted equally strong with these proteins, the extent of their co-localization, as seen by confocal immunofluorescence microscopy, differed: AP-1 and AP-3 showed better co-localization with Rab38 than with Rab32 (48 and 35% for AP-3, 57 and 37% for AP-1, respectively), whereas both Rabs only showed a partial co-localization with BLOC-2. Moreover, Bultema and colleagues also reported that, while Rab32 presence is essential to maintain normal Tyrp2 levels (as its depletion dramatically reduced Tyrp2 transport to the maturing melanosome), absence of Rab38 did not have any effect on this melanin-synthesizing enzyme, suggesting that they indeed have different functions.

Similar results were reported by the Pietro group in platelet dense granules, organelles belonging to the group of LROs; they were able to show by confocal immunofluorescence microscopy and by thin-section immunogold electron microscopy that both Rab38 and 32 are present in immature dense granules. Importantly, they also reported that these Rabs are individually essential for tethering or fusing the immature vesicle with the mature organelle, as the depletion of one Rab could not be fully

compensated by the presence of the other (Ambrosio et al., 2012). These results suggest that Rab32 and 38 are both very important for cargo transport to LROs, but their functions are not 100% redundant.

1.3.1.2. Rab32 and the MAM

Initially, Rab32 was found to localize to mitochondria on cells that lack LROs. This fact made this Rab protein very interesting to our lab, since it suggested that it might regulate MAM formation and targeting of proteins to this specialized subdomain. Indeed, our lab found by immunofluorescence microscopy that Rab32 not only co-localized with mitochondria, but also overlapped with the ER marker PDI (protein disulfide isomerase, an oxidoreductase involved in protein folding) both individually and together with mitochondria (Bui et al., 2010). Moreover, Opti-prep gradient fractionation (a protocol designed in our lab that allows the separation of membranes of the secretory pathway, the RER, and the MAM/mitochondria) revealed that Rab32 is indeed a MAM-enriched protein. This was confirmed by a different fractionation method (the Percoll gradient, which is used to distinguish between mitochondria and MAM membranes), where Rab32 was again found to be enriched in the MAM, as well as in microsomes and mitochondria (Bui et al., 2010).

The MAM-enrichment of Rab32 depends on its activation state. The constitutively active mutant Rab32 Q85L showed less enrichment on the MAM, and appeared to be more abundant in peripheral membranes and in the cytosol. On the other hand, the signal of the inactive mutant Rab32 T39N was higher in the perinuclear membranes of the ER and the MAM (Bui et al., 2010). Furthermore, our lab was able to reproduce and confirm that overexpression of the mutant Rab32 T39N causes the collapse of mitochondria around the nucleus, as seen before by Alto and colleagues (Alto et al., 2002).

Lastly, Rab32 appears to regulate MAM composition, since active Rab32 (as seen by the exogenous expression of the Q85L mutant) redistributes the MAM-enriched chaperone calnexin away from the MAM to other membranes within the ER (Bui et al., 2010).

1.3.1.3. Rab32 and autophagy

Autophagy is a well conserved lysosome-dependent pathway for the degradation of damaged cellular components, as well as for the break-down of non-essential macromolecules that can be reused by the cell (Uchiyama et al., 2008). Initially, a cup-shaped double membrane structure, named isolation membrane or phagophore, engulfs cytoplasmic materials, including damaged organelles or protein aggregates. After a gradual curved elongation, the isolation membrane eventually closes forming a proper autophagosome. Finally, the autophagosome fuses with the lysosome, which leads to the degradation of the engulfed components by the hydrolases contained in this organelle (Rubinsztein et al., 2012). To date, over 35 autophagy (Atg)-related genes have been involved in this process, i.e. Atg1, Atg6, and Atg14 which are involved in autophagosome formation (Kraft and Martens, 2012).

In 2009, Hirota and colleagues identified Rab32 to be involved in autophagy. In this study, WT and active Rab32 were proven to be important for the formation of autophagic vacuoles derived from ER-membranes, as 54% of both WT- and Q85L-expressing cells showed large, spherical autophagic vacuole-like structures that contained LC3, a specific marker of autophagosomes. On the other hand, Rab32 T39N and depletion of Rab32 by siRNA were reported to impair autophagic vacuole formation altogether (Hirota and Tanaka, 2009). Moreover, this year a study confirmed that in fact the ER is responsible for providing the membranes for autophagosome formation, and that, excitingly, this event happens at ER-mitochondria contact sites (Hamasaki et al., 2013). This is the first direct evidence of the MAM playing a role in the autophagic pathway.

1.3.2. Rab38

Rab38 was initially identified to be a 26kDa melanocyte-specific protein (Jäger et al., 2000). As Rab32, Rab38 has been mainly studied for its role in melanosome transport. In 2002, a comparative genomic study reported that mouse Rab38 had a similar expression profile to melanocyte control genes. Moreover, Rab38 was found to be contained in a locus that contains a mutation involved in chocolate (cht) mice. cht/cht mice are easily identified mice with lighter skin and eyes in comparison with their darker parental strain, suggesting an abnormality in their pigmentation pathways. Accordingly, Rab38 was reported to be present in melanosomes, and the mutated form of Rab38 found

in *cht/cht* mice showed hypopigmentation in these organelles, as well as a reduced Tyrp1 staining. Together, these findings suggest it participates in the sorting of this melanogenic enzyme to pigmented melanosomes, and the mutation in *cht/cht* mice hinders this function (Loftus et al., 2002). More recent studies of Rab38 in melanosome biogenesis were described above in section 1.3.1.1.

Rab38's role in mechanisms other than sorting cargo in LROs is still poorly understood. However, its rat homologue was found to be expressed in alveolar type II cells and to be enriched in the ER in these cells (Osanai et al., 2001), suggesting it might have a different function in non-melanosomal cells.

1.3.3. *Rab29*

In 1997, Rab29 was identified as a small GTP-binding protein highly homologous to Rab7, which was why it was initially designated Rab7-like 1 protein, or Rab7L1 (Shimizu et al., 1997). A few years later, Pereira and Seabra proposed to change the name to Rab29 since it appeared to be a rat Rab29 homolog (93% sequence homology) (Pereira-Leal and Seabra, 2000; Pereira-Leal and Seabra, 2001).

Since these studies, not much information was found about this protein. It was not until 2009 when a genome-wide association study identified the Rab29 gene to be contained in a locus related with Parkinson's disease (PD), called *PARK16* (Simón-Sánchez et al., 2009). PD is a neurodegenerative disease associated with the progressive loss of dopaminergic neurons that ultimately leads to disorders in the motor system. Since neurons are highly dynamic cells and require great amounts of energy to carry out their metabolic pathways, they are especially dependent on functional mitochondria, the main cellular power source (Sai et al., 2012). Therefore, it is not surprising that mutations in many genes that encode proteins important for mitochondrial physiology are related to PD. For example, loss-of-function mutations in parkin, an E3 ubiquitin ligase involved in mitochondrial fission, has been shown to play a role in the pathology of PD; moreover, several studies have shown that some substrates of parkin are involved in maintaining mitochondrial morphology and its contacts with other organelles, such as VDAC and mitofusin 1 and 2 (Lee et al., 2012). Similarly, mutations in PINK1 (PTEN-induced putative kinase 1), a gene that encodes a mitochondrial serine/threonine-protein kinase localized at the outer mitochondrial membrane, are known to cause a form of autosomal

recessive early-onset PD; PINK1 has been reported to act together with parkin to promote mitochondrial division (Henchcliffe and Beal, 2008).

Likewise, a study in 2010 reported a novel mutation (K157R) in the Rab29 gene to be associated with a pathologically proven PD case (Tucci et al., 2010). In addition, a recent bioinformatics analysis identified that alterations within the Rab29 promoter region conferred protection from PD (Gan-Or et al., 2012). However, besides its PD association, not much is known about Rab29. Future studies will have to elucidate the mechanism, by which Rab29 increases the risk of developing PD, and if it is related to a different pathway other than neurodegeneration.

1.4. ER-shaping proteins

As mentioned in section 1.1.1., the ER comprises a non-uniform membranous organelle. It can be envisaged as sheet-like structures stretching from the nuclear envelope, and as an interconnected network of tubules in the cell periphery, conferring this organelle different domains with distinct properties (Park and Blackstone, 2010). ER-sheets are found predominantly in the perinuclear region and are known to be studded with ribosomes and to be sites for protein synthesis; tubules, on the other hand, lack ribosomes and have been found to be sites for vesicle formation and fusion, as well as for lipid synthesis and transport to other organelles (Shibata et al., 2006).

These different ER morphologies are very dynamic and can be rearranged depending on the cell's needs. It is thought that these reorganization events are orchestrated by two types of proteins, the reticulons and DP1/Yop1p families, and the atlastins (Park and Blackstone, 2010), and they will be described below.

1.4.1. Reticulons/DP1 and atlastins

Early fluorescence microscopy and video recording led to the discovery of the highly dynamic and localized movements of the ER network, mainly tubule fusion and fission, as well as the formation and elimination of three-way junctions in monkey kidney cells (Lee and Chen, 1988). These studies initially proposed that the changes in ER morphology require the interaction with the cytoskeleton; however, two years later, two different groups confirmed these to be cytoskeleton-independent events, since microtubule and actin depolymerization enhancers did not result in the alteration of the reticular network (Dreier and Rapoport, 2000; Prinz et al., 2000). Later studies showed

that the cytoskeleton is only required for ER tubule movement and extension, as they slide along the microtubule network through the interaction of the ER-resident protein STIM1 and the microtubule protein EB1 (Chen et al., 2013).

1.4.1.1. Reticulon/DPI families

One of the first proteins identified to be involved in shaping ER tubules was reticulon-4a (Rtn-4a/NogoA). Using ER-derived vesicles from *Xenopus laevis*, Voeltz and colleagues were able to assay for *de novo* ER-tubule formation, which seemed to require GTP hydrolysis and the presence of sulfhydryl (SH) groups. An assay based on biotinylation showed that the candidate proteins had a cytoplasmically exposed SH group, and after mass spectrometry, Rtn-4a was identified. Consistently, Rtn-4a's inhibition by antibodies against their SH-containing domains hindered ER network formation (Voeltz et al., 2006). Rtn-4a, which was previously found to inhibit neurite outgrowth (Chen et al., 2000), belongs to the ubiquitous reticulon protein family, including four genes in mammals (Rtn-1, -2, -3 and -4), found in most eukaryotes. These proteins have been found to be enriched in the ER and they all share two homologous C-terminal transmembrane domains (TMDs) that appear to form hairpin domains in the outer leaflet of the cellular membranes generating a wedge and conferring the curvature of the tubules (Oertle et al., 2003; van de Velde et al., 1994).

In the same initial study, Voeltz and colleagues also found that Rtn-4a interacted with another ER-resident membrane protein, DP1 (deleted in polyposis-1 protein, also called REEP for Recceptor Expression Enhancing Protein). Together, these proteins regulate the formation of the tubular ER network, since deletion of both proteins led to a disrupted peripheral ER and an increase in ER sheets. The DP1 family includes 6 genes in mammals and is also ubiquitously expressed in eukaryotes. Although they do not share sequence homology with the reticulon family, they also do have dual hydrophobic segments near their cytosolic tails, suggesting they share a similar function (Chen et al., 2013).

Two years later, the same group proved that it is the hetero- and homo-oligomerization of reticulons and DP1 proteins that confers them their ER-tubule localization as well as their ability to cause tubule curvature in this domain of the ER (Shibata et al., 2008). Interestingly, reticulon/DPI proteins have also been implicated in forming the narrow edges of ER sheets, but are excluded from their flat faces, indicating

that their ratio and prevalence dictates the abundance of each ER morphologic subdomain (Shibata et al., 2010).

1.4.1.2. Atlastins

Generating ER tubules is only one part of the equation, since normally the ER is found forming an intricate network of tubules. In 2009, two different groups published the finding that the protein known as atlastin was the one responsible for fusing ER tubules (Hu et al., 2009; Orso et al., 2009). The atlastins comprise a family of large, integral proteins belonging to the dynamin family of GTPases. Humans have three atlastin family members, where atlastin-1 is mainly brain-specific, atlastin-2 and -3 are more ubiquitously expressed, excluding the brain (Rismanchi et al., 2008). Atlastin-1 localizes predominantly to the Golgi, as seen by immunofluorescence co-localization studies with the Golgi markers p115 and GM130, as well as by immunogold electron microscopy (Zhu et al., 2003); in contrast, atlastin-2 and -3 show a prominent ER localization by the same techniques (Rismanchi et al., 2008). All three proteins have the conserved N-terminal GTPase domain, and two transmembrane hydrophobic domains, with both N- and C-termini facing the cytoplasm (Rismanchi et al., 2008).

In *Drosophila*, the depletion of the single atlastin family member results in ER fragmentation, and its overexpression led to an increase in membrane fusion as seen by expanded ER cisternae (Orso et al., 2009). This study also provided evidence showing that atlastins mediate the homotypic fusion of opposing ER tubules by a GTP-dependent trans-oligomer complex formation. Furthermore, a different study identified an interaction, by co-immunoprecipitation assays, between the mammalian atlastins -1, -2, and -3 and proteins from the reticulon family, Rtn-4a and Rtn-3c, as well as with the DP1 protein (Hu et al., 2009). These researchers were able to show that depletion of the atlastin proteins generated long unbranched tubules, while their overexpression resulted in the formation of aberrant sheet-like structures. Very interestingly, these results were reproducible in organisms other than mammals, as seen by *in vitro* studies using *Xenopus laevis* egg extracts, where inhibition of atlastin hindered ER network formation. Likewise, the atlastin yeast functional homolog Sey1p can also interact with the reticulon homologs and Yop1p, a DP1 yeast homolog. All of these interactions were crucial for the maintenance of a normal ER morphology, as deletion of both Sey1p/Rtn1 or Sey1p/Yop1p results in severely perturbed ER network and the formation of aberrant

structures as well (Hu et al., 2009). Accordingly, a recent study showed that the protein Lnp1p, member of the Lunapark family proteins, co-localizes with and antagonizes Sey1p at ER tubule junctions, and controls its interaction with Rtn1, thus regulating tubule fusion and ER network formation and balance (Chen et al., 2012).

Altogether, these studies show that the atlastins work with the reticulon/DPI1 families to generate three-way junctions that ultimately results in the fusion of neighbor ER tubule membranes, and thus generates the complex ER network.

1.5. Mitochondrial membrane dynamics

Mitochondria are very well known for being the source of energy for the cell, as they generate most of the ATP by oxidative phosphorylation required by the cell's metabolic pathways. Besides, they have also been proven to be essential for intracellular Ca^{+2} signalling and apoptosis, as described before in section 1.1.2.2. These organelles exist in the cell as a mix of bean or round-shaped solitary mitochondria, or a highly interconnected network. These diverse morphologies are a result of a balance of fusion and fission events that are named mitochondrial membrane dynamics (Oettinghaus et al., 2012). Both fusion and fission machineries are mainly composed of well-conserved GTPases related to the dynamin family and they will be described below.

1.5.1. Fusion machinery

The fusion of mitochondria is carried out in two main steps: fusion of the outer mitochondria membrane (OMM) regulated by the dynamin-like GTPases known as mitofusin-1 and -2 in mammals (Fzo1 in yeast), and fusion of the inner mitochondrial membrane (IMM) mediated by the optic atrophy 1 protein or OPA1 (Mgm1 in yeast). Both processes require GTP binding and hydrolysis to mediate fusion (Hoppins et al., 2007).

Mitofusin-1 and -2 are inserted in the OMM membrane by a bipartite transmembrane domain, with both the C-terminus, containing a coiled-coil domain, and the N-terminus, containing the GTPase domain, facing the cytosol (Benard and Karbowski, 2009). Both mitofusin proteins form homo- and heterotypic complexes with each other to fuse together adjacent mitochondria. Moreover, deletion of these proteins leads to 85-95% fragmented mitochondria, and their overexpression leads to the formation of long tubules and an extensive mitochondrial network (Chen et al., 2003).

On the other hand, OPA1 is anchored to the IMM and is in charge of mediating the fusion of these membranes. As in the case of mitofusins, OPA1 forms homotypic oligomeric complexes to tether distinct IMM, and its depletion and overexpression also causes mitochondria fragmentation and promotes mitochondrial elongation, respectively (Belenguer and Pellegrini, 2013). Also, a study done in 2003 showed that downregulation of OPA1 leads to a disorganization of the mitochondrial cristae, as well as a loss in mitochondrial membrane potential and enhanced apoptosis derived from cytochrome c release (Olichon et al., 2003). Interestingly OPA1 has also been implicated in preserving mitochondrial DNA (mtDNA), since mutations in this protein leads to mtDNA instability and inhibits its replication (Amati-Bonneau et al., 2008; Elachouri et al., 2011).

1.5.2. Fission machinery

A master regulator of mitochondrial fission or division is dynamin-related protein 1 or Drp1. Drp1, the mammalian homolog of the yeast protein Dnm1 (Ishihara et al., 2012), is a ubiquitous protein related to dynamin. This founding member of the family is known to participate in endocytosis by oligomerizing from the cytosol into spirals around clathrin-coated vesicles and pinching them off from the plasma membrane (Takei et al., 1995). When Drp1 was first discovered early in 1998, it was found to localize mainly to two pools, one in the cytosol and one that associates with ER tubules, unlike dynamin that localizes to the endocytic pathway (Yoon et al., 1998).

Months later, a different group of researchers discovered that when they transfected cells with a mutant version of Drp1 (K38A, similar to K44A in dynamin that inhibits its activity), it caused the collapse of mitochondria in the perinuclear region, as seen by electron microscopy. With this version of Drp1, mitochondria exhibited a great variety of morphologies, including long tubules, club-, cup-, and ring-shaped mitochondria (Smirnova et al., 1998). In a similar study, Pitts and colleagues found that inactivation of Drp1 not only caused the collapse of mitochondria around the nucleus, but also deteriorated the ER network morphology (Pitts et al., 1999). These were the first pieces of evidence leading towards Drp1 having a role in mitochondria physiology.

It was not until two years later when this role was confirmed. Smirnova and colleagues found by immunofluorescent time-lapse experiments that Drp1 was present at sites where mitochondrial division occurred, and that it functioned very similarly as its close relative dynamin, since they were able to identify ring-like structures comprising

GTP-dependent oligomerized Drp1 around mitochondria (Smirnova et al., 2001). Recently, the Voeltz group very elegantly showed that ER tubules cross over and wrap around mitochondria leading to an initial mitochondrial constriction; this is then followed by Drp1 recruitment at these sites, which ultimately results in fission of mitochondria (Friedman et al., 2011). Different studies showed that both OMM-localized proteins mitochondrial fission factor (Mff) and mitochondrial fission protein 1 (Fis1) are the machinery components responsible for the recruitment of Drp1 to mitochondria division sites (Otera et al., 2010; Yoon et al., 2003).

As all dynamin-related proteins, Drp1 contains an N-terminal GTP-binding domain, a middle domain responsible for the self-oligomerization ability of Drp1, a small insert known as insert B or variable domain, and a C-terminal GTPase effector domain (or GED) which mediates its inter- and intramolecular interactions (Ishihara et al., 2012). The main difference to dynamin is the lack of the C-terminal proline-rich domain and a pleckstrin homology domain present in many members of the dynamin family which are important for their protein-membrane interactions (Oettinghaus et al., 2012).

Drp1 can be posttranslationally modified in many ways to regulate its function. One modification that has been greatly studied in the last years is phosphorylation. A study done in 2007 reported that mitochondria, which are normally fragmented in mitosis, were seen as long tubules upon Drp1 depletion; moreover, this same study identified serine 616 in humans (585 in rats) to be phosphorylated by the mitosis promoting factor (MPF, also known as cyclin-dependent kinase 1 or CDK1/cyclinB) complex, leading to Drp1 activation and enhanced mitochondrial fission (Taguchi et al., 2007). On the other hand, two parallel studies identified that phosphorylation by PKA of serine 637 (656 in rats) inactivates Drp1, thus shifting the balance towards mitochondrial fusion (Cribbs and Strack, 2007; Chang and Blackstone, 2007); since serine 637 lies within the GED domain, it hinders Drp1 of its intramolecular associations, as well as impairing its GTPase activity (Chang and Blackstone, 2007). This can be reversed by dephosphorylation of this serine by calcineurin, a cytosolic Ca^{+2} -dependent phosphatase also known as protein phosphatase 2B or PP2B (Cereghetti et al., 2008; Cribbs and Strack, 2007). Furthermore, phosphorylation of this residue also controls Drp1's subcellular distribution, as the phosphomimetic mutant S637D was mainly cytosolic, whereas the opposite mutant (S637A) localized almost exclusively to mitochondria

(Cereghetti et al., 2008). Since the rat amino acid sequence S656 is widely or preferably used in this field, it will also be used to represent the human S637 mutants in this thesis.

Sumoylation, which consists of the addition of small ubiquitin-like modifier (Sumo) to a protein, is another modification that regulates Drp1. This attachment protects the modified protein from being degraded and sometimes alters its subcellular localization. In the case of Drp1, Sumo attachment stabilizes Drp1 levels, enhances mitochondrial fragmentation, and sometimes leads to apoptosis, since Drp1's binding to mitochondria, and its activity, is supported (Knott et al., 2008).

Similarly, a posttranslational modification known as ubiquitination, has also been implicated in regulating mitochondrial dynamics. In this process, the binding of ubiquitin to a protein targets it to proteasomal degradation. The OMM protein membrane associated RING-CHV or MARCH5 is an ubiquitin ligase that has been reported to ubiquitinate Drp1, however, rather than targeting it for destruction, it stabilizes Drp1 in this organelle; in contrast, parkin-mediated ubiquitination of Drp1 does target it for degradation (Oettinghaus et al., 2012; Reddy et al., 2011).

Lastly, S-nitrosylation of Drp1 has been implicated in neurotoxicity. This modification consists of the alteration of thiols by nitric oxide (NO) and has been implicated in both increasing and decreasing enzymatic activity. S-nitrosylation of Cysteine644 of Drp1 was found to trigger mitochondrial fission; moreover, inhibition of this process prevented neurotoxicity as seen by abrogated synaptic loss and neuronal damage and death (Chang and Blackstone, 2010; Cho et al., 2009).

All in all, regulation of Drp1 is crucial to maintain a normal mitochondrial network, as well as normal mitochondrial physiology.

1.6. Comparative genomics and phylogenetics

The functional data mentioned above was obtained mainly in animal cells, however, membrane trafficking is a feature found in the diversity of eukaryotes. Eukaryotic organisms can be classified in six major supergroups, based on genomic, ultrastructural, and phylogenetic evidence: Opisthokonts (including animals and fungi), Amoebozoa (comprising amoebae and ameboid flagellates), Excavates (which includes mainly flagellates and major human parasites), Archaeplastida (comprising plants and red and green algae), SAR (including alveolates and the human parasite *Plasmodium*), and CCTH (including many algae as well) (Walker et al., 2011).

A way of comparing common features between organisms of these supergroups is to look at their ultimate genetic map, or genome. Therefore, the presence or absence of specific genes might confer an organism a different set of functions or abilities, setting it apart from closely related species. Similarly, identifying genes that are conserved throughout eukaryotes can also be achieved by comparative genomics (Hardison, 2003). For example, comparing the genomes of humans with chimpanzees was useful to determine which encoded proteins were conserved, and if these had similar functions. These organisms have very short phylogenetic distances, or measures of the extent of separation in the tree of eukaryotic life across time. This is probably why a great variety of their proteins are highly conserved; however, organisms with higher phylogenetic distances between them might not show a high level of conservation between their genomes (Hardison, 2003).

A popular way to visualize phylogenetic relationships between a group of organisms is using phylogenetic or evolutionary trees. Phylogenetic trees are generated in four main steps: 1) alignment of a sequence dataset; 2) determining an evolutionary model that best fits the dataset; 3) building the tree; and 4) visualizing and evaluating the tree. These trees are composed of branches, each representing a unique sequence or organism, and nodes, delineating the relationship between the sequences across evolution in respect with the root of the tree, or the common ancestor of all the taxa analyzed. Related sequences group together in clades, or groups of sequences including the common ancestor and all of its descendants. The resulting branching of the tree is called topology, and the branch lengths typically represent the number of changes that occurred in the branch (Hall, 2011).

In addition, the different phylogenetic relationships between organisms or sequences can be termed in three main ways. In general, two sequences that are descendants from a common ancestor are known as homologs. Orthologs, a type of homologous relationship, constitute two sequences from different species that evolved from a common ancestor sequence, normally retaining the same function as the ancestor. Paralogs, on the other hand, are a result of gene duplication within a genome, and they usually obtain new or different functions when compared to the ancestor (Hall, 2011). These terms will be used extensively throughout this thesis.

1.7. Goal of this thesis

The goal of this thesis is to determine the interactors of Rab32 that mediate its effects in mitochondrial membrane dynamics, and how Rab32 regulates the activity of its interactors. In addition, we want to determine if these interactions can be extrapolated to the other two members of the Rab32 family proteins, Rab38 and Rab29. Moreover, we also aim to elucidate the evolution of the Rab32 family across eukaryotic evolution and to determine which is the most ancient member of the family and when did the other members appear in time.

CHAPTER 2:

Materials and Methods

2. MATERIALS AND METHODS

2.1. MATERIALS AND REAGENTS

The materials, chemicals, and reagents used for this thesis were purchased from the indicated suppliers below and used according to the manufacturers' recommendations, unless otherwise stated.

Table 2.1. Chemicals and reagents

Chemical/Reagent	Source
10x PhosStop	Roche
25x Complete Protease Inhibitors	Roche
6x DNA Gel Loading Buffer	New England BioLabs
Acetic Acid	Fisher Scientific
Acetone	BDH Chemicals
Acrylamide (30%)	BioRad
Agarose (Ultrapure)	Invitrogen
Ammonium Chloride	Sigma
Ammonium Persulfate (APS)	BioRad
Ampicillin	Sigma
β -Mercaptoethanol	BioShop
Bovine Serum Albumin (BSA)	Sigma
Bromophenol Blue	BioRad
3-[(3-Cholamidopropyl) dimethylammonio]-1-propanesulfonate (CHAPS)	Sigma-Aldrich
Dimethyl Sulfoxide (DMSO)	Caledon
Dithiothreitol (DTT)	Fisher Scientific
Dithiobis Succinimidyl Propionate (DSP)	Thermo Scientific
100mM dNTPs set	Invitrogen
Dulbecco's Modified Eagle Medium (DMEM)	Gibco
Ethylene diamine tetraacetic acid (EDTA)	EMD
Ethylene glycol tetraacetic acid (EGTA)	OmniPur
Ethanol	Commercial Alcohols
Fetal Bovine Serum (FBS)	Gibco
Glucose	Fluka
Glycerol	BDH
Glycine	Fisher Scientific
4-(2-hydroxyethyl)-1-piperazieethanesulfonic acid (HEPES)	Sigma
Isopropanol	Fisher Scientific
Lipofectamine 2000	Invitrogen
Luria-Bertani (LB) Agar, Miller	BD Biosciences
Luria Broth Base, Miller	BD Biosciences
Magnesium Chloride (Molecular Biology purity)	Finnzymes
Magnesium Chloride	EM Science
Metafectene Pro	Biontex
Methanol	Fisher Chemicals

MitoTracker Red CMX Ros	Invitrogen
Nitrocellulose Trans-blot	BioRad
Nonyl phenoxypolyethoxyethanol (NP-40)	CalbioChem
Opti-MEM	Gibco
Paraformaldehyde (PFA)	Sigma
Dulbecco's Phosphate Buffered Saline (DPBS) 10X	Cellgro Mediatech, Inc.
Phosphate Buffer Saline with Calcium and Magnesium (PBS++) 10X	Cellgro Mediatech, Inc.
ProLong Antifade Resin (PLAF)	Invitrogen Molecular Probes
Protein A Sepharose (PAS) Beads CL-4B	GE Healthcare BioSciences
Saponin	Fluka
Sodium Acetate	EMD
Sodium Azide	ICN Biomedical Inc.
Sodium Bicarbonate	EMD
Sodium Carbonate	EMD
Sodium Chloride	Fisher Scientific
Sodium Deoxycholate	Sigma-Aldrich
Sodium Dodecyl Sulphate (SDS)	J.T. Baker
Sodium Hydroxide	BDH
Sucrose	EMD
SYBR® Safe	Invitrogen
Tetramethylethylenediamine (TEMED)	OmniPur/EMD
Tris	Bio Basic Inc.
Triton X-100	Sigma
Trypsin 2.5%	Gibco
UltraPure Water	Invitrogen

Table 2.2. Primary antibodies

Antibody	Source	Host	Antibody Clonality	Working Dilution	Application	Species Reactivity
Atlastin-2	Protein Tech Group	Rabbit	Polyclonal	1:1200	WB	H, Ms, R
Atlastin-3	Protein Tech Group	Rabbit	Polyclonal	1:1200	WB	H, Ms, R
Drp1 (Dnm1L)	Abcam	Mouse	Monoclonal	1:1000	WB	H, R
Dynamin-2	Millipore	Rabbit	Polyclonal	1:1000	WB	H
Flag	Rockland	Rabbit	Polyclonal	1:1000	WB	---
				1:100	IP, IF	
Flag	Rockland	Mouse	Monoclonal	1:1000	WB	---
Flag	Century Biochemicals	Rabbit	Polyclonal	1:1000	WB	---

GFP	Dr. Luc Berthiaume's Lab	Rabbit	Polyclonal	1:50,000	WB	---
HA	Covance	Mouse	Monoclonal	1:1000	WB	---
p115	Affinity Bio-Reagents	Rabbit	Polyclonal	1:100	IF	Ms, R
PDIA6	Abcam	Rabbit	Polyclonal	1:100	IF	H, Ms, R, Hm, X, Z
PDI	Thermo Scientific	Mouse	Monoclonal	1:5000	WB	H, Ms, R, Hm, P
Rab32	Dr. John Scott's Lab	Rabbit	Polyclonal	1:1000	WB	---
Rab38	Abnova	Mouse	Monoclonal	1:1000	WB	H
Rab38	Abcam	Rabbit	Polyclonal	1:1000	WB	H, M, R, Ch, C
Rab29 (Rab7L1)	GeneTex, Inc	Mouse	Monoclonal	1:1000	WB	H
Reticulon-4	Protein Tech Group	Rabbit	Polyclonal	1:1500	WB	H, Ms, R
Syntaxin-17	Sigma-Aldrich	Rabbit	Polyclonal	1:1000	WB	H

WB: Western Blot

IF: Immunofluorescence

IP: Immunoprecipitation

H: Human

Ms: Mouse

R: Rat

Ch: Chicken

C: Cow

Hm: Hamster

P: Pork

X: *Xaenopus laevis*

Mk: Monkey

Z: Zebrafish

D: Dog

A: Avian

2.3. Table of secondary antibodies

Antibody	Source	Host	Antibody Clonality	Working Dilution	Application
Alexa Fluor 750 anti-Rabbit	Invitrogen – Molecular Probes	Goat	Polyclonal	1:5000	WB
Alexa Fluor 680 anti-Mouse	Invitrogen – Molecular Probes	Goat	Polyclonal	1:5000	WB
Alexa Fluor 350 anti-Rabbit	Invitrogen – Molecular Probes	Goat	Polyclonal	1:500	IF
Alexa Fluor 488 anti-Mouse	Invitrogen – Molecular Probes	Goat	Polyclonal	1:500	IF

Alexa Fluor 488 anti-Rabbit	Invitrogen – Molecular Probes	Goat	Polyclonal	1:500	IF
Alexa Fluor 350 anti-Mouse	Invitrogen – Molecular Probes	Goat	Polyclonal	1:500	IF

WB: Western Blot

IF: Immunofluorescence

Table 2.4. Cell lines

Mammalian Cell Line	Source
Drp1 WT MEFS	Dr. Katsuyoshi Mihara, Japan
Drp1 KO MEFS	Dr. Katsuyoshi Mihara, Japan
HEK 293T	ATCC
HeLa	ECACC
Bacterial cells	Source
DH5 α <i>E. Coli</i>	Dr. Gary Eitzen, University of Alberta

Table 2.5. Molecular size standards

Molecular Size Standard	Source
O'GeneRuler 1Kb Plus DNA Ladder	Fermentas
Precision Plus Protein Dual Colour Standards	BioRad

Table 2.6. Multicomponent systems

Multicomponent system	Source
Phusion High Fidelity PCR Kit	Finnzymes
Platinum® Pfx DNA Polymerase	Invitrogen
QIAGEN Plasmid Midi Kit	QIAGEN
QIAQuick Gel Extraction Kit	QIAGEN

Table 2.7. Enzymes

Enzyme	Source
Restriction Endonucleases	Fermentas and New England BioLabs
T4 DNA ligase	Invitrogen

2.1.1 Common buffers and solutions

The buffers and solutions that were commonly used for the completion of this thesis, as well as their composition, are listed in the table below.

Table 2.8. Commonly used buffers and solutions

Buffer / Solution	Composition
1x TAE	40mM Tris, 20mM Acetic Acid, 1mM EDTA
4x Separating Buffer	1.5M Tris pH 8.8, 0.4% SDS
4x Stacking Buffer	0.5M Tris pH 6.8, 0.4% SDS
Carbonate Transfer	10mM NaHCO ₃ , 3mM Na ₂ CO ₃ , 20% Methanol

Buffer	
CHAPS Lysis Buffer	10mM Tris pH 7.4, 150mM NaCl, 1mM EDTA, 1% CHAPS
CoIp Buffer for Rabs	20mM HEPES pH 7.4, 150mM NaCl, 5mM MgCl ₂ , 1% NP-40
ER Tubulation Buffer	10mM MgCl ₂ , 10mM HEPES pH 7.4, 0.25M Sucrose
Gel Running Buffer	25mM Tris, 200mM Glycine, 0.1% SDS
IF Blocking Solution	1X DPBS, 2% BSA, 0.5% Saponin
IF Fixing Solution	1X DPBS, 4% Paraformaldehyde
IF Wash Solution	PBS++, 0.2% BSA, 0.1% Triton X-100
Laemli (Sample) Buffer	60mM Tris pH 6.8, 2% SDS, 10% Glycerol, 5% β-Mercaptoethanol, 0.01% Bromophenol Blue
Mild Lysis Buffer	20mM HEPES pH 7.0, 50mM NaCl, 1mM EDTA, 0.5mM EGTA, 10mM DTT, 1% Triton X-100
Miniprep Solution I	50mM glucose, 10mM EDTA, 25mM Tris pH 8.0
Miniprep Solution II	0.2N NaOH, 1% SDS
Miniprep Solution III	3M NaAc pH 5.0
Mitochondria Homogenization Buffer	250mM Sucrose, 10mM HEPES pH 7.4, 1mM EDTA
M-RIPA Lysis Buffer	1% NP-40, 0.25% deoxycholine, 150mM NaCl, 50mM Tris pH 7.4
Tris Buffered Saline-Triton X100 (TBS-T)	10mM Tris pH 8.0, 0.15M NaCl, 0.05% Triton X-100
Western Blocking Solution	1x DPBS, 2% BSA
Western Blot Antibody Solution	TBS-T, 2% Milk (Carnation, skim milk powder)

2.1.2. Plasmids and primers

The plasmid vectors used in this study are found in the table below, followed by tables of primers, their sequences, and the strategies used to generate mutations from the original constructs. In addition, Table 2.12 lists the siRNAs and shRNAs that were also used for the completion of this study.

Table 2.9. Plasmids

Plasmid Name	Tag	Vector	Bacterial Resistance	Promoter	Plasmid Type	Source
Rab32 WT	Flag	pcDNA ₃	Ampicillin	CMV	Mammalian Expression	Dr. John Scott's Lab
Rab32 Q85L	Flag	pcDNA ₃	Ampicillin	CMV	Mammalian Expression	Dr. John Scott's Lab
Rab32 T39N Flag	Flag	pcDNA ₃	Ampicillin	CMV	Mammalian Expression	Dr. John Scott's Lab
Rab32 T57N	Flag	pcDNA ₃	Ampicillin	CMV	Mammalian Expression	*

Rab38 WT	HA/Flag	pcDNA ₃	Ampicillin	CMV	Mammalian Expression	Dr. John Scott's Lab / *
Rab38 Q69L	Flag	pcDNA ₃	Ampicillin	CMV	Mammalian Expression	*
Rab38 T23N	Flag	pcDNA ₃	Ampicillin	CMV	Mammalian Expression	*
Rab29 WT	Flag	pcDNA ₃	Ampicillin	CMV	Mammalian Expression	Dr. John Scott's Lab
Rab29 Q67L	Flag	pcDNA ₃	Ampicillin	CMV	Mammalian Expression	Dr. John Scott's Lab
Rab29 T21N	Flag	pcDNA ₃	Ampicillin	CMV	Mammalian Expression	*
Rab33B WT	Flag	pcDNA ₃	Ampicillin	CMV	Mammalian Expression	Applied Biological Materials, Inc.
Rab33B Q92L	Flag	pcDNA ₃	Ampicillin	CMV	Mammalian Expression	*
Rab33B T47N	Flag	pcDNA ₃	Ampicillin	CMV	Mammalian Expression	*
Rab3D WT	Flag	pcDNA ₃	Ampicillin	CMV	Mammalian Expression	*
Drp1 WT	HA	pEGFP C1	Kanamycin	CMV	Mammalian Expression	Dr. Stephan Strack's Lab
Drp1 S656A	HA	pEGFP C1	Kanamycin	CMV	Mammalian Expression	Dr. Stephan Strack's Lab
Drp1 S656D	HA	pEGFP C1	Kanamycin	CMV	Mammalian Expression	Dr. Stephan Strack's Lab
RUTBC1 WT	GFP	pEGFP C1	Kanamycin	CMV	Mammalian Expression	Dr. Suzanne Pfeffer's Lab
RUTBC1 R803A	GFP	pEGFP C1	Kanamycin	CMV	Mammalian Expression	Dr. Suzanne Pfeffer's Lab
Evi-5 WT	Myc	pcDNA ₃	Ampicillin	CMV	Mammalian Expression	Gene Copoeia
LRRK2 WT	GFP	pAcGFP -C1	Kanamycin	CMV	Mammalian Expression	Addgene

LRRK2 G2019S	GFP	pcDNA- DEST53	Ampicillin	CMV	Mammalian Expression	Addgene
-----------------	-----	------------------	------------	-----	-------------------------	---------

* Mutant made as part of my project in the Simmen Lab.

Table 2.10. Primer combinations for the generation of DNA constructs

Construct	Primer Name		DNA template	Source	Restriction Endonucleases	Target Animal
	Forward	Reverse				
Rab38 WT Flag	TS367	TS386	Rab38 WT HA	Sigma-Aldrich	Acc65I and XhoI	Mammalian expression
Rab38 T23N Flag	T7	TS388	Rab38 WT Flag	Sigma-Aldrich	Acc65I and XhoI;	Mammalian expression
	TS387	Sp6		Sigma-Aldrich	Acc65I and XhoI;	Mammalian expression
Rab38 Q69L Flag	T7	TS390	Rab38 WT Flag	Sigma-Aldrich	Acc65I and XhoI; (XbaI)*	Mammalian expression
	TS389	Sp6		Sigma-Aldrich	Acc65I and XhoI; (XbaI)*	Mammalian expression
Rab29 T21N Flag	T7	TS407	Rab29 WT Flag	Sigma-Aldrich	Acc65I and XhoI; (SpeI)*	Mammalian expression
	TS406	Sp6		Sigma-Aldrich	Acc65I and XhoI; (SpeI)*	Mammalian expression
Rab32 T57N Flag	T7	TS457	Rab32 WT Flag	Sigma-Aldrich	Acc65I and XhoI; (Sall)*	Mammalian expression
	TS456	Sp6		Sigma-Aldrich	Acc65I and XhoI; (Sall)*	Mammalian expression
Rab3D WT Flag	TS468	TS469	Rab3D WT HA	Sigma-Aldrich	Acc65I and XhoI	Mammalian expression
Rab29 K157R Flag	T7	TS472	Rab29 WT Flag	Sigma-Aldrich	Acc65I and XhoI; (NruI)*	Mammalian expression
	TS471	Sp6		Sigma-Aldrich	Acc65I and XhoI; (NruI)*	Mammalian expression
Rab33B WT Flag	TS477	TS480	Rab33B WT		EcoRI and BamHI	Mammalian expression
Rab33B T47N Flag	TS477	TS478	Rab33B WT Flag	Sigma-Aldrich	EcoRI and BamHI (SnaBI)*	Mammalian expression
	TS479	TS480		Sigma-	EcoRI	Mammalian

				Aldrich	and BamHI (SnaBI)*	expression
Rab33B Q92L Flag	TS477	TS482	Rab33B WT Flag	Sigma- Aldrich	EcoRI and BamHI (XhoI)*	Mammalian expression
	TS481	TS480		Sigma- Aldrich	EcoRI and BamHI (XhoI)*	Mammalian expression

* Restriction endonuclease used to determine if the site directed mutation was successful.

Table 2.11. Primer sequences

Construct	Orientation	Primer	Nucleotide Sequence
Rab38 WT Flag	Forward	TS367	ATATCTCGAGCTAGGATTTGGCACAGC CAGAGCAGCTGGC
	Reverse	TS386	ATATGGTACCGCCAGGATGGACTACAA GGACGACGATGACAAGGGACAGGCCCC GCACAAGGAGCAC
Rab38 T23N Flag	Forward	TS387	GGGCGTGGGAAGAATTCTATCATCAA GCGCTAC
	Reverse	TS388	GTAGCGCTTGATGATAGAATTCTTCCCC ACGCC
Rab38 Q69L Flag	Forward	TS389	GATATCGCAGGTCTAGAAAGATTTGGA AAC
	Reverse	TS390	GTTTCAAATCTTTCTAGACCTGCGATA TC
Rab29 T21N Flag	Forward	TS406	GCAGTGGGCAAGAACTCACTAGTGCAG CGATATTCC
	Reverse	TS407	GGAATATCGCTGCACTAGTGAGTTCTTG CCCACTGC
Rab32 T57N Flag	Forward	TS456	CAGCACTACCGGGCCAACATCGGGGTC GACTT CGCCCTCAAG
	Reverse	TS457	CTTGAGGGCGAAGTCGACCCCGATGTT GGCCC GGTAGTGCTG
Rab3D WT Flag	Forward	TS468	ATATGGTACCGCCACCATGGACTACAA GGACGACGATGACAAGGGAGCATCAGC TGGAGACACCCAGGCAG
	Reverse	TS469	ATATCTCGAGCCATCTCTAGCAGCTGCA GCTGCTGGGC
Rab29 K157R Flag	Forward	TS471	GGTTGGACAGAAACATCAGTTCGCGAG AACAA AAATATTAATGAG
	Reverse	TS472	CTCATTAATATTTTTGTTCTCGCGAACT GATGTTTCTGTCCAACC
Rab33B WT Flag	Forward	TS477	ATATGGATCCGCCAGGATGGACTACAA GGACGACGATGACAAGGGAGCTGAGG

			AGATGGAGTCGTCG
	Reverse	TS480	ATATGAATTCTTAGCACCAGCACGTCAT TGCAGGCTTTGG
Rab33B T47N Flag	Forward	TS479	TCCAATGTGGGCAAGAATTGCCTTACG TACCGCTTCTGC
	Reverse	TS478	GCAGAAGCGGTACGTAAGGCAATTCTT GCCCACATTGGA
Rab33B Q92L Flag	Forward	TS481	TGGGACACAGCAGGACTCGAGCGATTC AGAAAGAGCATG
	Reverse	TS482	CATGCTCTTTCTGAATCGCTCGAGTCCT GCTGTGTCCCA

Table 2.12. siRNAs and shRNAs used in this study

Type	Name	ID	Source	Nucleotide Sequence	Target Animal
siRNA	RAB32 HSS116975	209983 B02	Invitrogen	CCGGAUGGU UUGAAACCU CUGCAA	Mammalian expression
siRNA	RAB32 HSS116975	209983 B03	Invitrogen	UUUGCAGAG GUUCAAAC CAUCCGG	Mammalian expression
siRNA	RAB32 HSS116976	209983 B04	Invitrogen	CCGGUCCU AGUGGAGAA AGAUUCU	Mammalian expression
siRNA	RAB32 HSS116976	209983 B05	Invitrogen	AAGAAUCUU CUCCACUAG GAACCGG	Mammalian expression
siRNA	RAB32 HSS174021	209983 B06	Invitrogen	GAAGUCCA CAUUUGAGG CAGUCUU	Mammalian expression
siRNA	RAB32 HSS174021	209983 B07	Invitrogen	AAGACUGCC UCAAUGUG GAACUUC	Mammalian expression
siRNA	RAB38 HSS119155	209983 B08	Invitrogen	GGAAGACCA GUAUCAUCA AGCGCUA	Mammalian expression
siRNA	RAB38 HSS119155	209983 B09	Invitrogen	UAGCGCUUG AUGAUACUG GUCUCC	Mammalian expression
siRNA	RAB38 HSS119156	209983 B10	Invitrogen	CCGAGAAGC UAUGGGUGC AUUUAU	Mammalian expression
siRNA	RAB38 HSS119156	209983 B11	Invitrogen	AAUAAAUGC ACCAUAGC UUCUCGG	Mammalian expression
siRNA	RAB38 HSS119157	209983 B12	Invitrogen	CCAAGUUA GUCUCCUA AUGGCAA	Mammalian expression
siRNA	RAB38	209983	Invitrogen	UUGCCAUA	Mammalian

	HSS119157	C01		GGGAGACUU AACUUGG	expression
siRNA	RAB7L1 HSS113226	209983 C02	Invitrogen	GGGACUACA UCAAUCUAC AAACCAA	Mammalian expression
siRNA	RAB7L1 HSS113226	209983 C03	Invitrogen	UUGGUUUGU AGAUUGAUG UAGUCCC	Mammalian expression
siRNA	RAB7L1 HSS189668	209983 C04	Invitrogen	CGAUAUUCC CAGGACAGC UUCAGCA	Mammalian expression
siRNA	RAB7L1 HSS189668	209983 C05	Invitrogen	UGCUGAAGC UGUCCUGGG AAUAUCG	Mammalian expression
siRNA	RAB7L1 HSS189669	209983 C06	Invitrogen	AAUUCACCA GAAGUAUUC AUGUCUU	Mammalian expression
siRNA	RAB7L1 HSS189669	209983 C07	Invitrogen	AAGACAUGA UAUCUUCUG UGGAAUU	Mammalian expression
shRNA	HSH018891- 1-CH1	REEP5-1	Gene Copoeia	CTGCAACCT GATAGGATT T	Mammalian expression
shRNA	HSH018891- 2-CH1	REEP5-2	Gene Copoeia	GGTCAAGGA CCTTAAAGA C	Mammalian expression
shRNA	HSH018891- 3-CH1	REEP5-3	Gene Copoeia	CCTACTGGA GCTTGATGTT	Mammalian expression
shRNA	HSH018891- 4-CH1	REEP5-4	Gene Copoeia	CAAAGCGGA GAAACATGT T	Mammalian expression
shRNA	HSH001118- 1-mH1	RAB32-1	Gene Copoeia	CCGCGAGCA CCTCTTCAAG	Mammalian expression
shRNA	HSH001118- 2-mH1	RAB32-2	Gene Copoeia	CCAGGTGGA CCAATTCTGC	Mammalian expression
shRNA	HSH001118- 3-mH1	RAB32-3	Gene Copoeia	GAAACCTCT GCAAAGGAT A	Mammalian expression
shRNA	HSH001118- 4-mH1	RAB32-4	Gene Copoeia	CCTAGTGGA GAAGATTCTT	Mammalian expression

2.1.3. Software and equipment

The software and equipment used throughout this study are listed in the tables below.

Table 2.13. Detection and analysis software

Software	Source
Odyssey Infrared Imaging System	LiCor

Ultraviolet Transilluminator (GelDoc)	Fisher Scientific
Axiovision 4 Acquisition Software	Zeiss
ImageJ Software	Rasband, W.S., ImageJ, U.S. National Institutes of Health, http://rsb.info.nih.gov/ij/

Table 2.14. Software used for comparative genomics and phylogenetic studies

Software	Source
BLASTp	NCBI; http://blast.ncbi.nlm.nih.gov/Blast.cgi
Coulson Plot Generator	(Field et al., 2013); http://sourceforge.net/projects/coulson/
FigTree v1.2	Rambaut, A.; http://tree.bio.ed.ac.uk/software/figtree/
MacClade 4.08	Maddison, D., and Maddison, W.; http://macclade.org/macclade.html
MUSCLE v3.6	(Edgar, 2004)
ProTest 1.3	(Abascal et al., 2005); http://darwin.uvigo.es
RAxML v2.2.3	(Stamatakis, 2006)
PhyML v2.4.4	(Guindon and Gascuel, 2003)
MR BAYES v3.1.2	(Ronquist and Huelsenbeck, 2003)

Table 2.15. Equipment

Equipment	Source
Microcentrifuge (room temperature)	Eppendorf
Microcentrifuge (4°C)	Eppendorf
Mastercycler PCR machine	Eppendorf
Ultracentrifuge	Beckman
Centrifuge (big 4°C)	Beckman
Li-Cor Scanner	Odyssey
Axiobserver Microscope	Zeiss
TLA 120.2 rotor	Beckman

2.2. METHODS

2.2.1. Mammalian cell culture techniques

2.2.1.1. Maintenance of Cell Lines

Cell cultures were maintained in Dulbecco's Modified Eagle Medium (DMEM, Table 2.1.) supplemented with 10% Fetal Bovine Serum (FBS, Table 2.1.). All cell lines were incubated at 37°C in an environment of 95% air and 5% CO₂. HEK 293T and HeLa cells were passaged twice per week, and WT and Drp1 KO MEFs were passaged 3 times per week, using Trypsin 2.5% to a maximum passage number of 45.

2.2.1.2. Experiment set up

Cell cultures were trypsinized (see above) and resuspended in 10mL DMEM + 10% FBS. After counting the cells using a hemacytometer, the desired amount of cells were resuspended in a specific volume of DMEM + 10% FBS, and then seeded in 6-well plates or 10cm dishes (depending on the conditions and cell concentration needed for each individual experiment), allowing them to become 80-90% confluent before starting the experiment.

2.2.1.3. Transient Transfection of Cell Lines

Cell cultures were transfected with exogenous DNA, siRNA or shRNA using two lipid based systems, Lipofectamine and Metafectene (see figure legends of individual experiments). The following morning after seeding the cells (see above), they were transfected using 7 and 10 μ L of Lipofectamine 2000 reagent and Metafectene Pro reagent (Table 2.1.), respectively, and 2 μ L of plasmid DNA, according to manufacturer's instructions; overexpression levels versus endogenous protein levels were in the order of 2-4 fold. The cell culture media was changed to fresh DMEM + 10% FBS after 4 hours of transfection, and plasmid expression was allowed to proceed for 16-72 hours (see figure legends of individual experiments) before harvesting and processing the cultures for various experiments. Note: Lipofectamine transfections were done using OptiMEM (Table 2.1.), and sterile 1X PBS for Metafectene reactions, according to manufacturer's instructions.

2.2.2. Basic Biochemical Techniques

2.2.2.1. Preparation of Whole Cell Lysates

Cells were harvested using cell scrapers (BD Falcon) and lysed using the desired lysis buffer (Table 2.8.) and 25X complete protease inhibitors to prevent protein degradation by proteases. After spinning down the nuclei at 800rpm at 4°C, Laemmli buffer was added to the samples and boiled for 10min.

2.2.2.2. Phosphorylation Assays

Cells were harvested as mentioned above, but 10X PhosStop reagent was included in the lysis buffer, which protects my proteins of interest from a broad range of phosphatases in the lysate and conserves their individual phosphorylation state.

2.2.2.3. Protein Precipitation

Proteins were precipitated using a 1:5 volume ratio of sample with 100% Acetone (Table 2.1.) and then incubated overnight at -20°C. The next morning, samples were spun down at 16,000 rpm at 4°C for 5 min and the pellets were resuspended using Laemmli buffer (Table 2.8.) and boiled for 10 min.

2.2.2.4. Sodium Dodecyl Sulfate-Polyacrylamide Gel Electrophoresis (SDS-PAGE)

Denatured samples were separated by the SDS-PAGE technique. Briefly, protein samples and standards were separated using a 4% stacking gel and a 8, 10, 12 or 15% separating gel, depending on the size of the protein or proteins of interest. The stacking buffer is composed of 125mM Tris pH 6.8, 0.1% SDS, 0.1% TEMED, and 0.2% APS, while the separating buffer contained 375mM Tris pH 8.8, 0.1% SDS, 0.1% TEMED, and 0.1% APS (Tables 2.1. and 2.8.). SDS-PAGE was done using the Mighty Small II gel running system (Amersham) under 150Volts for 60-80mins, depending on the gel percentage.

2.2.2.5. Western Blot

After separating the protein samples by SDS-PAGE, the gels were transferred onto a nitrocellulose membrane using a Mini Transblot Cell apparatus (BioRad) at 400mA for 2 hours at 4°C, in Carbonate Transfer Buffer (Table 2.8.). Then, the membrane was incubated in Western Blocking Solution (Table 2.8.) for 1 hr at room temperature. The membrane was later incubated with the Western Blot Antibody Solution (Table 2.8.), including the primary antibodies (Table 2.2.) and 0.04% sodium azide (Table 2.1.) to prevent contamination, either overnight at 4°C or 1 hr at room temperature, according to the specifications of each antibody. The next morning, the membrane was washed 3 times with TBS-T (Table 2.8.) for 5min each on a rocker at room temperature, and then incubated with Western Blot Antibody Solution containing the secondary antibodies for 1 hr (Table 2.3.). Lastly, the membranes were washed again (see above) and visualized using the Odyssey Infrared Scanner.

2.2.3. Cell Fractionation Technique

Approximately 10,000,000 HEK 293T cells were washed twice with chilled 1X PBS++ before being scraped from 10-cm dishes using 600 μ L of Mitochondria Homogenization Buffer (Table 2.8.) per dish and 25X Complete protease inhibitors. This cell suspension was passed 7-10 times through a syringe with a 18G x 1 ½ needle, for transfected and untreated cells, respectively. This homogenate was then spun down for 10 min at 800 rpm using a 4°C microcentrifuge (Table 2.15). The pelleted nuclei were discarded and the supernatant was centrifuged again at 10,000 rpm for 10 min in the same temperature conditions. The resulting pellet, called Heavy Membranes (HM), was resuspended using Laemmli Buffer and frozen at -86°C, while the supernatant was spun down using an ultracentrifuge in a TLA 120.2 rotor (Table 2.15) for 1 hr at 60,000 rpm at 4°C. The pellet, called Light Membranes (LM), was also resuspended in Laemmli Buffer and stored at -86°C. The protein supernatant was precipitated as mentioned above (section 2.2.2.3.).

2.2.4. Immunoprecipitation experiments

2.2.4.1. Immunoprecipitation of Flag- or HA-tagged proteins

For immunoprecipitation experiments, around 450,000 HEK 293T cells per mL of DMEM + 10% FBS were seeded in 6-well plates, allowing an expression time of 16-72 hrs after being transfected. On the day of the experiment, the cells were first washed twice with chilled PBS++ to prevent cell detachment and were then harvested after the addition of 150 μ L of lysis buffer to each well; the lysis buffer used depended on the proteins being pulled down (see figure legends of each individual experiment). The cell lysates were vortexed for 10 seconds and spun down at 4°C using a microcentrifuge at 800 rpm for 5 min. The pellet (nuclei) was discarded and the supernatant was incubated with 20 μ L of Protein A Sepharose (PAS) beads (Table 2.1.) for 1 hr in a 4°C rocker. The samples were then centrifuged for 1min at 800rpm and 4°C. 25 μ L of the supernatant was set aside with 25 μ L of Laemmli Buffer to be frozen at -86°C and used as loading control; the remaining supernatant was incubated overnight with 5 μ L of anti-Flag or anti-HA antibodies (Table 2.2.) in a 4°C rocker. The next morning, 25 μ L of PAS beads was added to the samples, allowing another hour of incubation in the 4°C rocker. After washing the samples 3 times with 400 μ L of lysis buffer (the same used at the beginning of the

experiment), 25 μ L of Laemmli Buffer was added to the pelleted beads and boiled for 10 min.

2.2.4.2. Protein Crosslinking

Cells were washed twice with room temperature 1X PBS++. After preparing the exact volume of 200mM stock of DSP in DMSO, the 2mM working solution was made by suspending the stock in room temperature 1X DPBS, including 25X protease inhibitors (1mL per well of a 6-well plate). Since DSP hydrolyses rapidly in water, cells were incubated immediately with this solution for 30min at room temperature. After washing the cultures 3 times with 1mL of 10mM NH₄Cl in PBS++ to quench the crosslinking reaction, cells were lysed as mentioned above for immunoprecipitation experiments.

2.2.5. Immunofluorescence experiments

2.2.5.1. Preparation of slides and data acquisition

250,000 cells/mL of DMEM + 10% FBS were seeded in glass coverslips in 6-well plates and incubated overnight at 37°C. The next day, 2 μ L of MitoTracker (Table 2.1.) was carefully added to the wells by lifting the plate to a 45° angle and slowly releasing the volume near the bottom of the well, allowing it to dilute in the media and being very careful not to let it be in direct contact with the cells. After gently mixing the plate a few times, it was incubated for 20-30 min at 37°C. The laboratory lights were turned off and the plate was covered with aluminum foil and carried to the bench. The cells were first washed 3 times with 1X DPBS and then incubated with 2mL IF fixing solution (Table 2.8.) per well at room temperature for 20min. After, the cells were incubated with 2mL IF washing solution (Table 2.8.) for 1-2 min, washed twice with 1X PBS++, and incubated with IF blocking solution. The primary antibody solution was prepared in IF blocking solution and a drop (approximately 30 μ L) of it per well was deposited in a wet chamber consisting of wet Whatman paper and parafilm on top. The coverslip was then placed “cells down” onto the primary antibody solution drop and incubated for 1 hour at room temperature; the chamber was covered with aluminum foil during all incubation periods.

5min before the primary incubation was over, the secondary antibody solution was prepared (Table 2.8.), also in IF blocking solution. The coverslips were removed

from the wet chamber and placed “cells up” in their corresponding well in the 6-well plate and were washed with 1X PBS++ twice. The used parafilm was removed from the chamber and replaced with a new piece, containing a drop of secondary antibody solution. The coverslips were placed again “cells down” in the wet chamber and incubated for 30 min at room temperature. Glass slides were labeled and a drop of mounting PLAF resin (Table 2.1.) was added on top; normally two separate drops were deposited per slide, accommodating two separate coverslips. The coverslips were washed again two times as mentioned above and placed “cells down” on top of the resin. The slides are allowed to dry overnight or for at least 1 hr inside a drawer on the bench before being analyzed using an Axioobserver Microscope and AxioCam digital camera.

NOTE: If the cells required transient expression of a plasmid, they were transfected (see above) the very next day after being seeded in glass coverslips and the protocol was executed on the third day.

2.2.5.2. Image quantification

To quantify alteration of the mitochondria phenotype in four different cell types (untransfected control cells, and cells expressing Flag-Rab32 T29N, Flag-Rab38 T23N, and Flag-Rab29 T21N), an ImageJ algorithm previously published by us and our colleagues was used (Bravo et al., 2011). Briefly, images were acquired on an Axioobserver Microscope using an AxioCam digital camera. Then, every cell was manually delineated, determining the cell’s outline, and the center of the nucleus of each cell was manually indicated. Next, the total fluorescence intensity was concentrically measured by the algorithm (quantifying fluorescence intensity per pixel) starting at the previously chosen center of the nucleus. Finally, pixel distances were then converted into micrometers to determine the distance of the peak fluorescence from the center of the nucleus for each cell type. The average distances of the peak fluorescences from the center of the nucleus were graphed as the percentage relative to control untransfected cells.

2.2.6. Molecular Biology Techniques

2.2.6.1. Simple Polymerase Chain Reaction (PCR)

This technique was used to generate some of the constructs used in this project and was performed following the instructions of the Phusion High Fidelity PCR kit

(Table 2.6.) and using a Mastercycler PCR machine (Table 2.15.). All primers were custom designed and synthesized by Sigma Genosys. The primers and enzyme combination used to generate each individual construct are summarized in Table 2.10.

2.2.6.2. PCR-based splicing by overlap extension

This was the technique that was used to generate the great majority of the mutant constructs used in this study. For the case of site directed mutagenesis, internal primers carrying the mutation and an engineered restriction site were used to perform an initial PCR reaction along with their corresponding outside primers (primarily the commercially available primers T7 (forward) and SP6 (reverse), creating overlapping complementary sequences (products). A sequential PCR reaction using these products and the outside primers was then performed, generating the whole gene carrying the mutation. A list of inside and outside primers as well as DNA templates' combinations is provided in Table 2.10.

For example, to create the Rab32 T57N Flag mutant, separate reactions containing the forward outside primer T7 paired with the internal primer TS457 carrying the mutation, and the reverse outside primer SP6 paired with the internal primer TS456 (also carrying the mutation), both using Rab32 WT Flag as the DNA template. The products of each individual reaction were then used as template for the following single PCR reaction, using the outside primers T7 and SP6, generating a whole Rab32 T57N Flag mutant.

2.2.6.3. Separation of DNA fragments by agarose gel electrophoresis

A 1.5% agarose gel was prepared using 1X TAE buffer containing 1X SYBR Safe (Table 2.1.) and submerged in an apparatus containing 1X TAE buffer. The final products of the PCR reactions were mixed with 6X DNA loading buffer (Table 2.8.), loaded into the gel, and then electrophorized at 100V for 30-40 min. The DNA was visualized using an ultraviolet transilluminator and a digital camera (Table 2.13).

2.2.6.4. DNA extraction from agarose gel

The DNA fragments of interest were excised from the gel using a razor blade and purified using a QIAQuick Gel Extraction Kit (Table 2.6) following the handbook instructions.

2.2.6.5. Restriction Digest

Restriction digest was performed, both to introduce a WT/mutated gene inside a vector or to check if the mutation (performed by PCR-based splicing by overlap extension) was successful. In both cases, the restriction endonucleases were used according to manufacturer's instructions, and incubated at 37°C for at least 1 hr up to 1.5 hrs. When preparing PCR products for ligation the vector pcDNA₃ was used in all cases.

2.2.6.6. DNA ligation

The DNA inserts prepared above were ligated into a pcDNA₃ vector using the T4 DNA ligase and the buffer provided by the manufacturer (Table 2.7.). The ratio of vector to insert varied between 1:10 to 1:50, including an empty control. The ligation was allowed to proceed overnight at room temperature.

2.2.6.7. Bacterial Transformation

-86°C stored competent DH5α *E. coli* bacteria were used for this protocol. First, bacteria were thawed on ice. Next, 100μL of thawed bacteria (Table 2.4.) were incubated on ice for 20min with 1μL of DNA or 5μL of ligation product. Bacteria were then heat-shocked for 45s in a 45°C water bath and mixed with 1mL of sterile LB broth, prepared according to manufacturer's instructions, was added. In the case of DNA, bacteria were then pelleted down using a microcentrifuge (Table 2.15.) for 30s at maximum speed, resuspended in 100μL of LB, and plated onto LB agar containing the appropriate antibiotic. In the case of ligation product, the heat-shocked bacteria resuspended in 1mL of LB were allowed a recovery period of 1 hr at 37°C in a rotary shaker at 200 rpm; bacteria were then pelleted and treated as mentioned above. Finally, the LB agar plates were incubated overnight at 37°C.

2.2.6.8. Bacterial Culture

Colonies of DH5α *E. coli* containing the DNA or ligation product were picked and grown in 50 or 2mL of LB, respectively, with the appropriate antibiotic overnight at 37°C in a 220 rpm rotary shaker. The next day, the 50mL cultures were pelleted down and either stored frozen at -20°C for a short period of time or at -87°C for a long period, or submitted to DNA isolation protocol (see below). For the case of the 2mL ligation products cultures, the tubes were placed at room temperature the next day, and in the

evening were transferred to 50mL of LB with the appropriate antibiotic. These cultures were treated as mentioned above.

2.2.6.9. Isolation of plasmid DNA from bacteria

2.2.6.9.1. Midiprep protocol

The QIAGEN Plasmid Midiprep Kit (Table 2.6.) was used to isolate plasmid DNA from 50mL bacterial cultures, according to the manufacturer's instructions.

2.2.6.9.2. Miniprep protocol

For the case of 2mL cultures, bacteria was transferred to 1.5mL Eppendorf tubes and pelleted down using a room temperature Microcentrifuge for 30 seconds at maximum speed. The supernatants were discarded, and the bacterial pellets were resuspended by vortexing with 100µL of ice cold Miniprep Solution I (Table 2.8.) until obtaining a uniform suspension. Next, 200µL of Miniprep Solution II was added and mixed by inverting the tube 4 times. 150µL of Miniprep Solution III were then added and mixed by vortexing for 10s. The tubes were centrifuged for 30s at room temperature at maximum speed and the supernatants were transferred to new Eppendorf tubes and re-centrifuged in the same conditions. After transferring the supernatants to new Eppendorf tubes, the DNA was precipitated with 1mL of 100% ethanol (Table 2.1.) and washed once with 80% ethanol. Finally, the tubes were allowed to dry at room temperature for 10-15 min, the DNA was dissolved in 40µL of UltraPure water (Table 2.1.), and analyzed by restriction digestion as mentioned above.

After visualizing the DNA in an agarose gel (see above), the cultures exhibiting positive colonies were selected and what was left of the tubes containing the 2mL cultures was transferred to 50mL LB with the proper antibiotic and grown overnight at 37°C in a 220 rpm rotary shaker. These cultures were submitted to the Midiprep protocol as mentioned above.

2.2.6.10. DNA Sequencing

Constructs were sent to be sequenced either by the Molecular Biology Facility in the Department of Biological Sciences or The Applied Genomics Centre in the Department of Medicine, both in the University of Alberta, using the BigDye Terminator v3.1 cycle sequencing kit.

2.2.7. Comparative genomics and phylogenetic studies

2.2.7.1. Homology searching

Candidate Rab32 family proteins' sequences were identified in representative lineages of the major eukaryotic supergroups using the BLAST (Basic Local Alignment Search Tool) algorithm for proteins (BLASTp). Genome sequences were obtained by the databases of the National Centre for Biotechnology Information (NCBI), the Joint Genomes Institute (JGI), Origins of Multicellularity of the Broad Institute, and individual genome projects (see Appendix Table 7.1 and 7.2). Protein sequences for *Schyliorhinus canicula* were translated manually using the software Sequencher v4.9.

For the BLASTp searches conducted in NCBI, the nr-database was restricted to the organism in question, thus being careful not to overlap with other organisms included in the analysis. The BLASTp searches conducted in the JGI database were also restricted to the genome data set of each individual organism.

Sequences identified with an E-value <0.05 were considered candidate homologous sequences, and were validated by a variation of the RBH method described in (Schlacht et al., 2013). Briefly, a candidate sequence is considered homologous when a reciprocal BLASTp search retrieves the query as the best scoring hit. Then, to confidentially assign a candidate sequence to a specific family member, it had to retrieve the initial query with E-values at least two or five-orders of magnitude smaller than the next best scoring hit, creating a less or more stringent classification, respectively. It is important to state that, since the Rab domain is present in all Rab proteins, the initial cut-off E-value of 0.05 was identifying a lot of Rab proteins outside the Rab32 family. So, after getting all the homologous sequences of the Rab32 family members in each individual BLASTp search, the next 5 sequences with the smallest E-value were verified with reciprocal BLASTp searches to confirm they were not members of our family of interest.

2.2.7.2. Homology visualization

When the homology search was finished, all the positive and negative hits were visualized using the Coulson Plot Generator, and manually fixed using Adobe Illustrator.

2.2.7.3. *Phylogenetic analysis*

After collecting and classifying all the homologous protein sequences throughout the eukaryotic supergroups, they were first aligned using MUSCLE v3.6 (Edgar, 2004) in Hydra and Fugu interface, and then manually adjusting the alignment using MacClade v4.08. Briefly, a mask layer was created and all highly homologous or conserved or slightly conserved domains were included, and highly divergent portions of the sequences were deleted. Next, ProtTest 1.3 (Abascal et al., 2005) was used for model testing with a Gamma rate distribution.

Trees were built using two maximum likelihood methods, RAxML v2.2.3 (Stamatakis, 2006) and PhyML v2.4.4 (Guindon and Gascuel, 2003), and a Bayesian inference method, MrBayes v3.1.2 (Ronquist and Huelsenbeck, 2003). Maximum likelihood methods search for a tree with high probability of observing the data under a proposed model of evolution. Bayesian inference, on the other hand, produces a set of trees with approximately similar likelihoods and then evaluates the posterior probabilities and identifies the tree with maximum probability given the data and model of evolution (Hall, 2011). For MrBayes trees, 30 000 000 Markov Chain Monte Carlo generations were used with a stop rule of <0.01 average standard deviation of split frequencies; the burn-in value was determined in a graph manner using Excel, removing usually the first 25% of the trees preceding the plateau. Maximum-likelihood bootstrap values were obtained using PhyML and Phylip 3.66 for RAxML trees, with 100 pseudoreplicates.

Trees were visualized using FigTree v1.2 and adjusted using Adobe Illustrator. After a few trials, highly divergent sequence, as well as persistent long branches, were removed, since they often lead to the attraction of not closely-related sequences and their incorrect positioning in the tree; this phenomenon is called long-branch attraction (LBA) and it occurs because fast-evolving sequences accumulate mutations or changes that converge and attract other highly divergent sequences, as well as very different species with high phylogenetic distances between them (Dacks and Doolittle, 2001; Philippe et al., 2005).

CHAPTER 3:

Rab32 family interactors alter mitochondrial membrane dynamics

3. Rab32 family interactors alter mitochondrial membrane dynamics

3.1 Rationale

The ER and mitochondria are highly dynamic organelles that constantly change shape through fission and fusion events, and it is the balance between these processes that dictates their overall morphology. In 2011, Friedman and Voeltz showed that the ER is involved in determining mitochondrial morphology. In this study, ER tubules were shown to wrap around mitochondria creating an initial constriction of the energy organelle. This is followed by Drp1 recruitment and oligomerization around these constriction sites, which ultimately leads to mitochondrial division (Friedman et al., 2011).

Initial studies from our laboratory reported that the inactive GDP-bound form of Rab32 causes mitochondria to collapse around the nucleus (Bui et al., 2010), confirming the same observations published by the Scott group (Alto et al., 2002). For this reason, we hypothesized that the interactors that mediate the downstream effect of this Rab are proteins that affect the balance between mitochondrial fusion and fission events, known as mitochondrial membrane dynamics. Since the ER is also involved in regulating mitochondrial morphology, we decided to expand our attention to proteins involved in the machineries that regulate the morphology of both organelles. Moreover, Rab32 belongs to a family of proteins including Rab38 and Rab29 (Elias et al., 2012). Hence, we wanted to know if because they belong to the same family and may share similar functions, the inactive form of these proteins also caused a similar mitochondrial phenotype. Therefore, a potential Rab32-effector interaction might also be extrapolated to the other two members of the Rab32 family.

3.2 Results

3.2.1. Drp1 as a Rab32 effector

It is well known that the localization of an effector protein can be determined by its interaction with its Rab (Grosshans et al., 2006). Drp1 is known as one master regulator of mitochondrial division. This dynamin-related protein has been shown to be recruited to mitochondria, and after its homo-oligomerization around this organelle, it ultimately constricts mitochondria (Smirnova et al., 2001). In 2010, our lab published that the normal cellular distribution of Drp1 is altered in the presence of Rab32 (Bui et al., 2010). Briefly, post-nuclear supernatants of HEK 293T cells were submitted to a series of centrifugations that allows the separation of low-speed heavy membranes and high-speed

light membranes, which contain mitochondria and ER/microsomes, respectively, from cytosol. In this experiment, Drp1 is normally enriched in light membranes, with lower signal in the cytosol and heavy membranes; however, overexpression of Rab32 WT and T39N (Rab32 inactive GTP-binding deficient mutant) caused a shift of Drp1 from light membranes (ER) to heavy membranes (mitochondria), while constitutively active Rab32 (Q85L GTPase inactive mutant) did not show any apparent changes in its distribution (Bui et al., 2010). This suggested that Rab32 activity modulates the distribution of Drp1.

Moreover, this study also reported that, in addition to modulating the localization of Drp1, Rab32 also regulates Drp1 activity. The activity of Drp1 can be regulated by many post-translational modifications, including phosphorylation (Chang and Blackstone, 2010). Drp1's inactivation through phosphorylation on serine 656 by PKA shifts the balance of mitochondrial membrane dynamics towards enhanced fusion and mitochondrial elongation, while dephosphorylation of this serine residue by the phosphatase calcineurin activates Drp1, and results in increased mitochondrial division (Cribbs and Strack, 2007; Chang and Blackstone, 2007). Since Rab32 acts as an AKAP recruiting PKA to mitochondria (Alto et al., 2002), our lab wanted to know if Rab32 might also be affecting Drp1's activity through phosphorylation by this kinase. Indeed, overexpression of Rab32 WT and T39N Flag-tagged mutants increased Drp1's phosphorylation levels on this serine residue 2- and 2.5-fold, respectively (Bui et al., 2010). This suggested that the activity of Rab32 can modulate Drp1 activity through phosphorylation, and that this inactivation ultimately alters Drp1 subcellular localization.

Since overexpression of inactive Rab32 alters the mitochondrial phenotype, and Rab32 modulates the activity and localization of Drp1, Drp1 constituted a potential candidate to act as an effector of Rab32.

3.2.1.1. Endogenous and active Drp1 bind to Rab32

In order for Drp1 to act as an effector of Rab32, the proteins need to interact physically. To test whether there was a physical interaction between Rab32 and Drp1, we did co-immunoprecipitation assays using HEK 293T cells, for their ease of transfection. Briefly, these cells were transfected with Flag-tagged WT Rab32 and were allowed 48 hours of expression. After a cross-linking period, cells were lysed and analyzed for co-immunoprecipitation of the Flag-tagged proteins, and then visualized by SDS-PAGE and Western blot. Compared to control untransfected cells, endogenous Drp1 co-

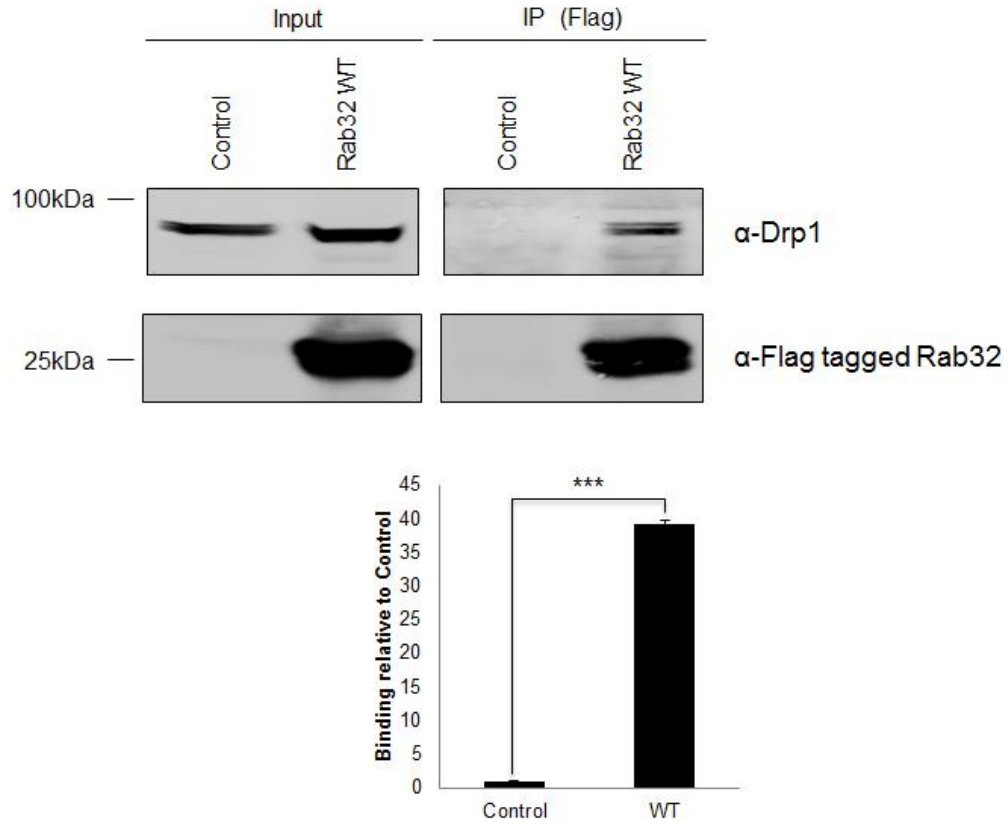


Figure 3.1. Endogenous Drp1 interacts with WT Rab32. HEK 293T cells were transfected with Flag-tagged Rab32 WT using Lipofectamine 2000, and were allowed 48 hours of expression. On the day of the experiment, the cells were cross-linked for 30min and then processed for co-immunoprecipitation analysis using M-RIPA buffer and anti-Flag antibodies; the samples were then analyzed by SDS-PAGE and Western blot with anti-Drp1 and anti-Flag monoclonal antibodies. This co-immunoprecipitation assay shows an interaction between endogenous Drp1 and WT Flag-tagged Rab32. The graph shows the average results for 4 independent experiments; *** stands for $p=0.0001$.

immunoprecipitated with Flag-tagged WT Rab32 ($p=0.0001$), as seen in Figure 3.1. This suggested that indeed there is a physical interaction between Drp1 and Rab32.

Next, to determine the meaning of this interaction, we used two Drp1 mutant constructs kindly provided by Dr. Stefan Strack (Iowa, USA): one constitutively active Drp1 HA-tagged mutant that cannot be phosphorylated, as it harbors a serine to alanine mutation in aminoacid 656 (Drp1 S656A), and an inactive pseudo-phosphorylated HA-tagged mutant harboring a serine to aspartic acid in the same aminoacid position (Drp1 S656D) (Merrill et al., 2011). First, Flag-tagged WT Rab32 was co-expressed in HEK 293T cells with both the active and inactive Drp1 HA-tagged mutants (S656A and S656D, respectively). Figure 3.2A shows that WT Rab32 binds predominantly with active Drp1. Then, to confirm the specificity of this interaction, we performed the reverse co-immunoprecipitation analysis co-expressing HEK 293T cells with WT Rab32 and active and inactive HA-tagged Drp1 constructs, but using anti-HA antibodies. This experiment also showed a higher amount of Rab32 WT being pulled-down with the active S656A mutant than with the inactive Drp1 mutant (Figure 3.2B). Lastly, it is well known that a good way to test whether a protein acts as an effector for a Rab protein, it should preferentially interact with the active form of the Rab (Grosshans et al., 2006). Hence, to determine if Drp1 showed a preference for active over inactive Rab32, HEK 293T cells were co-transfected with Drp1 S656A and both Rab32 Q85L and T39N mutants; as expected, there was a higher interaction between the active Rab32 Q85L mutant and active Drp1 (Figure 3.3), confirming our initial suspicions that the Rab32-Drp1 interaction might be Rab-effector in nature.

These three experiments suggest that Drp1 might be acting as an effector of Rab32, since we were able to detect a physical interaction between Rab32 and Drp1 that occurs preferentially between active Drp1 and active Rab32.

3.2.1.2. Knockout of Drp1 and inactivation of Rab32 by its GAP protein confirms that Drp1 acts as a Rab32 effector

To confirm our results from different angles, we used two different approaches. First, we used a Drp1 knockout mouse embryonic fibroblast cell line (Drp1 KO MEFs), kindly provided by Dr. Katsuyoshi Mihara (Japan) to analyze their mitochondrial phenotype. As expected, and as published before (Ishihara et al., 2009), these cells

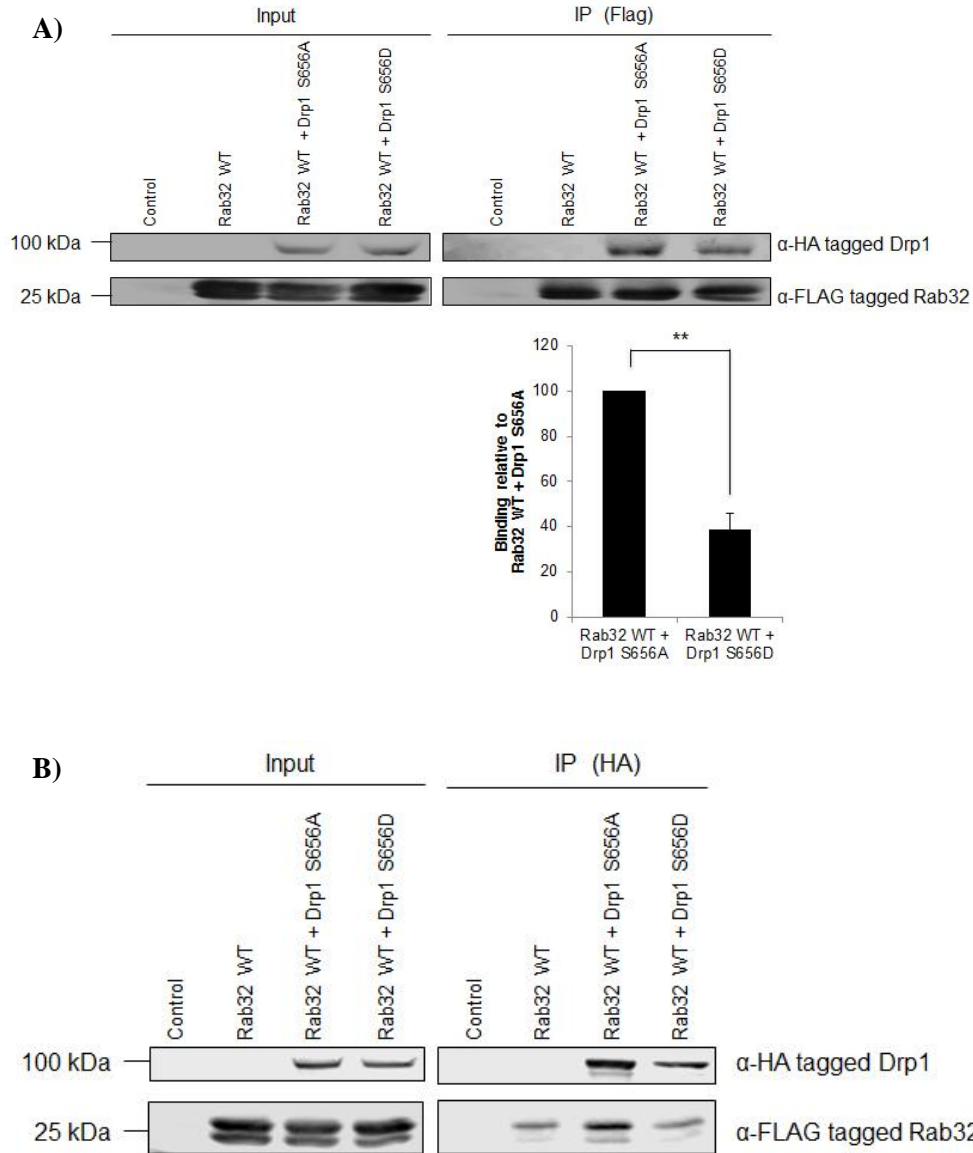


Figure 3.2. Rab32 preferentially interacts with active Drp1. HEK 293T cells were co-transfected with Flag-tagged Rab32 WT and active HA-tagged Drp1 S656A construct using Lipofectamine 2000, and were allowed 48 hours of expression. On the day of the experiment, the cells were cross-linked for 30min and then processed for co-immunoprecipitation analysis using M-RIPA buffer and anti-Flag antibodies in **A)** and HA-antibodies in **B)**; the samples were then analyzed by SDS-PAGE and Western blot with anti-HA and anti-Flag monoclonal antibodies. This co-immunoprecipitation assay shows a stronger interaction between WT Rab32 and active HA-tagged Drp1 S656A. The graph in **A)** represents the average result for 3 independent experiments; ** stands for $p=0.0018$.

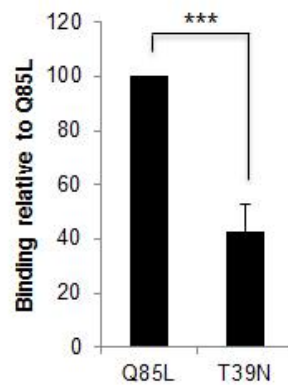
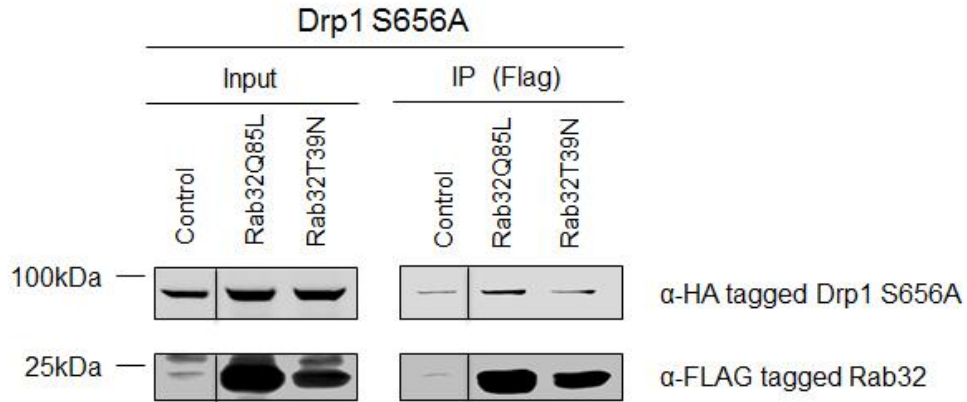


Figure 3.3. Active Drp1 preferentially interacts with active Rab32. HEK 293T cells were co-transfected with Flag-tagged Rab32 Q85L and T39N constructs and active HA-tagged Drp1 S656A construct using Lipofectamine 2000, and were allowed 48 hours of expression. On the day of the experiment, the cells were cross-linked for 30min and then processed for co-immunoprecipitation analysis using M-RIPA buffer and anti-Flag antibodies; the samples were then analyzed by SDS-PAGE and Western blot with anti-HA and anti-Flag monoclonal antibodies. This co-immunoprecipitation assay shows a stronger interaction between active Drp1 and active Flag-tagged Rab32 Q85L, suggesting Drp1 might be acting as an effector for Rab32. The graph represents the average result for 4 independent experiments; *** stands for $p=0.0002$.

exhibited clusters of mitochondria in the perinuclear region, similar to the effect seen when the inactive Rab32 mutant is being expressed (Figure 3.4). This suggests that Drp1 mediates the downstream effects of active Rab32, because the absence of its effector simulates the effect seen when Rab32 is inactive.

We then took advantage of the fact that the activity of a Rab protein is regulated by its GAP. As mentioned before, Rab GAPs accelerate the rate at which GTP hydrolysis takes place, and thus they promote Rab inactivation. In 2011, such a protein was identified for Rab32. In this study, a protein called RUTBC1 was found to increase several orders of magnitude the GAP-catalyzed GTP hydrolysis of Rab32 and another Rab known as Rab33B (Nottingham et al., 2011). RUTBC1 contains a RUN domain that has been reported to interact with Ras-like GTPases, and a TBC domain responsible for the GAP activity of the protein, as described earlier in the Introduction. Since RUTBC1 activity would, in principle, enhance inactivation of Rab32, we sought to investigate the effect it would have in the Rab32-Drp1 interaction. HEK 293T cells were co-transfected with Flag-tagged Rab32 WT and GFP-tagged WT RUTBC1, construct kindly provided by Dr. Suzanne Pfeffer (Stanford, California). Consistent with RUTBC1 acting as a GAP for Rab32, RUTBC1 overexpression resulted in a decreased interaction (about 60% from Rab32 WT alone) between Drp1 and Rab32, confirming that Drp1 preferentially binds to active Rab32 (Figure 3.5).

Altogether, these experiments reiterate that Drp1 acts as an effector of Rab32, since the depletion of the effector protein resembles the effect seen with inactive Rab32, and inactivation of Rab32 through its GAP decreases its interaction with Drp1.

3.2.2. Other Rab32 interactors

Besides Drp1, there are other proteins that also regulate ER and mitochondrial morphology. Therefore, we sought to identify if there were other protein interactors, within the protein machineries that dictate the overall morphology of these two organelles. The morphology of the ER is mainly regulated by two families of proteins, atlastins and reticulons. Atlastins participate in generating three-way junctions within the ER reticular network by promoting tubule branching by fusing neighboring tubules. Reticulons, on the other hand, are a family of GTPases that are involved in the formation of the tubular ER; they are transmembrane proteins located in the outer face of the ER membrane and create a wedge-induced curvature, giving rise to the tubular network of the

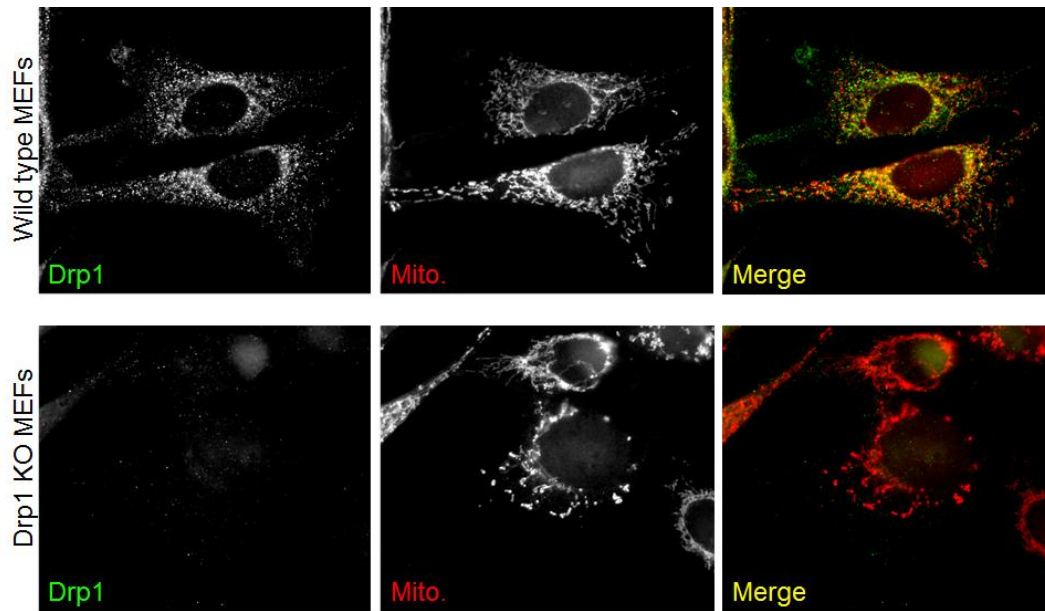


Figure 3.4. Drp1 knockout MEFs resemble dominant-negative Rab32's mitochondrial phenotype. Drp1 WT and KO MEFs were seeded in coverslips 24hrs before being fixed using 4% PFA and processed for immunofluorescence analysis; MitoTracker was used to visualize mitochondria (red) and mouse anti-Drp1 antibodies (green) to detect Drp1 knockout. Knockout of Drp1 results in the aggregation of mitochondria in the perinuclear region of the cell, similar to the effect of dominant-negative Rab32 expression.

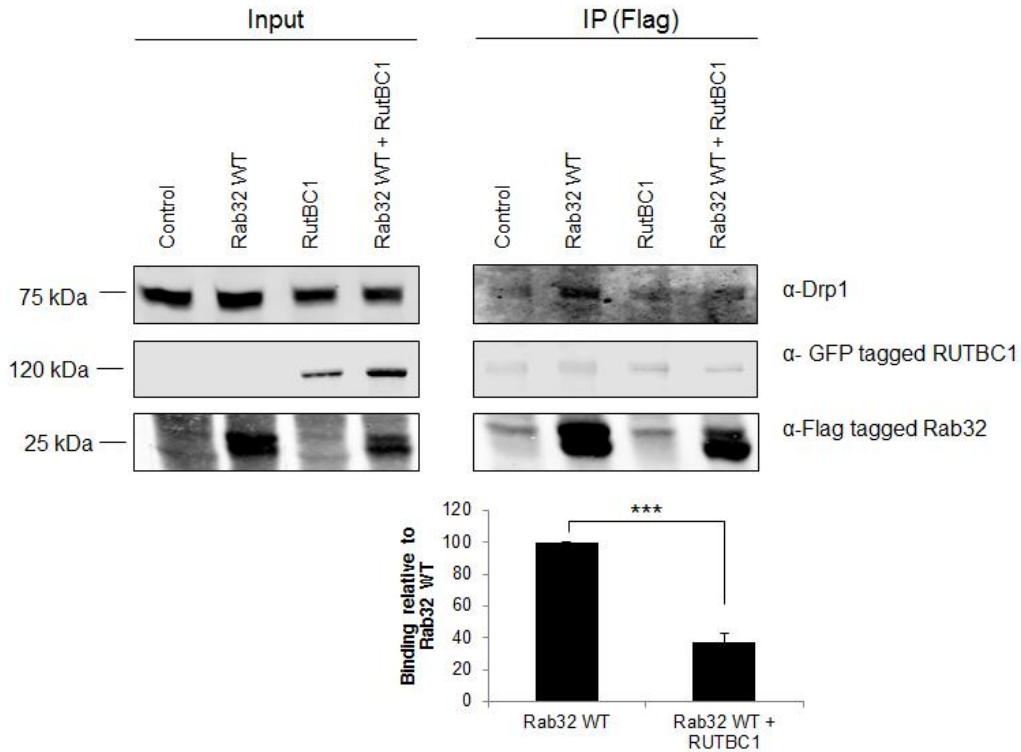


Figure 3.5. Rab32's GAP, RUTBC1, decreases its interaction with Drp1. HEK 293T cells were co-transfected with Flag-tagged Rab32 WT and GFP-tagged RUTBC1 constructs using Metafectene and were allowed 24 hours of expression. On the day of the experiment, the cells were cross-linked for 30min and then processed for co-immunoprecipitation analysis using CoIp buffer and anti-Flag antibodies; the samples were then analyzed by SDS-PAGE and Western blot for endogenous Drp1 (monoclonal), GFP (polyclonal), and Flag (polyclonal). This co-immunoprecipitation assay confirms that Drp1 might be acting as an effector of the Rab32 protein, since its inactivation by RUTBC1 decreases its interaction with this GTPase. The graph represents the results of 3 independent experiments; *** stands for $p=0.0006$.

ER (Park and Blackstone, 2010). Since both families regulate ER network formation, they were interesting candidates for possible interacting proteins participating in the regulation of the activity of Rab32.

3.2.2.1. Rab32 interacts with reticulons and atlastins

We decided to test whether Rab32 interacted with atlastins and reticulon by co-immunoprecipitation assays. These experiments were carried out using transiently transfected 293T cells with Flag-tagged Rab32 WT, Rab32 Q85L and Rab32 T39N. Since atlastin-1 is mostly expressed in the brain and atlastin-2 and -3 are ubiquitously expressed (Rismanchi et al., 2008), we focused our attention in the latter two. After analyzing the samples through SDS-PAGE and Western blot, we were able to identify atlastin-2 as an interacting protein (Figure 3.6). WT Rab32 showed the highest interaction with the ER-shaping protein atlastin-2, whereas the dominant-negative T39N and the dominant-active mutant Q85L showed a lower level of interaction. Unfortunately, however, we were unable to determine an interaction between atlastin-3 and Rab32 WT and any of its mutants, since the primary antibody used for this preliminary experiment failed to detect atlastin-3 even in the loading control lanes. Thus, this experiment should be repeated with different antibodies to conclude if this interaction is specific to atlastin-2 or if it is also positive for atlastin-3.

Next, we searched for an interaction with the most well-known reticulon protein, reticulon-4. Similar preliminary studies using our co-immunoprecipitation technique revealed an interaction between Rab32 and this protein (Figure 3.7). Like atlastin-2, reticulon-4 showed a strong interaction with WT Rab32, but very weak interaction with both active and inactive Rab32. This suggests that there is a physical interaction between Rab32 and the ER-shaping proteins. However, more experiments are needed to confirm these interactions and to determine its GTP/GDP specificity. As well, more experiments will be required to determine if there is an interaction with the other proteins of the atlastin and reticulon families, and how they regulate the activity of Rab32.

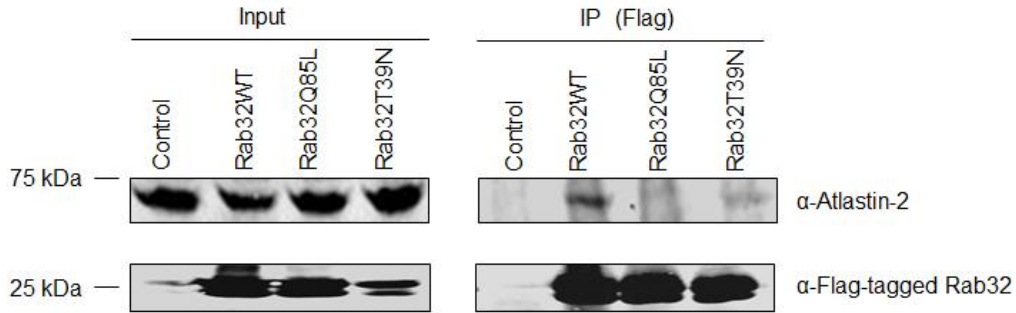


Figure 3.6. Rab32 interacts with atlastin-2. HEK 293T cells were co-transfected with Flag-tagged Rab32 WT and GFP-tagged RUTBC1 constructs using Lipofectamine 2000 and were allowed 24 hours of expression. On the day of the experiment, the cells were cross-linked for 30min and then processed for co-immunoprecipitation analysis using CoIp buffer and anti-Flag antibodies; the samples were then analyzed by SDS-PAGE and Western blot for atlastin-2 (polyclonal) and Flag (monoclonal). This co-immunoprecipitation assay shows that WT Rab32 interacts stronger with atlastin-2, than with active and inactive Rab32.

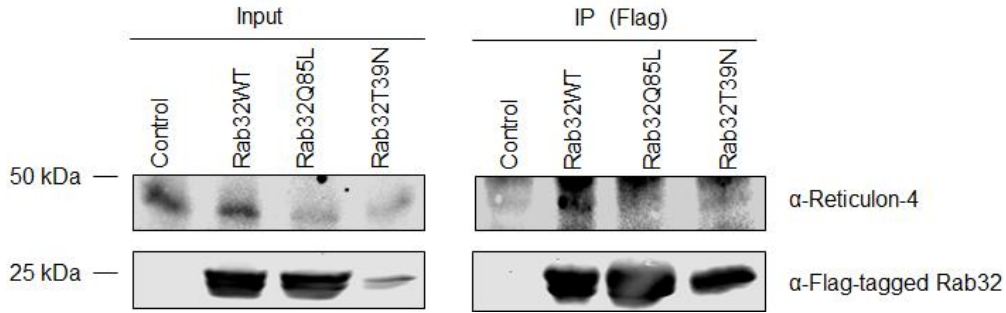


Figure 3.7. Rab32 WT interacts with reticulon-4. HEK 293T cells were co-transfected with Flag-tagged Rab32 WT and GFP-tagged RUTBC1 constructs using Lipofectamine 2000 and were allowed 24 hours of expression. On the day of the experiment, the cells were cross-linked for 30min and then processed for co-immunoprecipitation analysis using CoIp buffer and anti-Flag antibodies; the samples were then analyzed by SDS-PAGE and Western blot for reticulon-4 (polyclonal) and Flag (monoclonal). This co-immunoprecipitation assay shows that WT Rab32 interacts with reticulon-4.

3.2.3. Rab32 family proteins

3.2.3.1. Subcellular distribution of the Rab32 family proteins

Evolutionary studies showed that Rab32 belongs to a family of proteins including Rab38 and Rab29 (Elias et al., 2012). Rab32 and Rab38 have been previously shown to be present in melanosomes of cells that contain those organelles (Wasmeier et al., 2006). However, cells that do not have melanosomes also express Rab32 and Rab38, suggesting they might have different roles in cells that lack these organelles. Similarly, not much is known about the subcellular distribution and function of Rab29 in general. However, because these proteins are related and may have similar functions, they might be found in similar subcellular compartments as Rab32. Hence, we wanted to determine the cellular localization of Rab38 and Rab29 in cells that lack melanosomes using two different approaches: immunofluorescence and subcellular fractionation, using HeLa and HEK293T cells, respectively. As seen in Figure 3.8A, Rab38 shows a nice spread out distribution across the cell and a co-localization with both the ER marker PDI and mitochondria (MitoTracker); this is very similar to what our lab had published before for Rab32 (Bui et al., 2010). However, this was not seen with Rab29, as it rather exhibited a more specific and localized distribution close to the nucleus and its staining pattern co-localized with the Golgi marker p115, which targets ER-derived vesicles to the Golgi (Cao et al., 1998b). This suggests that the function performed by Rab32 and Rab38 might be more similar between them than to that performed by Rab29.

Furthermore, to determine a more specific cellular localization of Rab38 and Rab29 and confirm if Rab38 and Rab29's distribution were more or less similar to that of Rab32, respectively, we used a subcellular fractionation technique with which our lab has expertise; this technique allows the separation of low-speed heavy membranes (containing mitochondria), high-speed light membranes (containing ER/microsomes and Golgi), and cytosol (Bui et al., 2010; Gilady et al., 2010; Myhill et al., 2008). This experiment revealed a similar pattern for the distribution of Rab32 and Rab38, being present proportionally in all fractions, but moderately enriched in the heavy membranes (Figure 3.8B). Rab29, however, was mostly enriched in the light membranes, as expected for Golgi-enriched proteins (Gilady et al., 2010; Myhill et al., 2008). This reiterates that the function performed by Rab29 might be different from the function of Rab32 and Rab38.

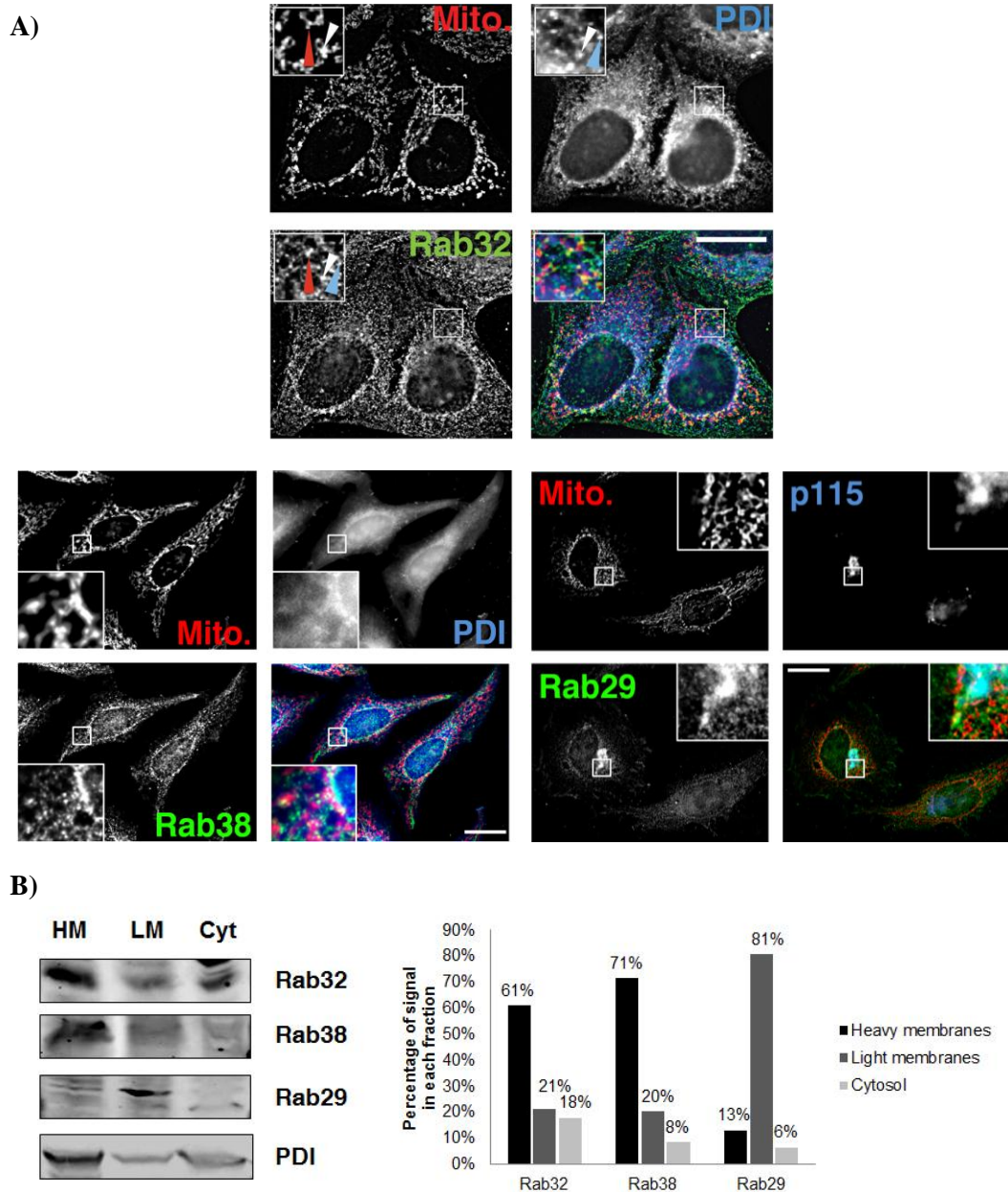


Figure 3.8. Subcellular distribution of the Rab32 family proteins. A) HeLa cells were seeded in coverslips 24hrs before being fixed using 4% PFA and processed for immunofluorescence; MitoTracker was used to visualize mitochondria (red); rabbit anti-Rab32 and anti-Rab38, and mouse anti-Rab29 antibodies (green) were used to visualize the endogenous distribution of the Rab32 family proteins; mouse anti-PDI and anti-p115 antibodies (blue) were used as ER and Golgi markers, respectively. Rab32's panel has been published previously by our lab (Bui et al., 2010). Scale bars: 25 μ m. **B)** HEK 293T cells were processed for subcellular fractionation analysis, separating heavy membranes (HM) from light membranes (LM) and cytosol. Samples were then analyzed by SDS-PAGE and Western blot for endogenous Rab32, Rab38, and Rab29 distribution; PDI was used as a marker of the integrity of the fractions. The graph shows the quantification of the Rab signal in each fraction.

3.2.3.2. Rab32 family proteins alter mitochondria morphology

Rab32 has been reported to cause the aggregation of mitochondria in the perinuclear region when its inactive GDP-bound form is overexpressed (Alto et al., 2002). Therefore, we wanted to test if the other members of the family, Rab38 and Rab29, had a similar effect on mitochondria morphology. First, we overexpressed in HeLa cells grown in coverslips the inactive Flag-tagged mutants of the three Rabs (Rab32 T39N, Rab38 T23N, and Rab29 T21N), and after 24 hours of transfection, they were fixed and stained for immunofluorescence analysis. Figure 3.9 shows that all inactive Rab32 family members cause an alteration in the mitochondria morphology to a similar extent.

We then wanted to know which of the three members of the family, if any, showed a stronger effect on the mitochondrial network. For this purpose, 50 cells per condition (untransfected control, and the inactive mutants Rab32 T39N, Rab38 T23N, and Rab29 T21N) were counted manually, separating cells with normal mitochondria phenotype (where the mitochondrial network is seen nicely spread out throughout the cell), from cells with altered mitochondria phenotype (where there was a disrupted network of mitochondria, including their clustering in the perinuclear region and mitochondria that have altered morphology). This analysis showed that the stronger effect seen on the mitochondria phenotype was with Rab32, and in minor degree with Rab38 and Rab29 (Figure 3.10A).

In addition, these same cells were then analyzed using an ImageJ algorithm previously published together with our collaborators in Chile (Bravo et al., 2011), that allows the radial quantification of the fluorescence intensity of mitochondria, starting from the nucleus towards the plasma membrane (see Materials and Methods section 2.2.5.2.). Figure 3.10B shows that there is a statistically significant reduction of 15% of the distance of the peak fluorescence from the center of the nucleus between control untransfected cells and all three inactive mutants; however, this method of quantification could not identify a significant difference between the distance of peak fluorescence intensities of the three Rab subfamily members.

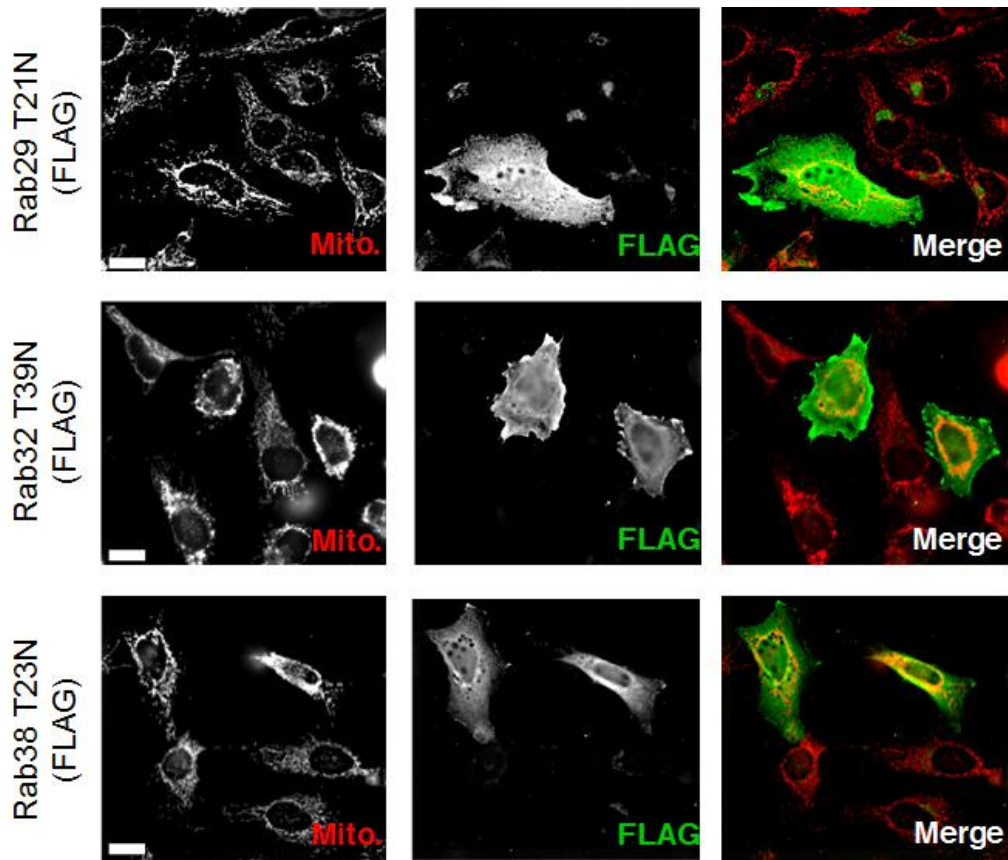
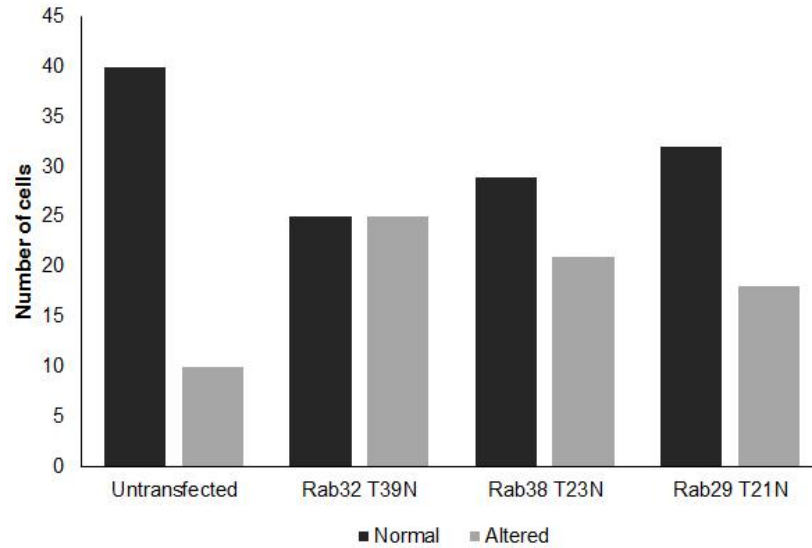


Figure 3.9. Inactive Rab32 family proteins disrupt the mitochondrial network. HeLa cells were seeded in coverslips 24hrs before being transiently transfected with Flag-tagged Rab32 T39N, Rab38 T23N, and Rab29 T21N. The cells were fixed using 4% PFA and processed for immunofluorescence; MitoTracker was used to visualize mitochondria (red), and mouse anti-Flag antibodies (green) to visualize transfected cells. This figure shows that all inactive Rab32 family proteins alter the mitochondria phenotype.

A)



B)

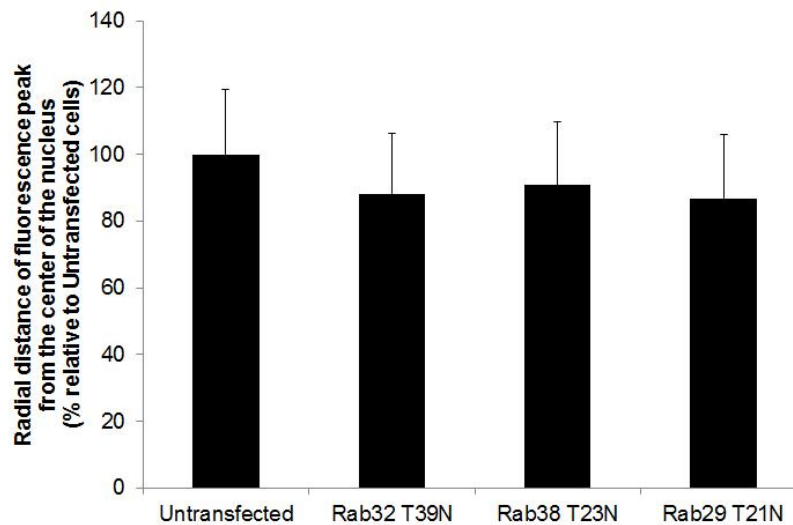


Figure 3.10. Inactive Rab32 family proteins alter the normal mitochondrial network phenotype. **A)** HeLa cells were seeded in coverslips 24hrs before being transiently transfected with Flag-tagged Rab32 T39N, Rab38 T23N, and Rab29 T21N. The cells were fixed using 4% PFA and processed for immunofluorescence; MitoTracker was used to visualize mitochondria (red), and mouse anti-Flag antibodies (green) to visualize transfected cells. 50 cells per condition were counted manually and separated between cells with a normal mitochondrial network spread out throughout the cell, or altered mitochondrial phenotype, which could be seen as clusters in the perinuclear region or disruption of the mitochondrial network. **B)** This graph shows the radial distance of the fluorescence peak from the center of the nucleus (50 cells per condition), represented as percentages relative to untransfected cells (see Materials and Methods section 2.2.5.2).

It is important to note, however, that this measurement differs from the one above in that the manual count was done taking into account the morphology of mitochondria, which the automated ImageJ algorithm could not do. Therefore, there are additional differences in the mitochondria phenotype observed within these inactive mutants for which measuring their fluorescence intensities are not accounted.

3.2.3.3. Rab38 and Rab29 also interact with Drp1

Since Rab38 and 29 also displayed an altered mitochondrial phenotype when their inactive forms were overexpressed, we wanted to investigate if they also interacted with Drp1 as Rab32, and whether this interaction explained the alteration of the mitochondrial phenotype with their inactive mutants. Although they are not AKAP's, and thus cannot bind and recruit PKA (Alto et al., 2002), they might share the sequence important for Rab32 to interact with Drp1, allowing Rab38 and 29 to interact with this protein as well. For this purpose, we repeated our co-immunoprecipitation assays using HEK 293T cells; these cells were first transiently transfected with Flag-tagged WT Rab38 and WT Rab29, then were lysed and analyzed for co-immunoprecipitation of the Flag-tagged proteins, and finally visualized by SDS-PAGE and Western blot. These experiments demonstrated that both family members also co-immunoprecipitate Drp1 (Figure 3.11A and B). This interaction was also confirmed with the reciprocal co-immunoprecipitation performed with HA-tag antibodies on HEK 293T cells with co-transfected Flag-tagged WT Rab38 and 29, and either the active or inactive Drp1 mutants. Like Rab32, Rab38 and 29 showed a higher interaction with the active S656A mutant than with inactive S656D Drp1 (Figure 3.12A and B), suggesting that Drp1 needs to be preferentially active to interact with all three family members.

These co-immunoprecipitation experiments, as well as the experiments done before for Rab32, were quantified and compared to see which showed the stronger interaction with Drp1. As seen in Figure 3.13, even though all Rab32 family members interact with Drp1, Rab32 seems to be the stronger interactor. This is in accordance with our finding that Rab32 shows the stronger effect in the alteration of the mitochondrial network phenotype.

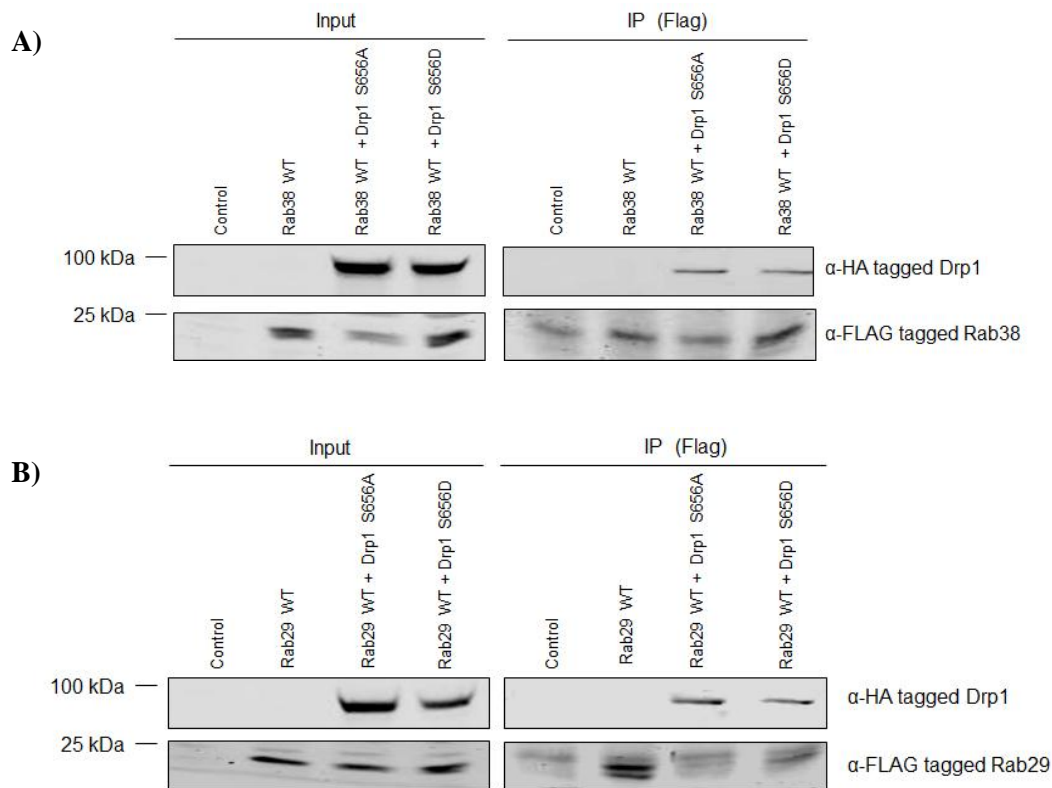


Figure 3.11. Rab38 and Rab29 preferentially interact with active Drp1. **A)** HEK 293T cells were co-transfected with Flag-tagged Rab38 WT and active and inactive HA-tagged Drp1 S656A and S656D constructs, respectively, using Lipofectamine 2000, and were allowed 48 hours of expression. On the day of the experiment, the cells were cross-linked for 30min and then processed for co-immunoprecipitation analysis using M-RIPA buffer and anti-Flag antibodies; the samples were then analyzed by SDS-PAGE and Western blot. This co-immunoprecipitation assay shows a slight preference in the interaction between WT Rab38 and active HA-tagged Drp1. **B)** HEK 293T cells were co-transfected with Flag-tagged Rab29 WT and active and inactive HA-tagged Drp1 S656A and S656D constructs, respectively, using Lipofectamine 2000, and were allowed 48 hours of expression; then they were then treated as in A). This co-immunoprecipitation assay shows a slight preference in the interaction between WT Rab29 and active HA-tagged Drp1 as well.

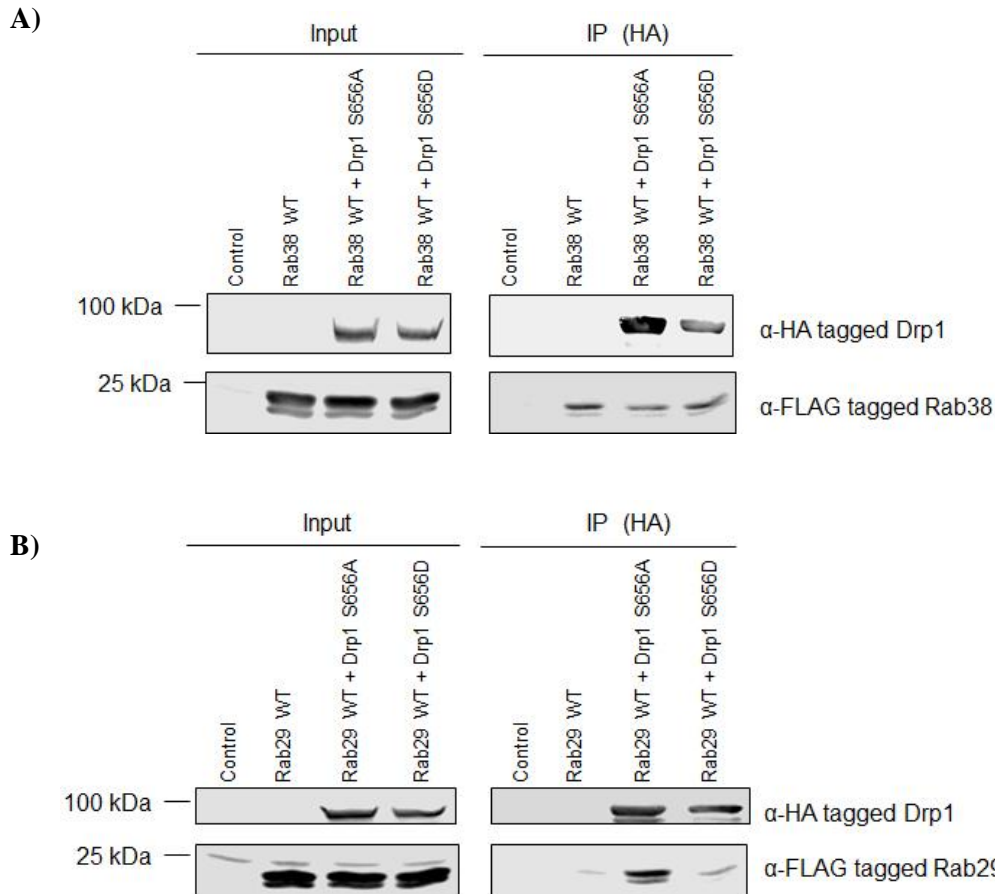


Figure 3.12. Rab38 and Rab29 preferentially interact with active Drp1. **A)** HEK 293T cells were co-transfected with Flag-tagged Rab38 WT and active and inactive HA-tagged Drp1 S656A and S656D, respectively using Lipofectamine 2000, and were allowed 48 hours of expression. On the day of the experiment, the cells were cross-linked for 30min and then processed for co-immunoprecipitation analysis using M-RIPA buffer and anti-HA antibodies; the samples were then analyzed by SDS-PAGE and Western blot with anti-HA and anti-Flag antibodies. This co-immunoprecipitation assay shows a slight preference in the interaction between active HA-tagged Drp1 and Rab38 WT. **B)** HEK 293T cells were co-transfected with Flag-tagged Rab29 WT and active and inactive HA-tagged Drp1 constructs using Lipofectamine 2000, and were allowed 48 hours of expression; they were then treated as A). This co-immunoprecipitation assay shows a slight preference in the interaction between active Drp1 and Rab29 WT.

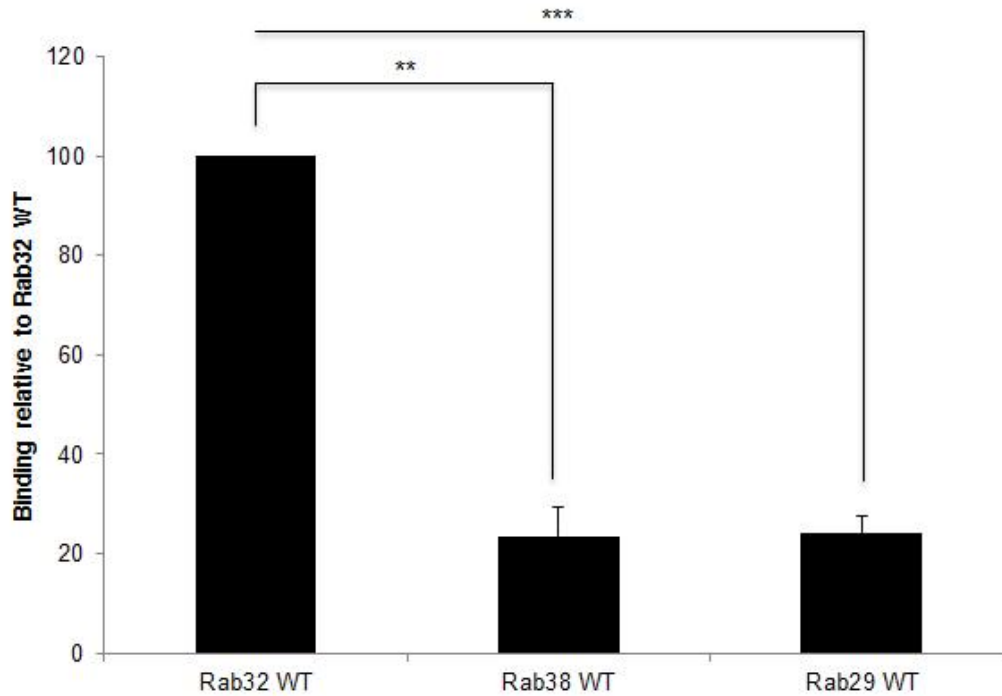


Figure 3.13. Rab32 is the strongest Drp1 interactor of the Rab32 family proteins. HEK 293T cells were transfected with Flag-tagged Rab32, Rab38, and Rab29 WT constructs using Metafectene and allowed to be expressed for 48 hours. On the day of the experiment, the cells were cross-linked for 30min and then processed for co-immunoprecipitation analysis using CoIp buffer and anti-Flag antibodies; the samples were then analyzed by SDS-PAGE and Western blot with anti-Drp1 and anti-Flag antibodies. The graph represents the average result of 3 independent experiments per Rab analyzed; *** stands for $p=0.0035$; ** stands for $p=0.0121$.

3.2.3.4. Absence of Drp1 alters the distribution of the Rab32 family proteins

It is well known that the correct localization of effectors ultimately determines the distribution of Rabs by the specificity of their interaction in a GTP-dependent manner (Grosshans et al., 2006). Hence, we used Drp1 knockout (KO) cells to determine if the absence of the effector protein would alter the distribution of the Rab32 family proteins. Post-nuclear supernatants of Drp1 WT and KO cells were analyzed by our subcellular fractionation technique, separating heavy membranes from light membranes. As expected, Figure 3.14 shows how the distribution of Rab32 and Rab38 shifts from heavy membranes to light membranes in Drp1 KO cells; Rab29, however, shows almost no effect in its distribution. This is in accordance with the fact that Rab29 showed a weaker interaction with Drp1 in comparison with Rab32 and Rab38, and thus its distribution is not that much affected with the absence of Drp1.

3.2.3.5. Rab32 family proteins interact with dynamin-2

In this thesis we identified that Rab32 interacts stronger with Drp1 than the other two members of the family. However, we wanted to determine if this interaction was specific to Drp1 or if other dynamin-related proteins could also interact with the Rab32 family proteins. Drp1, as its name states, belongs to the dynamin family of proteins. Dynamin is a 100kDa protein that is mainly involved in the formation of vesicles from the plasma membrane during endocytosis (Herskovits et al., 1993; Vallee et al., 1993). Since the mechanism by which Drp1 severs mitochondria is similar to the process by which dynamin functions, we wanted to know if the sequence similarity between these two proteins was enough for Rab32 family proteins to interact with dynamin as well. While Drp1 is ubiquitously expressed (Smirnova et al., 1998), dynamin is encoded by three genes in mammals: while dynamin-1 is brain specific, dynamin-2 is ubiquitously expressed, and dynamin-3 is expressed mainly in brain, testis, and lung (Cook et al., 1996; Obar et al., 1990; Sontag et al., 1994). Thus, we decided to use dynamin-2 as a general representative of this family for our co-immunoprecipitation studies. Again, HEK 293T cells were transfected with WT Rab32, Rab38, and Rab29, and analyzed by co-immunoprecipitation. As seen in Figure 3.15, the Rab32 family proteins all interact with dynamin-2 with diverse intensities. The strongest interaction was seen with Rab29, whereas Rab32 and 38 showed an equally weaker interaction. So, even though they all

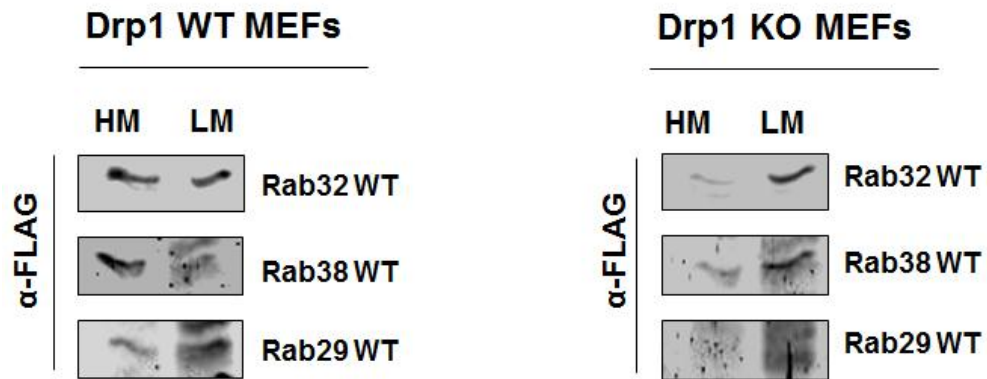


Figure 3.14. Drp1 knockout alters the distribution of the Rab32 family proteins. Drp1 wild-type and knockout mouse embryonic fibroblasts were transfected with Flag-tagged Rab32, Rab38, and Rab29 WT constructs using Metafectene and allowed to be expressed for 24 hours. Cells were then processed for subcellular fractionation analysis, separating heavy membranes (HM) from light membranes (LM). Samples were then analyzed by SDS-PAGE and Western blot for Flag. This experiment showed that the distribution of the Rab32 family proteins is altered when its effector Drp1 is absent.

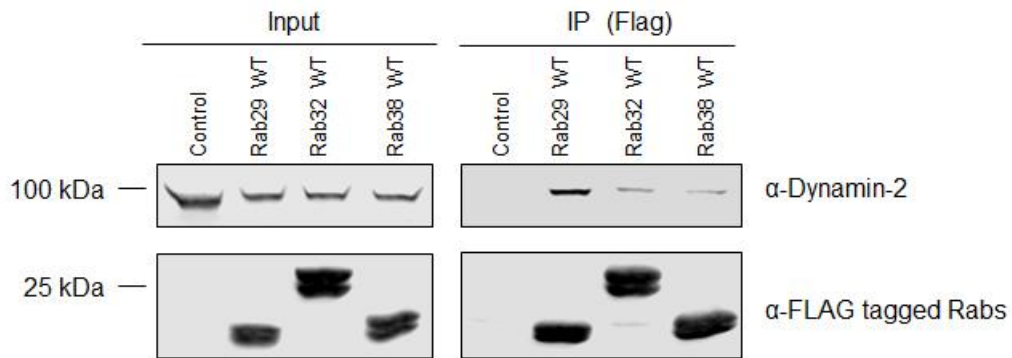


Figure 3.15. Rab29 interacts stronger with dynamin-2. HEK 293T cells were transfected with Flag-tagged Rab32, Rab38, and Rab29 WT using Metafectene and were allowed 24 hours of expression. On the day of the experiment, the cells were cross-linked for 30min and then processed for co-immunoprecipitation analysis using CoIp buffer and anti-Flag antibodies; the samples were then analyzed by SDS-PAGE and Western blot for dynamin-2 and Flag. This co-immunoprecipitation assay shows that Rab29 is the main interactor of dynamin-2 from the Rab32 family proteins.

interact with dynamin-2 albeit to different extent, they do not show the same pattern as in their Drp1 interaction.

This suggests that the differences between the sequences of Drp1 and dynamin-2 allow them to have different affinities for each of the Rab32 family proteins: Drp1 binding stronger to Rab32 but weaker to Rab38 and 29, and dynamin-2 interacting stronger to Rab29 than to Rab38 and Rab32. This encourages the idea that the Rab32 family proteins harbor sequence similarities that allows them to interact with dynamin-related proteins.

3.2.4 Rab32 interacts with the SNARE syntaxin-17

After finding the exciting Rab32 family-Drp1 interaction, we continued our search for more Rab32 family interactors. SNARE proteins have been found to interact directly with Rab proteins or indirectly with Rab effectors to perform their function in membrane fusion (Grote and Novick, 1999; Hutagalung and Novick, 2011; Lupashin and Waters, 1997). Interestingly, this year, a SNARE protein known as syntaxin-17 was shown to localize at ER-mitochondria contact sites upon autophagy activation by induced starvation (Hamasaki et al., 2013). These findings made this protein very interesting to us, since Rab32 is both found to be enriched in the MAM and to participate in autophagy as well (Bui et al., 2010; Hirota and Tanaka, 2009).

Syntaxin-17 is a Qa-SNARE that was initially found to be localized generally to the ER by immunofluorescence (Steggmaier et al., 1998), but it was later found to be enriched in the smooth domains of the ER using cryoimmunogold electron microscopy (Steggmaier et al., 2000). Moreover, this SNARE was demonstrated to play an important role in maintaining the normal morphology of the ERGIC and the Golgi, as its deletion causes the disintegration of the first one and the fragmentation of the latter (Muppirala et al., 2011). In 2012, syntaxin-17 was identified to localize to the outer membrane only of mature autophagosomes, where it interacts with the R-SNARE VAMP8 in the endosome/lysosome, as well as with the Qbc-SNARE SNAP-29, in complex to mediate the fusion between these two organelles (Itakura et al., 2012).

To determine if Rab32 and syntaxin-17 interacted physically, we returned to our initial co-immunoprecipitation assays. These experiments revealed that indeed, Flag-tagged Rab32 WT pulled down syntaxin-17 (Figure 3.16). In addition, these experiments also included the expression of Flag-tagged WT Rab38 and Rab29; however, Rab29

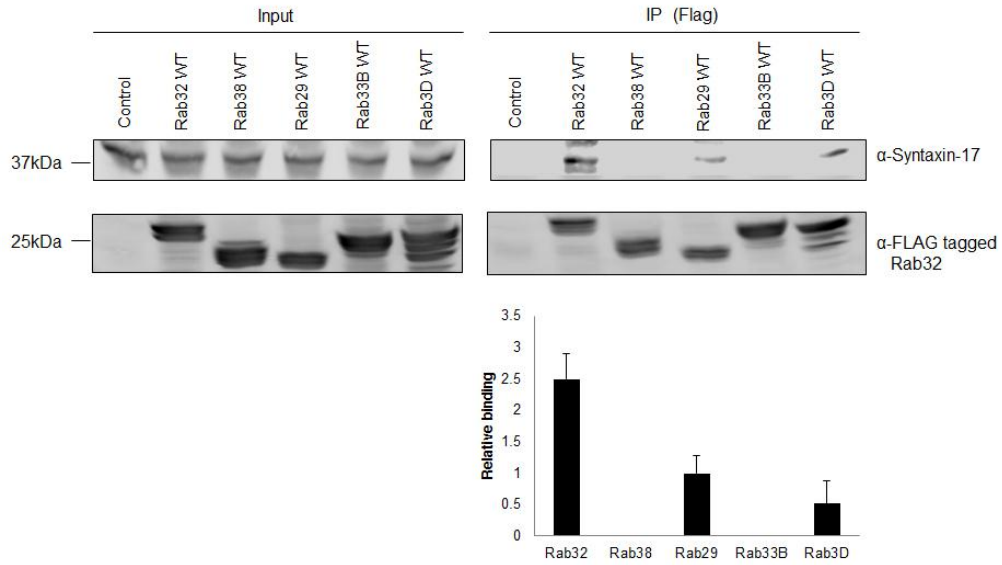


Figure 3.16. Rab32 interacts with syntaxin-17. HEK 293T cells were co-transfected with Flag-tagged Rab32 WT and GFP-tagged RUTBC1 constructs using Metafectene and were allowed 24 hours of expression. On the day of the experiment, the cells were cross-linked for 30min and then processed for co-immunoprecipitation analysis using CoIp buffer and anti-Flag antibodies; the samples were then analyzed by SDS-PAGE and Western blot for syntaxin-17 and Flag. This co-immunoprecipitation assay shows that Rab32 is the main interactor of syntaxin-17 from the Rab32 family proteins. Rab33B and Rab3D were used as negative controls. The graph shows the results of 3 independent experiments.

seemed to bind 2-fold weaker to syntaxin-17, and Rab38 showed no interaction at all with this protein. Rab33B and Rab3D were used as negative controls for these set of experiments, since Rab33B has also been shown to have a role in autophagy and it is also a substrate for RUTBC1, but it is not related to the Rab32 family proteins (Itoh et al., 2008; Nottingham et al., 2011), and Rab3D is not related to this family as well (Elias et al., 2012).

This suggests that Rab32 and syntaxin-17 interact physically to mediate autophagosome formation. More experiments are needed to elucidate the GDP/GTP-binding specificity for this interaction, and how overexpression of either protein's active or inactive form affect autophagosome formation as well.

CHAPTER 4:
Rab32 family evolution

4. Rab32 family evolution

4.1. Rationale

According to evolutionary studies, the Rab32 family comprises Rab32, Rab38, and Rab29 (Elias et al., 2012). They were grouped together by their sequence similarity according to their Rab family and subfamily domains (Pereira-Leal and Seabra, 2000; Pereira-Leal and Seabra, 2001). Both Rab32 and Rab38 have mainly been a subject of melanosomal trafficking research (Cohen-Solal et al., 2003; Tamura et al., 2009; Wang et al., 2008; Wasmeier et al., 2006). In these studies, Rab38 and Rab32 were shown to have some overlapping functions, but they are not entirely redundant (Ambrosio et al., 2012; Bultema et al., 2012). Moreover, Rab32 has also been implicated in modulating mitochondrial membrane dynamics (Alto et al., 2002; Bui et al., 2010), suggesting that Rab32 has another role in cells that lack melanosomes. On the other hand, not much is known about the function of Rab29. Recent studies have found it to be a gene of potential risk for developing Parkinson's disease (Gan-Or et al., 2012; Simón-Sánchez et al., 2009; Tucci et al., 2010); as widely known, this disease develops in neurons, which are highly dependent on mitochondria to provide sufficient energy for their function (Henchcliffe and Beal, 2008).

Recently, Elias and colleagues detected an ancient split for the Rab32 family, which included Rab32A and Rab32B. Humans and other metazoans have only Rab32A, while Rab32B is present along with Rab32A in Excavates and other Holozoan and Amoebozoan organisms (Elias et al., 2012). This suggests that the function of Rab32 may have diverged early in evolution.

Altogether, these findings prompted us to question if this variety of functions among the Rab32 family proteins were gained throughout evolution, and when the expansion of the Rab32 family happen. For this purpose, we used comparative genomics to search for homologous proteins of Rab32A/B, Rab38, and Rab29 throughout many different eukaryotic organisms whose genomes are publicly available. This technique allows us to detect sequences that are conserved in different organisms, as well as gain, loss or mutation of genes that give new organisms unique characteristics and might give rise to new or different functions than the original protein. Previous studies had determined the distribution of Rab32 in many different eukaryotic organisms (Brighouse et al., 2010; Diekmann et al., 2011; Elias et al., 2012). However, we decided to increase

the taxonomic breadth in order to gain a better perspective of the evolution of this family of Rab GTPases.

4.2. Results

4.2.1. Rab32A and Rab32B are the most ancient members of the family

In this approach, I first used the human protein sequence of each individual Rab32 family protein to find their homologues using BLAST. Then, if a positive candidate was identified, I did a reverse BLAST search into the human genome to confirm if this protein sequence also recovered the original human protein sequence and, only then, consider it as a positive hit or homologous protein. The list of organisms used in this study is included in the Appendix section, along with a brief description of each organism (Appendix Table 7.1). To avoid bias on the search, at least two representative organisms were chosen from each of the six major eukaryotic supergroups: Opisthokonta, containing metazoans, fungi, and their unicellular relatives; Amoebozoa, including the slime mold *Dictyostelium discoideum*; Excavata, which includes the free-living organism *Naegleria gruberi* and the parasite *Trypanosoma brucei*; Archaeplastida, containing plants and red and green algae; SAR, including brown algae and phytoplankton species; and CCTH, that also includes many species of algae.

After many searches in various genome databases (including NCBI, JGI, Origins of Multicellularity of the Broad Institute, or specific genome projects), I was able to find several positive hits, or homologues, in each supergroup of eukaryotic life. Figure 4.1 shows a Coulson plot, which depicts the presence (colored) or absence (blank) of a homolog for each organism analyzed. As seen, Rab32A and Rab32B are the only members of the family that are present in all supergroups, except Archaeplastida; meanwhile, both Rab38 and Rab29 show a Holozoa-specific distribution. This suggests that Rab32A and B are the most ancient members of the family, and that the other two members were acquired through evolution in Holozoa.

4.2.2. Rab38 and Rab29 are descendants of Rab32A

As mentioned before, Rab32 showed an ancient split very early in evolution, which included Rab32A and Rab32B (Elias et al., 2012). Therefore, to determine which of the two (Rab32A or Rab32B) did Rab38 and Rab29 derive, we focused on the expansion of Holozoan taxa (since Rab38 and Rab29 showed a Holozoa-specific

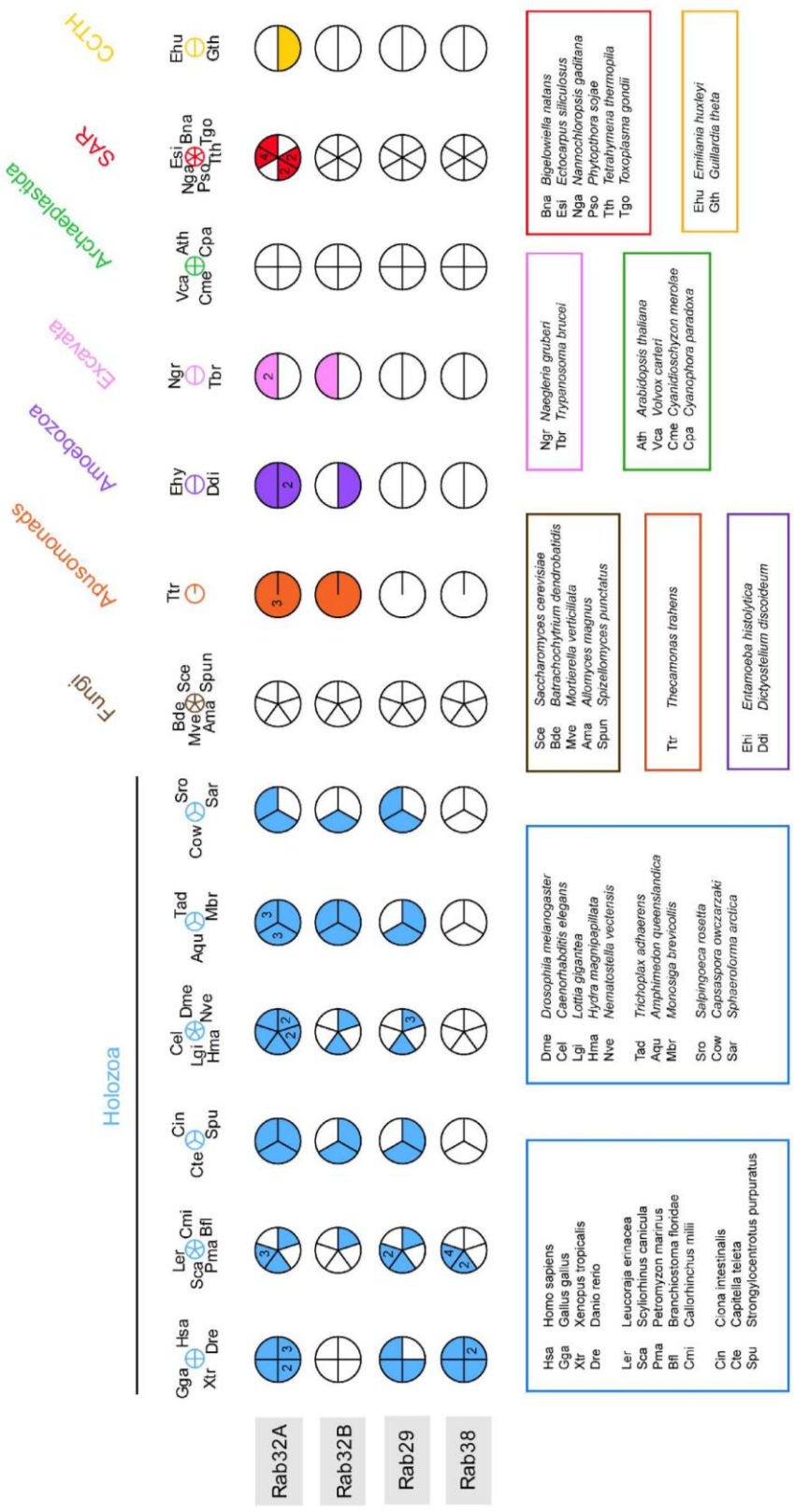


Figure 4.1. Distribution of the Rab32 family proteins across eukaryotic taxa. This Coulson plot represents the distribution of the Rab32 family proteins across different organisms of the six major eukaryotic supergroups. Colored or blank pieces of the pie chart indicate presence or absence of each Rab in each organism, respectively. The non-abbreviated name for each organism is included in their corresponding color boxes. All positive and negative hits were confirmed both by comparative genomics and phylogenetic studies in various genome databases. Numbers indicate when there was more than one homologue found in each specific organism.

distribution) used in previous studies (Brighthouse et al., 2010; Diekmann et al., 2011; Elias et al., 2012).

Interestingly, we were able to identify patterns of presence and absence between Rab32B and the other Rabs (Figure 4.1). We confirmed that the presence of Rab32B in the eukaryotes analyzed depended on the presence of Rab32A. Furthermore, when Rab38 appeared in higher eukaryotes, Rab32B was no longer present. This suggests that Rab38 might have arisen as an alternate for Rab32B when the latter was “lost”. Also, Rab29 is present in Holozoan organisms whenever Rab32A, Rab38 or Rab32B are also present. Altogether, these findings suggest that the appearance of Rab29 and Rab38 did not cause the loss of the other family members, and that these eukaryotic organisms require all of their functions to grow.

Next, to determine when these gene duplications occurred, phylogenetic analyses were performed. First, all the homologous sequences were aligned to allow the detection of regions with unambiguous homology. This alignment was then used to obtain phylogenetic trees by two different maximum likelihood methods (RAxML and PhyML), and a Bayesian inference method (Mr. Bayes). Figure 4.2 shows a representative tree for with the best Mr. Bayes tree topology. Interestingly, we can see that Rab38 and Rab29 were derived from Rab32A. Also, it seems that Rab29 diverged earlier from Rab32 than Rab38, since its split appeared closer to the root of the tree in Filazoa, while Rab38 appears to have arisen in Chordates. This suggests that the sequence of Rab32 is more similar to Rab38 than to Rab29, which is in accordance with our findings in Chapter 3 that the functions and subcellular distributions of Rab32 are more similar to Rab38 than to Rab29.

Finally, the final set of trees were Holozoa specific, since Rab38 and Rab29 appeared to have arisen at this moment of evolution (Figure 4.1), and we wanted to have better resolution and support for the trees of this specific supergroup. Figure 4.3 shows a representative tree from this last set of trees, using *Thecamonas trahens* (Ttr) as the root of the tree since it is the most basal organism included. In this tree we can see that all Rab38 sequences group nicely together, as well as Rab29 and Rab32 independently. Unlike in previous attempts, this specific set of trees did not show good support values to determine with certainty that Rab29 diverged earlier from Rab32A than Rab38. However, previous studies have been able to find that this indeed is the case with better support



Figure 4.2. Phylogenetic evolution of Rab32 family proteins. Phylogenetic tree of the Rab32 family proteins identified in representative eukaryotic organisms, depicted with the best Bayesian topology obtained. Clades containing sequences of each specific family member are color coded (Rab32B, yellow; Rab32A, orange; Rab29, blue; Rab38, green). Numerical values represent Bayesian posterior probabilities and maximum likelihood bootstrap values (RAxML and PhyML); black circles indicate 1.00/95/95 support values for MrBayes, RAxML, and PhyML, respectively.

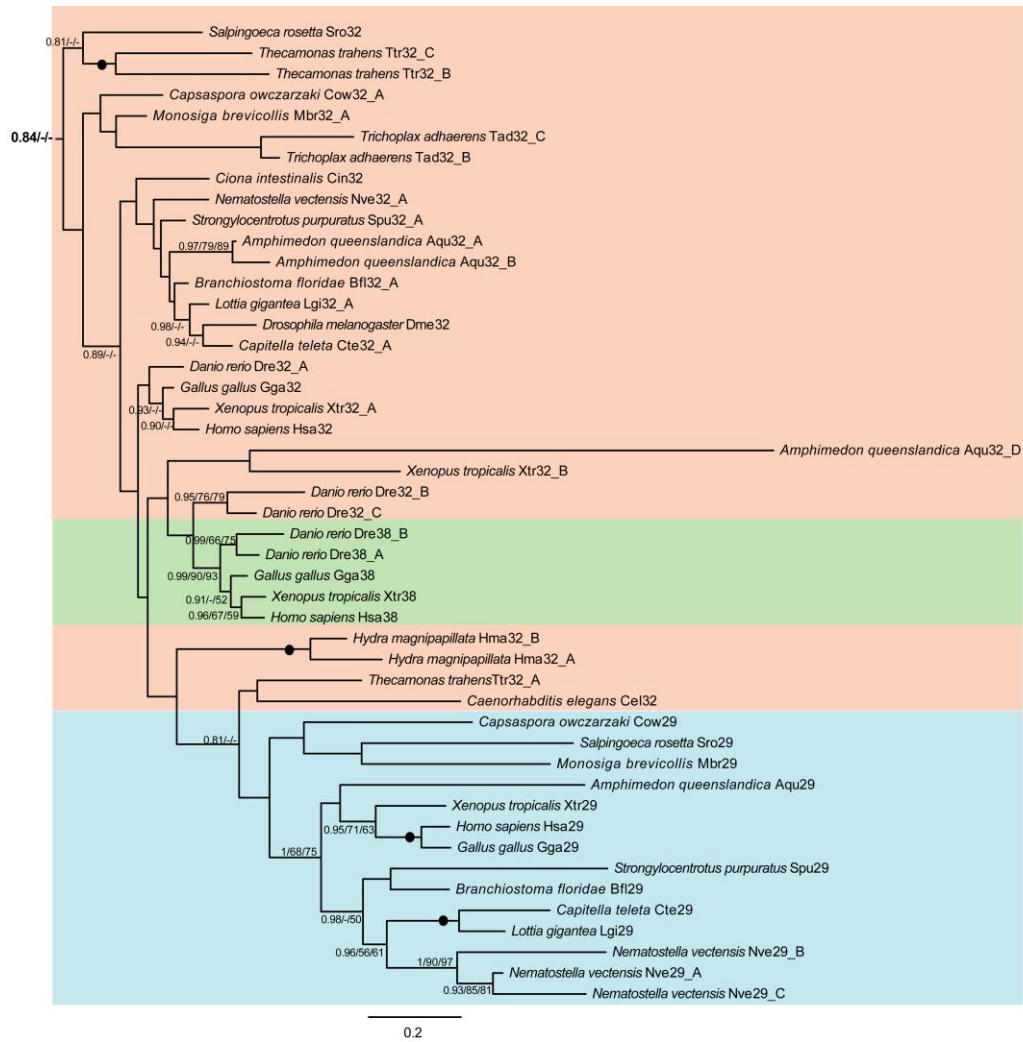


Figure 4.3. Holozoan evolution of Rab32 family proteins. Phylogenetic tree of the Rab32 family proteins identified in Holozoan organisms, depicted with the best Bayesian topology obtained. Clades containing sequences of each specific family member are color coded (Rab32A, orange; Rab29, blue; Rab38, green). Numerical values represent Bayesian posterior probabilities and maximum likelihood bootstrap values (RAxML and PhyML); black circles indicate 1.00/95/95 support values for MrBayes, RAxML, and PhyML, respectively.

values (Elias et al., 2012), suggesting that a reassessment of the sequences included and their alignment might aid in improving the support of this Holozoan tree. Unfortunately, additional variations of taxa, including the shark protein sequences, did not improve the resolution of the trees.

Altogether, these results suggest that both Rab38 and Rab29 are a result of Holozoan expansion of Rab32A. Also, we can infer that the functions performed by Rab29 and Rab38 are not entirely redundant from those of Rab32A and Rab32B, since their appearance in Holozoans did not cause the loss of the ancient variations of Rab32.

CHAPTER 5:
Discussion and
Future Perspectives

5. DISCUSSION AND FUTURE PERSPECTIVES

5.1. The interactors of Rab32 family proteins modulate both ER and mitochondrial membrane dynamics

In Chapter 3, we analyzed the distribution of the Rab32 family proteins, as well as their interaction with several proteins that regulate their activity throughout their cycle. In 2002, Rab32 had initially been found to disrupt the mitochondrial network when its inactive form was overexpressed in cells (Alto et al., 2002). Our lab was able to reproduce these observations, and to determine that in fact Rab32 showed a subcellular co-localization with both the ER and mitochondria, and more specifically, that it was enriched in the MAM (Bui et al., 2010). The reason for this distribution and the mitochondria phenotype observed with GDP-bound Rab32 became clearer when, in 2011, Friedman and colleagues showed that the ER is involved in mitochondrial membrane dynamics by initiating a constricting process around mitochondria that ultimately leads to the fission of this organelle (Friedman et al., 2011). Altogether, these findings suggested that the proteins regulating the Rab activity were proteins that either resided in these organelles or that are involved in shaping the ER or mitochondria.

It is well known that Rab proteins regulate their respective membrane trafficking pathways by recruiting several proteins that mediate at least one of their downstream effects, which is why these proteins are called effectors (Hutagalung and Novick, 2011). In this thesis, we were able to determine that Drp1, a regulator of mitochondrial fission, acts as an effector of Rab32, since it preferentially interacts with the active GTP-bound form of this Rab (Figure 3.3). This was confirmed by a decrease in this interaction when the Rab32 GAP protein (RUTBC1), which inactivates the Rab protein, was exogenously expressed (Figure 3.5). Consistent with this, we were also able to show that knocking out Drp1 resembled the effect seen in the cells expressing the inactive form of Rab32 (Figure 3.4), further confirming it acts downstream of the Rab, as expected for an effector.

Moreover, in 2010, our lab reported that the normal cellular distribution and activity of Drp1 is altered in the presence of inactive Rab32 (Bui et al., 2010). This occurs apparently through Rab32's AKAP activity, which mediates inactivation of Drp1 by PKA-mediated phosphorylation of serine 656 (Alto et al., 2002; Cribbs and Strack, 2007; Chang and Blackstone, 2007). However, this effect was not seen with the active

mutant of Rab32, Q85L (Bui et al., 2010). This is in agreement with the fact that Drp1 preferentially interacts with Rab32 Q85L in its active non-phosphorylated form. Altogether, these findings suggest that Rab32 acts through Drp1 to modulate mitochondrial membrane dynamics. Having found a specific Rab-effector interaction between Rab32 and Drp1, we would like to know how they bind to one another by creating domain-specific constructs of Drp1. This will aid elucidating which of these domains is necessary for the interaction to take place and alter mitochondrial dynamics.

Moreover, we were able to show that not only inactive Rab32, but also inactive Rab38 and Rab29, cause the alteration of the mitochondria phenotype and that they all interact with Drp1 (Figures 3.9 and 3.11). Even though Rab38 and Rab29 are not AKAPs and thus they cannot bind and recruit PKA, they still interact with Drp1, suggesting that the sequence that determines their binding specificity in these family proteins is not in the same region as the one that confers Rab32 AKAP activity. Recently, a study reported that the variable domain close to the C-terminus in Drp1's sequence modulates its ability to form higher-order oligomers around mitochondria, which ultimately leads to constriction of this organelle (Strack and Cribbs, 2012). Perhaps Rab38 and Rab29 associate with Drp1 through this domain to modulate its oligomerization around mitochondria, thus regulating in this way mitochondrial membrane dynamics. Indeed, generating Drp1 domain-specific constructs will help to uncover the mechanism of interaction between Drp1 and the Rab32 family proteins.

As mentioned before, the correct localization of an effector can determine the distribution of a Rab (Grosshans et al., 2006). In this thesis, we were able to show that knocking out Drp1 also altered the subcellular distribution of Rab38 and Rab29, which suggests that Drp1 might also be acting as an effector of Rab38 and Rab29 (Figure 3.14). Even though the experiment to confirm this was not done in this thesis, it can easily be shown by performing co-immunoprecipitation assays with active Drp1 and both active and inactive mutants of the Rabs. If this indeed is the case, we would see more binding of Drp1 to active Rab38 and Rab29, similarly to what we observed in the case of Rab32.

Interestingly, even though Rab29 staining overlapped with the Golgi marker protein p115 (Figure 3.8A), and showed a strong signal in light membranes in our fractionation protocol (Figure 3.8B), it still interacted with Drp1. In 2010, a study reported that Drp1 also localizes to the Golgi apparatus in a cell line-specific manner, as seen by its strong co-localization with the peripheral Golgi protein p115 and the TGN

protein in the monkey kidney fibroblast-like cell line Cos-7 and rat hepatoma FaO cells, but not in the human hepatocellular carcinoma cell line HepG2 (Bonekamp et al., 2010). This study implicated Drp1 in the delivery of a subset of cargo proteins in some cells from the TGN to the plasma membrane, and that depletion of Drp1 caused the dispersion of Golgi stacks. However, the Rab29-Drp1 interaction found as part of this thesis might more likely be taking place with the ER/MAM pools of Rab29 and Drp1, since the effects seen in our studies with inactive Rab29 involved only the mitochondrial network. In addition, we were able to identify a stronger interaction between dynamin-2 and Rab29 than with Rab38 and Rab32 (Figure 3.15). Dynamin-2 is widely known for its function in endocytosis by pinching off vesicles from the plasma membrane (Takei et al., 1995). However, a few studies have shown that dynamin-2 also localizes to another pool in the Golgi, and it is involved in the formation of secretory vesicles from the TGN (Cao et al., 1998a; Cao et al., 2000; Jones et al., 1998; Maier et al., 1996). This suggests that Rab29 is able to interact with both Drp1 and dynamin-2 because their subcellular distributions partially overlap. Nevertheless, new experiments are required to determine if inactive Rab29 also has an effect in the morphology of the Golgi apparatus and if the interaction between this Rab and Drp1 or dynamin-2 might also have an effect on this cellular compartment as well.

Besides interacting with Drp1 from the mitochondrial membrane dynamics machinery, we were also able to show that Rab32 interacts with some of the proteins that participate in ER network formation, including atlastin-2 and reticulon-4 (Figures 3.6 and 3.7). These two proteins are known to mainly reside in smooth ER tubules, but they are also present in rough ER-sheets, suggesting Rab32 might interact with these proteins when it is cycling back to the donor membrane to be activated again after performing its function, either in the cell's periphery or its perinuclear region. Indeed, our subcellular fractionation technique would be useful to determine the main distribution of these and the rest ER-shaping proteins and if it resembles that of Rab32. Likewise, it would be interesting to know if the other family proteins also interact physically with these ER-shaping proteins. This would help elucidate the protein machinery by which Rab32 cycles throughout the cell, and if it is similar to that of its fellow family members. In addition, it is very important to note that Drp1, atlastins, and reticulons belong to the family of dynamin-related proteins. In this way, it was not surprising that the Rab32 family proteins also interacted with dynamin-2. All of these interacting proteins share sequence

similarities that confer them the properties to either constrict or fuse membranes through homo- and hetero-oligomerization (which depends on GTP hydrolysis), and might also explain why they all interact with the Rab32 family.

5.2. Rab32 family proteins in autophagy

A rather exciting finding was Rab32's interaction with the ER-resident SNARE syntaxin-17, because they both have been proven to participate in autophagy (Hamasaki et al., 2013; Hirota and Tanaka, 2009). SNARE proteins have been found to act directly with Rab proteins, i.e. the t-SNARE Sed5 has been shown to act as an effector of Rab Ypt1. In this example, Ypt1 interaction with Sed5 liberates the SNARE protein from its regulator Sly1p and allows it to form a complex with its specific v-SNAREs to mediate membrane fusion (Lupashin and Waters, 1997). Moreover, other Rabs have been implicated in regulating autophagy as well, including: Rab7, which has been reported to participate in the final stages of late autophagic vacuoles mediating their fusion with the lysosome (Jäger et al., 2004); Rab11, participating in the fusion of late endosomes with autophagosomes (Fader et al., 2008); and Rab24, which appears to be required for the formation of autophagosomes in cells under starvation (Munafó and Colombo, 2002). However, a study done in 2008 reported the first direct link between an autophagy-related protein and a Rab protein (Itoh et al., 2008). Itoh and colleagues have shown that Rab33B, which is a *cis*-Golgi-resident Rab, interacts with Atg16L (a crucial factor for the formation of the isolation membrane) to regulate both autophagosome formation and maturation; also, this same team was later able to show that expression of a stronger Rab33B GAP different from RUTBC1, called OATL1, decreased its interaction with its effector Atg16L, hampering the fusion of autophagosomes with lysosomes (Itoh et al., 2008; Itoh et al., 2011).

Similarly, this thesis shows the first direct evidence of the MAM enriched Rab32 interacting with syntaxin-17, a protein from the autophagic machinery (Figure 3.16). It would be interesting to know how syntaxin-17 regulates Rab32 activity and what role it plays in this Rab's cycle. Similarly, we could determine if the interaction of Rab32 with syntaxin-17 is a Rab-effector type, by modulating this interaction with the overexpression of the Rab32 GAP protein RUTBC1. If this is indeed the case, it would also be useful to know if RUTBC1 has an effect on Rab32's ability to promote autophagosome formation, as was the case with its Drp1 interaction and its ability to modulate mitochondrial

membrane dynamics. This approach will also be very useful with the other newly found interacting proteins, since it will ultimately lead to uncovering the mechanistic requirements Rab32 needs to cycle around the cell performing its function.

Furthermore, a previous study identified human Rab32 to regulate autophagosome formation (Hirota and Tanaka, 2009). Similarly, in *Drosophila*, the inactive version of the sole orthologue of human Rab32 called RabRP1 (Rab related-protein 1, also known as lightoid) was reported to cause the accumulation of structures that resembled autophagosomes (Fujikawa et al., 2002), and it was later found to have an effect on lipid droplets and autophagosome formation (Wang et al., 2012). This orthologue is highly expressed in the fat body and it is mainly present in the autophagosomes, as shown by its subcellular co-localization with the autophagosome marker Atg8. Inactive RabRP1 expression generates small lipid droplets in these flies, suggesting that RabRP1's role in these cells is to regulate lipid storage through the autophagic pathway (Wang et al., 2012). This encourages the idea that Rab32 performs specific functions that are conserved, at least in metazoans.

Altogether, these findings suggest that not only Rab32 has cell-type specific roles, but also that it performs more than one function in cells that lack melanosomes. It appears that the distribution of active/inactive Rab32 that is available in the different regions of the cell, as well as the proximity of their binding partners at these given regions, dictates the variety of pathways regulated by this Rab protein.

5.3. Rab32 family evolution

The multiple roles of Rab32 in mammalian cells, and its partial redundancy with the other Rab32 family proteins, led us to question if these proteins were conserved in other eukaryotic organisms. In Chapter 4, we analyzed this family using comparative genomics and phylogenetics to determine when the gene duplication of Rab32 occurred. We found that Rab32A and Rab32B are the most ancient members of the family, and that both Rab38 and Rab29 were Holozoa-specific expansions of Rab32A, possibly diverging with slightly different function and sequence specificity (Figures 4.1, 4.2, and 4.3).

These results are consistent with previous attempts to resolve the evolution of Rab subfamilies (Diekmann et al., 2011; Elias et al., 2012). These two studies were able to determine the Rab repertoire that was present in the LECA (Last Ekaryotic Common Ancessor) through different approaches, which included 15 and 23 Rabs, respectively.

The method used by Diekmann and colleagues is based first on the identification if a protein sequences is or a not a Rab protein by the presence of conserved domains of GTPases and RabF motifs; then it classifies the putative Rab protein sequence under either pre-defined subfamilies or undetermined subfamily X (Diekmann et al., 2011). Elias and colleagues, on the other hand, relied on datasets that were constructed using the least divergent orthologous representatives of a putative Rab family within each eukaryotic supergroup; then these individual datasets were then cross-referenced to one another in order to determine a more accurate evolution of the Rab family across all eukaryotes (Elias et al., 2012). Both studies were able to determine that Rab32 was one of the Rab members present in the LECA, however, only the study done by Elias and colleagues was able to identify the ancient split of Rab32A and Rab32B. In line with these results, our expansion of taxa sampling increased the resolution of the Holozoan subgroup of both studies, allowing us to determine that Rab29 and Rab38 diverged from Rab32A in Holozoa and Metazoa, respectively, and not from Rab32B. This suggests that Rab32 already played a dual function in early organisms and that, even though Rab32B was lost in Metazoa, it may have been functionally replaced by Rab38.

It is important to note that all of the individual clades containing Rab-specific sequences show good support (bootstrap values) in my last Holozoa-specific tree; unfortunately, I was unable to obtain good resolution in the earlier branches (Figure 4.3). This occurs because, not only the sequences of the Rab family are very short and highly conserved, but also the sequences between Rab subfamilies are even more similar, causing the algorithms difficulties to classify them in separate clades. However, due to lack of time, I could not reassess the sequences used for this set of trees. Perhaps, better support for the earlier branches could have been obtained if we would have included only the best-behaved members of each clade from all the previous analyses. This way, we are still including the same eukaryotic organisms but fewer sequences that are highly divergent. Moreover, we can also see an example of a long branch in Figure 4.3, as showed by the *Aqu32_D sequence*; this suggests that this sequence is highly divergent from the rest of its paralogs. Therefore, removal of this sequence might help get better support values for its neighboring clades and re-position Xtr32_B sequence along with its paralogs, since it might have been attracted to the highly divergent *Aqu32_D* sequence, and aid in improving altogether the resolution of the tree.

Altogether, we can highlight the benefits of incorporating phylogenetics and comparative genomics to cell biology studies, since they are powerful tools that provide us with valuable evolutionary insights that improve our understanding of cellular processes.

5.4. Rab32 expression and function across eukaryotes

In humans, Rab32 and Rab38 have been implicated in melanosomal trafficking (Wasmeier et al., 2006). Similarly, these Rabs have also been found to be expressed in the primary retinal pigment epithelium cells in mice, and to localize primarily to the perimeter membrane of mature melanosomes in these tissues. Interestingly, it seems that the function of Rab32 and Rab38 in these cells is not redundant, since depletion of Rab38 caused a dramatic decrease in the number of melanosomes (Lopes et al., 2007), similarly to their human homologues (Ambrosio et al., 2012). This suggests that the sole presence of Rab32 can not compensate for the absence of its paralog Rab38.

In addition to its role in melanosomes, human Rab32 has also been reported to recruit PKA to mitochondria, and it is the only member of the family to have this AKAP activity (Alto et al., 2002). Very interestingly, the closely related Rab32 ortholog from *Xenopus* has also been reported to be highly expressed in pigmented epithelium of the retina and to act as an AKAP, recruiting PKA to melanosomes (Park et al., 2007; Voigt et al., 2005). Similarly, *Drosophila*'s sole Rab32 orthologue RabRP1, was also found to act as an AKAP by the Scott group in 2002 (Alto et al., 2002). However, Glo-1, the Rab32 orthologue in the nematode *Caenorhabditis elegans* does not exhibit AKAP activity (Hermann et al., 2005). This suggests that at least the ability of Rab32 to function as an AKAP is conserved in Holozoans and that this specific function might set Rab32 apart from its other paralog proteins in these organisms.

Moreover, in the bollworm *Helicoverpa armigera*, Rab32 was found to be present in the epidermis, midgut and fat body of larvae. Interestingly, levels of Rab32 increased by 50% in the epidermis and midgut in the metamorphosis stage, suggesting it is also important for late development of this organism (Hou et al., 2011). Similar observations were obtained in the notochord of zebrafish (*Danio rerio*), a very closely related metazoan (Ellis et al., 2013). In this study, Rab32 was found to be present in notochord vacuoles (LROs), and expression of its inactive GDP-form caused 90% fragmentation of these, as well as a shortening of the body axis and deformation of the

body and spine (Ellis et al., 2013). In *Trypanosoma cruzi*, a more distant eukaryote, Rab32 has been found to localize in the contractile vacuole bladder, which has been proven to control cell volume (Ulrich et al., 2011); orthologues of this protein, however, have not been found in other trypanosomatids, similarly to what we found in the evolutionary studies of this thesis. This suggests that the role of Rab32 expression during the development is at least partially conserved among various eukaryotic organisms.

5.5. Rab32 family in disease

Now that we have a broader perspective of the eukaryotic distribution of the Rab32 family proteins, as well as their tissue and subcellular distribution across eukaryotes, we can understand better the involvement of these family proteins in disease.

A recent study has reported a possible role for Rab29 in LROs. In 2011 Spanò and colleagues found that Rab29 was recruited to vacuoles containing *Salmonella typhi*, the causative agent of typhoid fever. Interestingly, this was not the case in vacuoles containing the broad-host *Salmonella typhimurium* which does not infect humans. These researchers were able to identify that the latter secretes a factor called GtgE, a protease that ultimately cleaves Rab29 within its GTPase domain and thus inactivates the Rab protein, preventing it from being recruited to the *S. typhimurium*-containing vacuole. Moreover, exogenous GtgE expression in *S. typhi* increased its ability to grow in epithelial cells, suggesting that Rab29 degradation creates a better environment for the bacteria to grow inside the cell (Spanò et al., 2011).

A year later, this same group reported that Rab32 and Rab38 can also be degraded by GtgE and they are also recruited to vacuoles containing *S. typhi* expressing GtgE; these vacuoles resembled LROs (lysosome-related organelles), explaining the Rab32 family recruitment and presence in this specific compartments. Interestingly, neither Rab29 nor Rab38's depletion by siRNA had an effect per se in the ability of *S. typhi* to survive in macrophages; in contrast, Rab32's depletion increased the bacteria count in the infected cells (Spanò and Galán, 2012).

Similarly, in macrophages, Rab32 and Rab38 were shown to localize in very low levels to phagosomes. Furthermore, expression of the inactive form of these two Rabs inhibited the recruitment of the lysosomal hydrolase cathepsin D to phagosomes. Macrophages infected with *Mycobacterium tuberculosis* showed impaired recruitment of Rab32 and 38 to phagosomes, and, subsequently, lysosomes did not fuse with these

organelles, suggesting that these proteins might play a role in phagosome maturation and phagolysosome biogenesis as well (Seto et al., 2011). Similarly, in 2011, a genome-wide association study reported that a genetic polymorphism in Rab32 increases susceptibility to *Mycobacterium leprae* infection (Zhang et al., 2011). The involvement of Rab32 in infection-related diseases is in line with the fact that Rab32 is involved in autophagy, since the infection by these microorganisms has been related to autophagy-mediated clearance of these intracellular bacteria in host defense (Deretic, 2010; Ponpuak et al., 2010; Zheng et al., 2009).

5.6. Conclusions

Our understanding on how MAM-associated Rab32 modulates mitochondrial membrane dynamics has increased with the results obtained in this thesis. I have identified that Drp1, a master regulator of mitochondrial fission, acts as an effector of Rab32. This interaction is potentially one way through which Rab32 modulates the morphology of this organelle, since it not only causes the clustering of mitochondria around the perinuclear region when inactive, but it also modulates Drp1 activity through PKA-mediated phosphorylation (Alto et al., 2002; Bui et al., 2010). In addition, I was also able to show that Rab38 and Rab29, members of the Rab32 family, also alter the mitochondria phenotype and also interact with Drp1, albeit to a weaker extent.

Moreover, I was also able to determine that Rab32 also interacts with syntaxin-17, a SNARE protein that has been identified to be enriched in the MAM and to participate in autophagy (Hamasaki et al., 2013), similar to Rab32. Importantly, autophagy was been implicated in participating in host defense against bacterial infections (Deretic, 2010), so studies yet to come will elucidate how this interaction might potentially be regulated to develop new strategies to combat human disease.

Lastly, I was also able to increase our understanding of the Rab32 family evolution and how all of their homologous proteins have conserved or divergent functions. Our results suggest that Rab32 performs specific functions that, up to now, cannot be extrapolated to its closely related paralogs, Rab38 and Rab29, including Rab32's AKAP activity and its role in animal development. However, some functions seem to be at least partially redundant (i.e. melanosomal trafficking); after all, these proteins are very closely related and it would be expected that their functions are related

as well. Indeed, studies yet to come will elucidate the functions of Rab32 homologs, and how, when, and why they diverged from their common ancestor protein sequence.

CHAPTER 6:

References

6. REFERENCES

- Abascal, F., R. Zardoya, and D. Posada. 2005. ProtTest: selection of best-fit models of protein evolution. *Bioinformatics*. 21:2104-2105.
- Aivazian, D., R.L. Serrano, and S. Pfeffer. 2006. TIP47 is a key effector for Rab9 localization. *J Cell Biol*. 173:917-926.
- Alexandrov, K., H. Horiuchi, O. Steele-Mortimer, M.C. Seabra, and M. Zerial. 1994. Rab escort protein-1 is a multifunctional protein that accompanies newly prenylated rab proteins to their target membranes. *Embo J*. 13:5262-5273.
- Alto, N.M., J. Soderling, and J.D. Scott. 2002. Rab32 is an A-kinase anchoring protein and participates in mitochondrial dynamics. *J Cell Biol*. 158:659-668.
- Amati-Bonneau, P., M.L. Valentino, P. Reynier, M.E. Gallardo, B. Bornstein, A. Boissière, Y. Campos, H. Rivera, J.G. de la Aleja, R. Carroccia, L. Iommarini, P. Labauge, D. Figarella-Branger, P. Marcorelles, A. Furby, K. Beauvais, F. Letournel, R. Liguori, C. La Morgia, P. Montagna, M. Liguori, C. Zanna, M. Rugolo, A. Cossarizza, B. Wissinger, C. Verny, R. Schwarzenbacher, M.A. Martín, J. Arenas, C. Ayuso, R. Garesse, G. Lenaers, D. Bonneau, and V. Carelli. 2008. OPA1 mutations induce mitochondrial DNA instability and optic atrophy 'plus' phenotypes. *Brain*. 131:338-351.
- Ambrosio, A.L., J.A. Boyle, and S.M. Di Pietro. 2012. Mechanism of platelet dense granule biogenesis: study of cargo transport and function of Rab32 and Rab38 in a model system. *Blood*. 120:4072-4081.
- Anant, J.S., L. Desnoyers, M. Machius, B. Demeler, J.C. Hansen, K.D. Westover, J. Deisenhofer, and M.C. Seabra. 1998. Mechanism of Rab geranylgeranylation: formation of the catalytic ternary complex. *Biochemistry*. 37:12559-12568.
- Andres, D.A., M.C. Seabra, M.S. Brown, S.A. Armstrong, T.E. Smeland, F.P. Cremers, and J.L. Goldstein. 1993. cDNA cloning of component A of Rab geranylgeranyl transferase and demonstration of its role as a Rab escort protein. *Cell*. 73:1091-1099.
- Arai, S., Y. Noda, S. Kainuma, I. Wada, and K. Yoda. 2008. Ypt11 functions in bud-directed transport of the Golgi by linking Myo2 to the coatomer subunit Ret2. *Curr Biol*. 18:987-991.
- Balderhaar, H.J., and C. Ungermann. 2013. CORVET and HOPS tethering complexes - coordinators of endosome and lysosome fusion. *J Cell Sci*. 126:1307-1316.
- Bannykh, S.I., T. Rowe, and W.E. Balch. 1996. The organization of endoplasmic reticulum export complexes. *J Cell Biol*. 135:19-35.
- Bao, X., A.E. Faris, E.K. Jang, and R.J. Haslam. 2002. Molecular cloning, bacterial expression and properties of Rab31 and Rab32. *Eur J Biochem*. 269:259-271.
- Barr, F., and D.G. Lambright. 2010. Rab GEFs and GAPs. *Curr Opin Cell Biol*. 22:461-470.
- Baughman, J.M., F. Perocchi, H.S. Girgis, M. Plovonich, C.A. Belcher-Timme, Y. Sancak, X.R. Bao, L. Strittmatter, O. Goldberger, R.L. Bogorad, V. Kotliansky, and V.K. Mootha. 2011. Integrative genomics identifies MCU as an essential component of the mitochondrial calcium uniporter. *Nature*. 476:341-345.
- Baumann, N.A., D.P. Sullivan, H. Ohvo-Rekilä, C. Simonot, A. Pottekat, Z. Klaassen, C.T. Beh, and A.K. Menon. 2005. Transport of newly synthesized sterol to the sterol-enriched plasma membrane occurs via nonvesicular equilibration. *Biochemistry*. 44:5816-5826.

- Belenguer, P., and L. Pellegrini. 2013. The dynamin GTPase OPA1: more than mitochondria? *Biochim Biophys Acta*. 1833:176-183.
- Benard, G., and M. Karbowski. 2009. Mitochondrial fusion and division: Regulation and role in cell viability. *Semin Cell Dev Biol*. 20:365-374.
- Bird, M.M. 1978. Presynaptic and postsynaptic organelles of synapses formed in cultures of previously dissociated mouse spinal cord. *Cell Tissue Res*. 194:503-511.
- Blümer, J., J. Rey, L. Dehmelt, T. Mazel, Y.W. Wu, P. Bastiaens, R.S. Goody, and A. Itzen. 2013. RabGEFs are a major determinant for specific Rab membrane targeting. *J Cell Biol*. 200:287-300.
- Boehning, D., D.O. Mak, J.K. Foskett, and S.K. Joseph. 2001. Molecular determinants of ion permeation and selectivity in inositol 1,4,5-trisphosphate receptor Ca²⁺ channels. *J Biol Chem*. 276:13509-13512.
- Boldogh, I.R., S.L. Ramcharan, H.C. Yang, and L.A. Pon. 2004. A type V myosin (Myo2p) and a Rab-like G-protein (Ypt11p) are required for retention of newly inherited mitochondria in yeast cells during cell division. *Mol Biol Cell*. 15:3994-4002.
- Bonekamp, N.A., K. Vormund, R. Jacob, and M. Schrader. 2010. Dynamin-like protein 1 at the Golgi complex: a novel component of the sorting/targeting machinery en route to the plasma membrane. *Exp Cell Res*. 316:3454-3467.
- Bos, J.L., H. Rehmann, and A. Wittinghofer. 2007. GEFs and GAPs: critical elements in the control of small G proteins. *Cell*. 129:865-877.
- Bravo, R., J.M. Vicencio, V. Parra, R. Troncoso, J.P. Munoz, M. Bui, C. Quiroga, A.E. Rodriguez, H.E. Verdejo, J. Ferreira, M. Iglewski, M. Chiong, T. Simmen, A. Zorzano, J.A. Hill, B.A. Rothermel, G. Szabadkai, and S. Lavandero. 2011. Increased ER-mitochondrial coupling promotes mitochondrial respiration and bioenergetics during early phases of ER stress. *J Cell Sci*. 124:2143-2152.
- Breckenridge, D.G., M. Stojanovic, R.C. Marcellus, and G.C. Shore. 2003. Caspase cleavage product of BAP31 induces mitochondrial fission through endoplasmic reticulum calcium signals, enhancing cytochrome c release to the cytosol. *J Cell Biol*. 160:1115-1127.
- Brighouse, A., J.B. Dacks, and M.C. Field. 2010. Rab protein evolution and the history of the eukaryotic endomembrane system. *Cell Mol Life Sci*. 67:3449-3465.
- Budnik, A., and D.J. Stephens. 2009. ER exit sites--localization and control of COPII vesicle formation. *FEBS Lett*. 583:3796-3803.
- Bui, M., S.Y. Gilady, R.E. Fitzsimmons, M.D. Benson, E.M. Lynes, K. Gesson, N.M. Alto, S. Strack, J.D. Scott, and T. Simmen. 2010. Rab32 modulates apoptosis onset and mitochondria-associated membrane (MAM) properties. *J Biol Chem*. 285:31590-31602.
- Bultema, J.J., A.L. Ambrosio, C.L. Burek, and S.M. Di Pietro. 2012. BLOC-2, AP-3, and AP-1 proteins function in concert with Rab38 and Rab32 proteins to mediate protein trafficking to lysosome-related organelles. *J Biol Chem*. 287:19550-19563.
- Cai, H., K. Reinisch, and S. Ferro-Novick. 2007. Coats, tethers, Rabs, and SNAREs work together to mediate the intracellular destination of a transport vesicle. *Dev Cell*. 12:671-682.
- Cantalupo, G., P. Alifano, V. Roberti, C.B. Bruni, and C. Bucci. 2001. Rab-interacting lysosomal protein (RILP): the Rab7 effector required for transport to lysosomes. *Embo J*. 20:683-693.
- Cao, H., F. Garcia, and M.A. McNiven. 1998a. Differential distribution of dynamin isoforms in mammalian cells. *Mol Biol Cell*. 9:2595-2609.

- Cao, H., H.M. Thompson, E.W. Krueger, and M.A. McNiven. 2000. Disruption of Golgi structure and function in mammalian cells expressing a mutant dynamin. *J Cell Sci.* 113 (Pt 11):1993-2002.
- Cao, X., N. Ballew, and C. Barlowe. 1998b. Initial docking of ER-derived vesicles requires Uso1p and Ypt1p but is independent of SNARE proteins. *Embo J.* 17:2156-2165.
- Carlucci, A., L. Lignitto, and A. Feliciello. 2008. Control of mitochondria dynamics and oxidative metabolism by cAMP, AKAPs and the proteasome. *Trends Cell Biol.* 18:604-613.
- Cereghetti, G.M., A. Stangherlin, O. Martins de Brito, C.R. Chang, C. Blackstone, P. Bernardi, and L. Scorrano. 2008. Dephosphorylation by calcineurin regulates translocation of Drp1 to mitochondria. *Proc Natl Acad Sci U S A.* 105:15803-15808.
- Cohen-Solal, K.A., R. Sood, Y. Marin, S.M. Crespo-Carbone, D. Sinsimer, J.J. Martino, C. Robbins, I. Makalowska, J. Trent, and S. Chen. 2003. Identification and characterization of mouse Rab32 by mRNA and protein expression analysis. *Biochim Biophys Acta.* 1651:68-75.
- Colombini, M. 2012. VDAC structure, selectivity, and dynamics. *Biochim Biophys Acta.* 1818:1457-1465.
- Collins, R.N. 2003. "Getting it on"--GDI displacement and small GTPase membrane recruitment. *Mol Cell.* 12:1064-1066.
- Cook, T., K. Mesa, and R. Urrutia. 1996. Three dynamin-encoding genes are differentially expressed in developing rat brain. *J Neurochem.* 67:927-931.
- COPELAND, D.E., and A.J. DALTON. 1959. An association between mitochondria and the endoplasmic reticulum in cells of the pseudobranch gland of a teleost. *J Biophys Biochem Cytol.* 5:393-396.
- Cribbs, J.T., and S. Strack. 2007. Reversible phosphorylation of Drp1 by cyclic AMP-dependent protein kinase and calcineurin regulates mitochondrial fission and cell death. *EMBO Rep.* 8:939-944.
- Croze, E.M., and D.J. Morré. 1984. Isolation of plasma membrane, golgi apparatus, and endoplasmic reticulum fractions from single homogenates of mouse liver. *J Cell Physiol.* 119:46-57.
- Csordás, G., C. Renken, P. Várnai, L. Walter, D. Weaver, K.F. Buttle, T. Balla, C.A. Mannella, and G. Hajnóczky. 2006. Structural and functional features and significance of the physical linkage between ER and mitochondria. *J Cell Biol.* 174:915-921.
- Chang, C.R., and C. Blackstone. 2007. Cyclic AMP-dependent protein kinase phosphorylation of Drp1 regulates its GTPase activity and mitochondrial morphology. *J Biol Chem.* 282:21583-21587.
- Chang, C.R., and C. Blackstone. 2010. Dynamic regulation of mitochondrial fission through modification of the dynamin-related protein Drp1. *Ann N Y Acad Sci.* 1201:34-39.
- Chavrier, P., J.P. Gorvel, E. Stelzer, K. Simons, J. Gruenberg, and M. Zerial. 1991. Hypervariable C-terminal domain of rab proteins acts as a targeting signal. *Nature.* 353:769-772.
- Chen, H., S.A. Detmer, A.J. Ewald, E.E. Griffin, S.E. Fraser, and D.C. Chan. 2003. Mitofusins Mfn1 and Mfn2 coordinately regulate mitochondrial fusion and are essential for embryonic development. *J Cell Biol.* 160:189-200.
- Chen, M.S., A.B. Huber, M.E. van der Haar, M. Frank, L. Schnell, A.A. Spillmann, F. Christ, and M.E. Schwab. 2000. Nogo-A is a myelin-associated neurite

- outgrowth inhibitor and an antigen for monoclonal antibody IN-1. *Nature*. 403:434-439.
- Chen, S., P. Novick, and S. Ferro-Novick. 2012. ER network formation requires a balance of the dynamin-like GTPase Sey1p and the Lunapark family member Lnp1p. *Nat Cell Biol*. 14:707-716.
- Chen, S., P. Novick, and S. Ferro-Novick. 2013. ER structure and function. *Curr Opin Cell Biol*.
- Cho, D.H., T. Nakamura, J. Fang, P. Cieplak, A. Godzik, Z. Gu, and S.A. Lipton. 2009. S-nitrosylation of Drp1 mediates beta-amyloid-related mitochondrial fission and neuronal injury. *Science*. 324:102-105.
- Choe, C.U., and B.E. Ehrlich. 2006. The inositol 1,4,5-trisphosphate receptor (IP3R) and its regulators: sometimes good and sometimes bad teamwork. *Sci STKE*. 2006:re15.
- Christoforidis, S., H.M. McBride, R.D. Burgoyne, and M. Zerial. 1999. The Rab5 effector EEA1 is a core component of endosome docking. *Nature*. 397:621-625.
- Dacks, J.B., and W.F. Doolittle. 2001. Reconstructing/deconstructing the earliest eukaryotes: how comparative genomics can help. *Cell*. 107:419-425.
- de Brito, O.M., and L. Scorrano. 2008. Mitofusin 2 tethers endoplasmic reticulum to mitochondria. *Nature*. 456:605-610.
- De Stefani, D., A. Raffaello, E. Teardo, I. Szabò, and R. Rizzuto. 2011. A forty-kilodalton protein of the inner membrane is the mitochondrial calcium uniporter. *Nature*. 476:336-340.
- Deretic, D., L.A. Huber, N. Ransom, M. Mancini, K. Simons, and D.S. Papermaster. 1995. rab8 in retinal photoreceptors may participate in rhodopsin transport and in rod outer segment disk morphogenesis. *J Cell Sci*. 108 (Pt 1):215-224.
- Deretic, V. 2010. Autophagy in infection. *Curr Opin Cell Biol*. 22:252-262.
- Diekmann, Y., E. Seixas, M. Gouw, F. Tavares-Cadete, M.C. Seabra, and J.B. Pereira-Leal. 2011. Thousands of rab GTPases for the cell biologist. *PLoS Comput Biol*. 7:e1002217.
- Dirac-Svejstrup, A.B., T. Sumizawa, and S.R. Pfeffer. 1997. Identification of a GDI displacement factor that releases endosomal Rab GTPases from Rab-GDI. *Embo J*. 16:465-472.
- Dreier, L., and T.A. Rapoport. 2000. In vitro formation of the endoplasmic reticulum occurs independently of microtubules by a controlled fusion reaction. *J Cell Biol*. 148:883-898.
- Edgar, R.C. 2004. MUSCLE: a multiple sequence alignment method with reduced time and space complexity. *BMC Bioinformatics*. 5:113.
- Elachouri, G., S. Vidoni, C. Zanna, A. Pattyn, H. Boukhaddaoui, K. Gaget, P. Yu-Wai-Man, G. Gasparre, E. Sarzi, C. Delettre, A. Olichon, D. Loiseau, P. Reynier, P.F. Chinnery, A. Rotig, V. Carelli, C.P. Hamel, M. Rugolo, and G. Lenaers. 2011. OPA1 links human mitochondrial genome maintenance to mtDNA replication and distribution. *Genome Res*. 21:12-20.
- Elias, M., A. Brighouse, C. Gabernet-Castello, M.C. Field, and J.B. Dacks. 2012. Sculpting the endomembrane system in deep time: high resolution phylogenetics of Rab GTPases. *J Cell Sci*. 125:2500-2508.
- Ellis, K., J. Bagwell, and M. Bagnat. 2013. Notochord vacuoles are lysosome-related organelles that function in axis and spine morphogenesis. *J Cell Biol*. 200:667-679.

- Fader, C.M., D. Sánchez, M. Furlán, and M.I. Colombo. 2008. Induction of autophagy promotes fusion of multivesicular bodies with autophagic vacuoles in k562 cells. *Traffic*. 9:230-250.
- Feliciello, A., M.E. Gottesman, and E.V. Avvedimento. 2001. The biological functions of A-kinase anchor proteins. *J Mol Biol*. 308:99-114.
- Field, H.I., R.M. Coulson, and M.C. Field. 2013. An automated graphics tool for comparative genomics: the Coulson plot generator. *BMC Bioinformatics*. 14:141.
- Frasa, M.A., K.T. Koessmeier, M.R. Ahmadian, and V.M. Braga. 2012. Illuminating the functional and structural repertoire of human TBC/RABGAPs. *Nat Rev Mol Cell Biol*. 13:67-73.
- Friedman, J.R., L.L. Lackner, M. West, J.R. DiBenedetto, J. Nunnari, and G.K. Voeltz. 2011. ER tubules mark sites of mitochondrial division. *Science*. 334:358-362.
- Fujikawa, K., A.K. Satoh, S. Kawamura, and K. Ozaki. 2002. Molecular and functional characterization of a unique Rab protein, RABRP1, containing the WDIAGQE sequence in a GTPase motif. *Zoolog Sci*. 19:981-993.
- Gabernet-Castello, C., A.J. O'Reilly, J.B. Dacks, and M.C. Field. 2013. Evolution of Tre-2/Bub2/Cdc16 (TBC) Rab GTPase-activating proteins. *Mol Biol Cell*. 24:1574-1583.
- Gan-Or, Z., A. Bar-Shira, D. Dahary, A. Mirelman, M. Kedmi, T. Gurevich, N. Giladi, and A. Orr-Urtreger. 2012. Association of sequence alterations in the putative promoter of RAB7L1 with a reduced parkinson disease risk. *Arch Neurol*. 69:105-110.
- Gilady, S.Y., M. Bui, E.M. Lynes, M.D. Benson, R. Watts, J.E. Vance, and T. Simmen. 2010. Ero1alpha requires oxidizing and normoxic conditions to localize to the mitochondria-associated membrane (MAM). *Cell Stress Chaperones*. 15:619-629.
- Giorgi, C., D. De Stefani, A. Bononi, R. Rizzuto, and P. Pinton. 2009. Structural and functional link between the mitochondrial network and the endoplasmic reticulum. *Int J Biochem Cell Biol*. 41:1817-1827.
- Grimm, S. 2012. The ER-mitochondria interface: the social network of cell death. *Biochim Biophys Acta*. 1823:327-334.
- Grosshans, B.L., D. Ortiz, and P. Novick. 2006. Rabs and their effectors: achieving specificity in membrane traffic. *Proc Natl Acad Sci U S A*. 103:11821-11827.
- Grote, E., and P.J. Novick. 1999. Promiscuity in Rab-SNARE interactions. *Mol Biol Cell*. 10:4149-4161.
- Guindon, S., and O. Gascuel. 2003. A simple, fast, and accurate algorithm to estimate large phylogenies by maximum likelihood. *Syst Biol*. 52:696-704.
- Guo, W., D. Roth, C. Walch-Solimena, and P. Novick. 1999. The exocyst is an effector for Sec4p, targeting secretory vesicles to sites of exocytosis. *Embo J*. 18:1071-1080.
- Hall, B.G. 2011. Phylogenetic Trees made easy: a how-to manual. Sinauer Associates.
- Hamasaki, M., N. Furuta, A. Matsuda, A. Nezu, A. Yamamoto, N. Fujita, H. Oomori, T. Noda, T. Haraguchi, Y. Hiraoka, A. Amano, and T. Yoshimori. 2013. Autophagosomes form at ER-mitochondria contact sites. *Nature*. 495:389-393.
- Hardison, R.C. 2003. Comparative genomics. *PLoS Biol*. 1:E58.
- Hayashi, T., R. Rizzuto, G. Hajnoczky, and T.P. Su. 2009. MAM: more than just a housekeeper. *Trends Cell Biol*. 19:81-88.
- Hayashi, T., and T.P. Su. 2007. Sigma-1 receptor chaperones at the ER-mitochondrion interface regulate Ca(2+) signaling and cell survival. *Cell*. 131:596-610.

- Henchcliffe, C., and M.F. Beal. 2008. Mitochondrial biology and oxidative stress in Parkinson disease pathogenesis. *Nat Clin Pract Neurol.* 4:600-609.
- Hermann, G.J., L.K. Schroeder, C.A. Hieb, A.M. Kershner, B.M. Rabbitts, P. Fonarev, B.D. Grant, and J.R. Priess. 2005. Genetic analysis of lysosomal trafficking in *Caenorhabditis elegans*. *Mol Biol Cell.* 16:3273-3288.
- Herskovits, J.S., C.C. Burgess, R.A. Obar, and R.B. Vallee. 1993. Effects of mutant rat dynamin on endocytosis. *J Cell Biol.* 122:565-578.
- Hirota, Y., and Y. Tanaka. 2009. A small GTPase, human Rab32, is required for the formation of autophagic vacuoles under basal conditions. *Cell Mol Life Sci.* 66:2913-2932.
- Hoppins, S., L. Lackner, and J. Nunnari. 2007. The machines that divide and fuse mitochondria. *Annu Rev Biochem.* 76:751-780.
- Hou, L., J.X. Wang, and X.F. Zhao. 2011. Rab32 and the remodeling of the imaginal midgut in *Helicoverpa armigera*. *Amino Acids.* 40:953-961.
- Hu, J., Y. Shibata, P.P. Zhu, C. Voss, N. Rismanchi, W.A. Prinz, T.A. Rapoport, and C. Blackstone. 2009. A class of dynamin-like GTPases involved in the generation of the tubular ER network. *Cell.* 138:549-561.
- Hutagalung, A.H., and P.J. Novick. 2011. Role of Rab GTPases in membrane traffic and cell physiology. *Physiol Rev.* 91:119-149.
- Ishihara, N., M. Nomura, A. Jofuku, H. Kato, S.O. Suzuki, K. Masuda, H. Otera, Y. Nakanishi, I. Nonaka, Y. Goto, N. Taguchi, H. Morinaga, M. Maeda, R. Takayanagi, S. Yokota, and K. Mihara. 2009. Mitochondrial fission factor Drp1 is essential for embryonic development and synapse formation in mice. *Nat Cell Biol.* 11:958-966.
- Ishihara, N., H. Otera, T. Oka, and K. Mihara. 2012. Regulation and Physiologic Functions of GTPases in Mitochondrial Fusion and Fission in Mammals. *Antioxid Redox Signal.*
- Itakura, E., C. Kishi-Itakura, and N. Mizushima. 2012. The hairpin-type tail-anchored SNARE syntaxin 17 targets to autophagosomes for fusion with endosomes/lysosomes. *Cell.* 151:1256-1269.
- Itoh, T., N. Fujita, E. Kanno, A. Yamamoto, T. Yoshimori, and M. Fukuda. 2008. Golgi-resident small GTPase Rab33B interacts with Atg16L and modulates autophagosome formation. *Mol Biol Cell.* 19:2916-2925.
- Itoh, T., E. Kanno, T. Uemura, S. Waguri, and M. Fukuda. 2011. OATL1, a novel autophagosome-resident Rab33B-GAP, regulates autophagosomal maturation. *J Cell Biol.* 192:839-853.
- Itoh, T., A. Watabe, A. Toh-E, and Y. Matsui. 2002. Complex formation with Ypt11p, a rab-type small GTPase, is essential to facilitate the function of Myo2p, a class V myosin, in mitochondrial distribution in *Saccharomyces cerevisiae*. *Mol Cell Biol.* 22:7744-7757.
- Iwasawa, R., A.L. Mahul-Mellier, C. Datler, E. Pazarentzos, and S. Grimm. 2011. Fis1 and Bap31 bridge the mitochondria-ER interface to establish a platform for apoptosis induction. *Embo J.* 30:556-568.
- Jäger, D., E. Stockert, E. Jäger, A.O. Güre, M.J. Scanlan, A. Knuth, L.J. Old, and Y.T. Chen. 2000. Serological cloning of a melanocyte rab guanosine 5'-triphosphate-binding protein and a chromosome condensation protein from a melanoma complementary DNA library. *Cancer Res.* 60:3584-3591.
- Jäger, S., C. Bucci, I. Tanida, T. Ueno, E. Kominami, P. Saftig, and E.L. Eskelinen. 2004. Role for Rab7 in maturation of late autophagic vacuoles. *J Cell Sci.* 117:4837-4848.

- John, L.M., J.D. Lechleiter, and P. Camacho. 1998. Differential modulation of SERCA2 isoforms by calreticulin. *J Cell Biol.* 142:963-973.
- Jones, S.M., K.E. Howell, J.R. Henley, H. Cao, and M.A. McNiven. 1998. Role of dynamin in the formation of transport vesicles from the trans-Golgi network. *Science.* 279:573-577.
- Jordens, I., M. Fernandez-Borja, M. Marsman, S. Dusseljee, L. Janssen, J. Calafat, H. Janssen, R. Wubbolts, and J. Neefjes. 2001. The Rab7 effector protein RILP controls lysosomal transport by inducing the recruitment of dynein-dynactin motors. *Curr Biol.* 11:1680-1685.
- Jordens, I., M. Marsman, C. Kuijl, and J. Neefjes. 2005. Rab proteins, connecting transport and vesicle fusion. *Traffic.* 6:1070-1077.
- Kahn, R.A., C.J. Der, and G.M. Bokoch. 1992. The ras superfamily of GTP-binding proteins: guidelines on nomenclature. *FASEB J.* 6:2512-2513.
- Kamhi-Nesher, S., M. Shenkman, S. Tolchinsky, S.V. Fromm, R. Ehrlich, and G.Z. Lederkremer. 2001. A novel quality control compartment derived from the endoplasmic reticulum. *Mol Biol Cell.* 12:1711-1723.
- Knott, A.B., G. Perkins, R. Schwarzenbacher, and E. Bossy-Wetzel. 2008. Mitochondrial fragmentation in neurodegeneration. *Nat Rev Neurosci.* 9:505-518.
- Kornmann, B., E. Currie, S.R. Collins, M. Schuldiner, J. Nunnari, J.S. Weissman, and P. Walter. 2009. An ER-mitochondria tethering complex revealed by a synthetic biology screen. *Science.* 325:477-481.
- Kraft, C., and S. Martens. 2012. Mechanisms and regulation of autophagosome formation. *Curr Opin Cell Biol.* 24:496-501.
- Lang, T., and R. Jahn. 2008. Core proteins of the secretory machinery. *Handb Exp Pharmacol.* 107-127.
- Lee, C., and L.B. Chen. 1988. Dynamic behavior of endoplasmic reticulum in living cells. *Cell.* 54:37-46.
- Lee, J., S. Giordano, and J. Zhang. 2012. Autophagy, mitochondria and oxidative stress: cross-talk and redox signalling. *Biochem J.* 441:523-540.
- Leitman, J., E. Ron, N. Ogen-Shtern, and G.Z. Lederkremer. 2013. Compartmentalization of endoplasmic reticulum quality control and ER-associated degradation factors. *DNA Cell Biol.* 32:2-7.
- Lewin, T.M., J.H. Kim, D.A. Granger, J.E. Vance, and R.A. Coleman. 2001. Acyl-CoA synthetase isoforms 1, 4, and 5 are present in different subcellular membranes in rat liver and can be inhibited independently. *J Biol Chem.* 276:24674-24679.
- Lewin, T.M., C.G. Van Horn, S.K. Krisans, and R.A. Coleman. 2002. Rat liver acyl-CoA synthetase 4 is a peripheral-membrane protein located in two distinct subcellular organelles, peroxisomes, and mitochondrial-associated membrane. *Arch Biochem Biophys.* 404:263-270.
- Lieberman, A.R. 1971. Microtubule-associated smooth endoplasmic reticulum in the frog's brain. *Z Zellforsch Mikrosk Anat.* 116:564-577.
- Lin, S., S. Sun, and J. Hu. 2012. Molecular basis for sculpting the endoplasmic reticulum membrane. *Int J Biochem Cell Biol.* 44:1436-1443.
- Lipatova, Z., A.A. Tokarev, Y. Jin, J. Mulholland, L.S. Weisman, and N. Segev. 2008. Direct interaction between a myosin V motor and the Rab GTPases Ypt31/32 is required for polarized secretion. *Mol Biol Cell.* 19:4177-4187.
- Loftus, S.K., D.M. Larson, L.L. Baxter, A. Antonellis, Y. Chen, X. Wu, Y. Jiang, M. Bittner, J.A. Hammer, and W.J. Pavan. 2002. Mutation of melanosome protein RAB38 in chocolate mice. *Proc Natl Acad Sci U S A.* 99:4471-4476.

- Lombardi, D., T. Soldati, M.A. Riederer, Y. Goda, M. Zerial, and S.R. Pfeffer. 1993. Rab9 functions in transport between late endosomes and the trans Golgi network. *Embo J.* 12:677-682.
- Lopes, V.S., C. Wasmeier, M.C. Seabra, and C.E. Futter. 2007. Melanosome maturation defect in Rab38-deficient retinal pigment epithelium results in instability of immature melanosomes during transient melanogenesis. *Mol Biol Cell.* 18:3914-3927.
- Lupashin, V.V., and M.G. Waters. 1997. t-SNARE activation through transient interaction with a rab-like guanosine triphosphatase. *Science.* 276:1255-1258.
- Lynes, E.M., and T. Simmen. 2011. Urban planning of the endoplasmic reticulum (ER): how diverse mechanisms segregate the many functions of the ER. *Biochim Biophys Acta.* 1813:1893-1905.
- Maier, O., M. Knoblich, and P. Westermann. 1996. Dynamin II binds to the trans-Golgi network. *Biochem Biophys Res Commun.* 223:229-233.
- McBride, H.M., V. Rybin, C. Murphy, A. Giner, R. Teasdale, and M. Zerial. 1999. Oligomeric complexes link Rab5 effectors with NSF and drive membrane fusion via interactions between EEA1 and syntaxin 13. *Cell.* 98:377-386.
- McGraw, C.F., A.V. Somlyo, and M.P. Blaustein. 1980. Localization of calcium in presynaptic nerve terminals. An ultrastructural and electron microprobe analysis. *J Cell Biol.* 85:228-241.
- McLauchlan, H., J. Newell, N. Morrice, A. Osborne, M. West, and E. Smythe. 1998. A novel role for Rab5-GDI in ligand sequestration into clathrin-coated pits. *Curr Biol.* 8:34-45.
- Meier, P.J., M.A. Spycher, and U.A. Meyer. 1981. Isolation and characterization of rough endoplasmic reticulum associated with mitochondria from normal rat liver. *Biochim Biophys Acta.* 646:283-297.
- Merrill, R.A., R.K. Dagda, A.S. Dickey, J.T. Cribbs, S.H. Green, Y.M. Usachev, and S. Strack. 2011. Mechanism of neuroprotective mitochondrial remodeling by PKA/AKAP1. *PLoS Biol.* 9:e1000612.
- Michel, A.H., and B. Kornmann. 2012. The ERMES complex and ER-mitochondria connections. *Biochem Soc Trans.* 40:445-450.
- Milburn, M.V., L. Tong, A.M. deVos, A. Brünger, Z. Yamaizumi, S. Nishimura, and S.H. Kim. 1990. Molecular switch for signal transduction: structural differences between active and inactive forms of protooncogenic ras proteins. *Science.* 247:939-945.
- Møller, J.V., C. Olesen, A.M. Winther, and P. Nissen. 2010. The sarcoplasmic Ca²⁺-ATPase: design of a perfect chemi-osmotic pump. *Q Rev Biophys.* 43:501-566.
- Moyer, B.D., B.B. Allan, and W.E. Balch. 2001. Rab1 interaction with a GM130 effector complex regulates COPII vesicle cis-Golgi tethering. *Traffic.* 2:268-276.
- Munafó, D.B., and M.I. Colombo. 2002. Induction of autophagy causes dramatic changes in the subcellular distribution of GFP-Rab24. *Traffic.* 3:472-482.
- Muppirala, M., V. Gupta, and G. Swarup. 2011. Syntaxin 17 cycles between the ER and ERGIC and is required to maintain the architecture of ERGIC and Golgi. *Biol Cell.* 103:333-350.
- Myhill, N., E.M. Lynes, J.A. Nanji, A.D. Blagoveshchenskaya, H. Fei, K. Carmine Simmen, T.J. Cooper, G. Thomas, and T. Simmen. 2008. The subcellular distribution of calnexin is mediated by PACS-2. *Mol Biol Cell.* 19:2777-2788.
- Norian, L., I.A. Dragoi, and T. O'Halloran. 1999. Molecular characterization of rabE, a developmentally regulated Dictyostelium homolog of mammalian rab GTPases. *DNA Cell Biol.* 18:59-64.

- Nottingham, R.M., I.G. Ganley, F.A. Barr, D.G. Lambright, and S.R. Pfeffer. 2011. RUTBC1 protein, a Rab9A effector that activates GTP hydrolysis by Rab32 and Rab33B proteins. *J Biol Chem.* 286:33213-33222.
- Novick, P., M. Medkova, G. Dong, A. Hutagalung, K. Reinisch, and B. Grosshans. 2006. Interactions between Rabs, tethers, SNAREs and their regulators in exocytosis. *Biochem Soc Trans.* 34:683-686.
- Obar, R.A., C.A. Collins, J.A. Hammarback, H.S. Shpetner, and R.B. Vallee. 1990. Molecular cloning of the microtubule-associated mechanochemical enzyme dynamin reveals homology with a new family of GTP-binding proteins. *Nature.* 347:256-261.
- Oertle, T., M. Klinger, C.A. Stuermer, and M.E. Schwab. 2003. A reticular rhapsody: phylogenetic evolution and nomenclature of the RTN/Nogo gene family. *FASEB J.* 17:1238-1247.
- Oettinghaus, B., M. Licci, L. Scorrano, and S. Frank. 2012. Less than perfect divorces: dysregulated mitochondrial fission and neurodegeneration. *Acta Neuropathol.* 123:189-203.
- Olichon, A., L. Baricault, N. Gas, E. Guillou, A. Valette, P. Belenguer, and G. Lenaers. 2003. Loss of OPA1 perturbs the mitochondrial inner membrane structure and integrity, leading to cytochrome c release and apoptosis. *J Biol Chem.* 278:7743-7746.
- Orso, G., D. Pendin, S. Liu, J. Toso, T.J. Moss, J.E. Faust, M. Micaroni, A. Egorova, A. Martinuzzi, J.A. McNew, and A. Daga. 2009. Homotypic fusion of ER membranes requires the dynamin-like GTPase atlastin. *Nature.* 460:978-983.
- Osanai, K., M. Iguchi, K. Takahashi, Y. Nambu, T. Sakuma, H. Toga, N. Ohya, H. Shimizu, J.H. Fisher, and D.R. Voelker. 2001. Expression and localization of a novel Rab small G protein (Rab38) in the rat lung. *Am J Pathol.* 158:1665-1675.
- Otera, H., C. Wang, M.M. Cleland, K. Setoguchi, S. Yokota, R.J. Youle, and K. Mihara. 2010. Mff is an essential factor for mitochondrial recruitment of Drp1 during mitochondrial fission in mammalian cells. *J Cell Biol.* 191:1141-1158.
- Palade, G. 1975. Intracellular aspects of the process of protein synthesis. *Science.* 189:867.
- Park, M., A.S. Serpinskaya, N. Papalopulu, and V.I. Gelfand. 2007. Rab32 regulates melanosome transport in *Xenopus* melanophores by protein kinase A recruitment. *Curr Biol.* 17:2030-2034.
- Park, S.H., and C. Blackstone. 2010. Further assembly required: construction and dynamics of the endoplasmic reticulum network. *EMBO Rep.* 11:515-521.
- Parys, J.B., and H. De Smedt. 2012. Inositol 1,4,5-trisphosphate and its receptors. *Adv Exp Med Biol.* 740:255-279.
- Pereira-Leal, J.B., A.N. Hume, and M.C. Seabra. 2001. Prenylation of Rab GTPases: molecular mechanisms and involvement in genetic disease. *FEBS Lett.* 498:197-200.
- Pereira-Leal, J.B., and M.C. Seabra. 2000. The mammalian Rab family of small GTPases: definition of family and subfamily sequence motifs suggests a mechanism for functional specificity in the Ras superfamily. *J Mol Biol.* 301:1077-1087.
- Pereira-Leal, J.B., and M.C. Seabra. 2001. Evolution of the Rab family of small GTP-binding proteins. *J Mol Biol.* 313:889-901.
- Perkins, G., C. Renken, M.E. Martone, S.J. Young, M. Ellisman, and T. Frey. 1997. Electron tomography of neuronal mitochondria: three-dimensional structure and organization of cristae and membrane contacts. *J Struct Biol.* 119:260-272.

- Pfeffer, S.R. 2007. Unsolved mysteries in membrane traffic. *Annu Rev Biochem.* 76:629-645.
- Philippe, H., Y. Zhou, H. Brinkmann, N. Rodrigue, and F. Delsuc. 2005. Heterotachy and long-branch attraction in phylogenetics. *BMC Evol Biol.* 5:50.
- Pichler, H., B. Gaigg, C. Hrastnik, G. Achleitner, S.D. Kohlwein, G. Zellnig, A. Perktold, and G. Daum. 2001. A subfraction of the yeast endoplasmic reticulum associates with the plasma membrane and has a high capacity to synthesize lipids. *Eur J Biochem.* 268:2351-2361.
- Pitts, K.R., Y. Yoon, E.W. Krueger, and M.A. McNiven. 1999. The dynamin-like protein DLP1 is essential for normal distribution and morphology of the endoplasmic reticulum and mitochondria in mammalian cells. *Mol Biol Cell.* 10:4403-4417.
- Ponpuak, M., A.S. Davis, E.A. Roberts, M.A. Delgado, C. Dinkins, Z. Zhao, H.W. Virgin, G.B. Kyei, T. Johansen, I. Vergne, and V. Deretic. 2010. Delivery of cytosolic components by autophagic adaptor protein p62 endows autophagosomes with unique antimicrobial properties. *Immunity.* 32:329-341.
- Prinz, W.A., L. Grzyb, M. Veenhuis, J.A. Kahana, P.A. Silver, and T.A. Rapoport. 2000. Mutants affecting the structure of the cortical endoplasmic reticulum in *Saccharomyces cerevisiae*. *J Cell Biol.* 150:461-474.
- Pylypenko, O., A. Rak, T. Durek, S. Kushnir, B.E. Dursina, N.H. Thomae, A.T. Constantinescu, L. Brunsveld, A. Watzke, H. Waldmann, R.S. Goody, and K. Alexandrov. 2006. Structure of doubly prenylated Ypt1:GDI complex and the mechanism of GDI-mediated Rab recycling. *Embo J.* 25:13-23.
- Ran, Q., R. Wadhwa, R. Kawai, S.C. Kaul, R.N. Sifers, R.J. Bick, J.R. Smith, and O.M. Pereira-Smith. 2000. Extramitochondrial localization of mortalin/mthsp70/PBP74/GRP75. *Biochem Biophys Res Commun.* 275:174-179.
- Raturi, A., and T. Simmen. 2013. Where the endoplasmic reticulum and the mitochondrion tie the knot: the mitochondria-associated membrane (MAM). *Biochim Biophys Acta.* 1833:213-224.
- Reddy, P.H., T.P. Reddy, M. Manczak, M.J. Calkins, U. Shirendeb, and P. Mao. 2011. Dynamin-related protein 1 and mitochondrial fragmentation in neurodegenerative diseases. *Brain Res Rev.* 67:103-118.
- Richardson, P.M., and L.I. Zon. 1995. Molecular cloning of a cDNA with a novel domain present in the *trc-2* oncogene and the yeast cell cycle regulators BUB2 and *cdc16*. *Oncogene.* 11:1139-1148.
- Riederer, M.A., T. Soldati, A.D. Shapiro, J. Lin, and S.R. Pfeffer. 1994. Lysosome biogenesis requires Rab9 function and receptor recycling from endosomes to the trans-Golgi network. *J Cell Biol.* 125:573-582.
- Rismanchi, N., C. Soderblom, J. Stadler, P.P. Zhu, and C. Blackstone. 2008. Atlastin GTPases are required for Golgi apparatus and ER morphogenesis. *Hum Mol Genet.* 17:1591-1604.
- Rizzuto, R., M. Brini, M. Murgia, and T. Pozzan. 1993. Microdomains with high Ca²⁺ close to IP₃-sensitive channels that are sensed by neighboring mitochondria. *Science.* 262:744-747.
- Rizzuto, R., P. Pinton, W. Carrington, F.S. Fay, K.E. Fogarty, L.M. Lifshitz, R.A. Tuft, and T. Pozzan. 1998. Close contacts with the endoplasmic reticulum as determinants of mitochondrial Ca²⁺ responses. *Science.* 280:1763-1766.
- Roderick, H.L., J.D. Lechleiter, and P. Camacho. 2000. Cytosolic phosphorylation of calnexin controls intracellular Ca²⁺ oscillations via an interaction with SERCA2b. *J Cell Biol.* 149:1235-1248.

- Rojas, R., T. van Vlijmen, G.A. Mardones, Y. Prabhu, A.L. Rojas, S. Mohammed, A.J. Heck, G. Raposo, P. van der Sluijs, and J.S. Bonifacino. 2008. Regulation of retromer recruitment to endosomes by sequential action of Rab5 and Rab7. *J Cell Biol.* 183:513-526.
- Ronquist, F., and J.P. Huelsenbeck. 2003. MrBayes 3: Bayesian phylogenetic inference under mixed models. *Bioinformatics.* 19:1572-1574.
- Rubinsztein, D.C., T. Shpilka, and Z. Elazar. 2012. Mechanisms of autophagosome biogenesis. *Curr Biol.* 22:R29-34.
- Rusiñol, A.E., Z. Cui, M.H. Chen, and J.E. Vance. 1994. A unique mitochondria-associated membrane fraction from rat liver has a high capacity for lipid synthesis and contains pre-Golgi secretory proteins including nascent lipoproteins. *J Biol Chem.* 269:27494-27502.
- Sai, Y., Z. Zou, K. Peng, and Z. Dong. 2012. The Parkinson's disease-related genes act in mitochondrial homeostasis. *Neurosci Biobehav Rev.* 36:2034-2043.
- Sandoval, C.O., and T. Simmen. 2012. Rab proteins of the endoplasmic reticulum: functions and interactors. *Biochem Soc Trans.* 40:1426-1432.
- Saraste, J., and K. Svensson. 1991. Distribution of the intermediate elements operating in ER to Golgi transport. *J Cell Sci.* 100 (Pt 3):415-430.
- Schlacht, A., K. Mowbrey, M. Elias, R.A. Kahn, and J.B. Dacks. 2013. Ancient Complexity, Opisthokont Plasticity, and Discovery of the 11th Subfamily of Arf GAP Proteins. *Traffic.* 14:636-649.
- Schlichting, I., S.C. Almo, G. Rapp, K. Wilson, K. Petratos, A. Lentfer, A. Wittinghofer, W. Kabsch, E.F. Pai, and G.A. Petsko. 1990. Time-resolved X-ray crystallographic study of the conformational change in Ha-Ras p21 protein on GTP hydrolysis. *Nature.* 345:309-315.
- Seabra, M.C., J.L. Goldstein, T.C. Südhof, and M.S. Brown. 1992. Rab geranylgeranyl transferase. A multisubunit enzyme that prenylates GTP-binding proteins terminating in Cys-X-Cys or Cys-Cys. *J Biol Chem.* 267:14497-14503.
- Seto, S., K. Tsujimura, and Y. Koide. 2011. Rab GTPases regulating phagosome maturation are differentially recruited to mycobacterial phagosomes. *Traffic.* 12:407-420.
- Shibata, Y., T. Shemesh, W.A. Prinz, A.F. Palazzo, M.M. Kozlov, and T.A. Rapoport. 2010. Mechanisms determining the morphology of the peripheral ER. *Cell.* 143:774-788.
- Shibata, Y., G.K. Voeltz, and T.A. Rapoport. 2006. Rough sheets and smooth tubules. *Cell.* 126:435-439.
- Shibata, Y., C. Voss, J.M. Rist, J. Hu, T.A. Rapoport, W.A. Prinz, and G.K. Voeltz. 2008. The reticulon and DP1/Yop1p proteins form immobile oligomers in the tubular endoplasmic reticulum. *J Biol Chem.* 283:18892-18904.
- Shimizu, F., T. Katagiri, M. Suzuki, T.K. Watanabe, S. Okuno, Y. Kuga, M. Nagata, T. Fujiwara, Y. Nakamura, and E. Takahashi. 1997. Cloning and chromosome assignment to 1q32 of a human cDNA (RAB7L1) encoding a small GTP-binding protein, a member of the RAS superfamily. *Cytogenet Cell Genet.* 77:261-263.
- Shore, G.C., and J.R. Tata. 1977. Two fractions of rough endoplasmic reticulum from rat liver. I. Recovery of rapidly sedimenting endoplasmic reticulum in association with mitochondria. *J Cell Biol.* 72:714-725.
- Shoshan-Barmatz, V., R. Zalk, D. Gincel, and N. Vardi. 2004. Subcellular localization of VDAC in mitochondria and ER in the cerebellum. *Biochim Biophys Acta.* 1657:105-114.

- Simmen, T., J.E. Aslan, A.D. Blagoveshchenskaya, L. Thomas, L. Wan, Y. Xiang, S.F. Feliciangeli, C.H. Hung, C.M. Crump, and G. Thomas. 2005. PACS-2 controls endoplasmic reticulum-mitochondria communication and Bid-mediated apoptosis. *Embo J.* 24:717-729.
- Simón-Sánchez, J., C. Schulte, J.M. Bras, M. Sharma, J.R. Gibbs, D. Berg, C. Paisan-Ruiz, P. Lichtner, S.W. Scholz, D.G. Hernandez, R. Krüger, M. Federoff, C. Klein, A. Goate, J. Perlmutter, M. Bonin, M.A. Nalls, T. Illig, C. Gieger, H. Houlden, M. Steffens, M.S. Okun, B.A. Racette, M.R. Cookson, K.D. Foote, H.H. Fernandez, B.J. Traynor, S. Schreiber, S. Arepalli, R. Zonozi, K. Gwinn, M. van der Brug, G. Lopez, S.J. Chanock, A. Schatzkin, Y. Park, A. Hollenbeck, J. Gao, X. Huang, N.W. Wood, D. Lorenz, G. Deuschl, H. Chen, O. Riess, J.A. Hardy, A.B. Singleton, and T. Gasser. 2009. Genome-wide association study reveals genetic risk underlying Parkinson's disease. *Nat Genet.* 41:1308-1312.
- Simonsen, A., J.M. Gaullier, A. D'Arrigo, and H. Stenmark. 1999. The Rab5 effector EEA1 interacts directly with syntaxin-6. *J Biol Chem.* 274:28857-28860.
- Siniosoglou, S., and H.R. Pelham. 2001. An effector of Ypt6p binds the SNARE Tlg1p and mediates selective fusion of vesicles with late Golgi membranes. *Embo J.* 20:5991-5998.
- Sitia, R., and J. Meldolesi. 1992. Endoplasmic reticulum: a dynamic patchwork of specialized subregions. *Mol Biol Cell.* 3:1067-1072.
- Sivars, U., D. Aivazian, and S.R. Pfeffer. 2003. Yip3 catalyses the dissociation of endosomal Rab-GDI complexes. *Nature.* 425:856-859.
- Smirnova, E., L. Griparic, D.L. Shurland, and A.M. van der Bliek. 2001. Dynamin-related protein Drp1 is required for mitochondrial division in mammalian cells. *Mol Biol Cell.* 12:2245-2256.
- Smirnova, E., D.L. Shurland, S.N. Ryazantsev, and A.M. van der Bliek. 1998. A human dynamin-related protein controls the distribution of mitochondria. *J Cell Biol.* 143:351-358.
- Somlyo, A.P. 1984. Cell physiology: cellular site of calcium regulation. *Nature.* 309:516-517.
- Sönnichsen, B., M. Lowe, T. Levine, E. Jämsä, B. Dirac-Svejstrup, and G. Warren. 1998. A role for giantin in docking COPI vesicles to Golgi membranes. *J Cell Biol.* 140:1013-1021.
- Sontag, J.M., E.M. Fykse, Y. Ushkaryov, J.P. Liu, P.J. Robinson, and T.C. Südhof. 1994. Differential expression and regulation of multiple dynamins. *J Biol Chem.* 269:4547-4554.
- Spanò, S., and J.E. Galán. 2012. A Rab32-dependent pathway contributes to Salmonella typhi host restriction. *Science.* 338:960-963.
- Spanò, S., X. Liu, and J.E. Galán. 2011. Proteolytic targeting of Rab29 by an effector protein distinguishes the intracellular compartments of human-adapted and broad-host Salmonella. *Proc Natl Acad Sci U S A.* 108:18418-18423.
- Stamatakis, A. 2006. RAxML-VI-HPC: maximum likelihood-based phylogenetic analyses with thousands of taxa and mixed models. *Bioinformatics.* 22:2688-2690.
- Steggmaier, M., V. Oorschot, J. Klumperman, and R.H. Scheller. 2000. Syntaxin 17 is abundant in steroidogenic cells and implicated in smooth endoplasmic reticulum membrane dynamics. *Mol Biol Cell.* 11:2719-2731.
- Steggmaier, M., B. Yang, J.S. Yoo, B. Huang, M. Shen, S. Yu, Y. Luo, and R.H. Scheller. 1998. Three novel proteins of the syntaxin/SNAP-25 family. *J Biol Chem.* 273:34171-34179.

- Stenmark, H., and V.M. Olkkonen. 2001. The Rab GTPase family. *Genome Biol.* 2:REVIEWS3007.
- Stone, S.J., and J.E. Vance. 2000. Phosphatidylserine synthase-1 and -2 are localized to mitochondria-associated membranes. *J Biol Chem.* 275:34534-34540.
- Strack, S., and J.T. Cribbs. 2012. Allosteric modulation of Drp1 mechanoenzyme assembly and mitochondrial fission by the variable domain. *J Biol Chem.* 287:10990-11001.
- Stroupe, C., and A.T. Brunger. 2000. Crystal structures of a Rab protein in its inactive and active conformations. *J Mol Biol.* 304:585-598.
- Suvorova, E.S., R. Duden, and V.V. Lupashin. 2002. The Sec34/Sec35p complex, a Ypt1p effector required for retrograde intra-Golgi trafficking, interacts with Golgi SNAREs and COPI vesicle coat proteins. *J Cell Biol.* 157:631-643.
- Szabadkai, G., K. Bianchi, P. Várnai, D. De Stefani, M.R. Wieckowski, D. Cavagna, A.I. Nagy, T. Balla, and R. Rizzuto. 2006. Chaperone-mediated coupling of endoplasmic reticulum and mitochondrial Ca²⁺ channels. *J Cell Biol.* 175:901-911.
- Taguchi, N., N. Ishihara, A. Jofuku, T. Oka, and K. Mihara. 2007. Mitotic phosphorylation of dynamin-related GTPase Drp1 participates in mitochondrial fission. *J Biol Chem.* 282:11521-11529.
- Takei, K., P.S. McPherson, S.L. Schmid, and P. De Camilli. 1995. Tubular membrane invaginations coated by dynamin rings are induced by GTP-gamma S in nerve terminals. *Nature.* 374:186-190.
- Tamura, K., N. Ohbayashi, Y. Maruta, E. Kanno, T. Itoh, and M. Fukuda. 2009. Varp is a novel Rab32/38-binding protein that regulates Tyrp1 trafficking in melanocytes. *Mol Biol Cell.* 20:2900-2908.
- Touchot, N., P. Chardin, and A. Tavitian. 1987. Four additional members of the ras gene superfamily isolated by an oligonucleotide strategy: molecular cloning of YPT-related cDNAs from a rat brain library. *Proc Natl Acad Sci U S A.* 84:8210-8214.
- Tucci, A., M.A. Nalls, H. Houlden, T. Revesz, A.B. Singleton, N.W. Wood, J. Hardy, and C. Paisán-Ruiz. 2010. Genetic variability at the PARK16 locus. *Eur J Hum Genet.* 18:1356-1359.
- Uchiyama, Y., M. Shibata, M. Koike, K. Yoshimura, and M. Sasaki. 2008. Autophagy-physiology and pathophysiology. *Histochem Cell Biol.* 129:407-420.
- Ulrich, P.N., V. Jimenez, M. Park, V.P. Martins, J. Atwood, K. Moles, D. Collins, P. Rohloff, R. Tarleton, S.N. Moreno, R. Orlando, and R. Docampo. 2011. Identification of contractile vacuole proteins in *Trypanosoma cruzi*. *PLoS One.* 6:e18013.
- Ungar, D., T. Oka, M. Krieger, and F.M. Hughson. 2006. Retrograde transport on the COG railway. *Trends Cell Biol.* 16:113-120.
- Vallee, R.B., J.S. Herskovits, J.G. Aghajanian, C.C. Burgess, and H.S. Shpetner. 1993. Dynamin, a GTPase involved in the initial stages of endocytosis. *Ciba Found Symp.* 176:185-193; discussion 193-187.
- van de Velde, H.J., A.J. Roebroek, N.H. Senden, F.C. Ramaekers, and W.J. Van de Ven. 1994. NSP-encoded reticulons, neuroendocrine proteins of a novel gene family associated with membranes of the endoplasmic reticulum. *J Cell Sci.* 107 (Pt 9):2403-2416.
- Vance, J.E. 1990. Phospholipid synthesis in a membrane fraction associated with mitochondria. *J Biol Chem.* 265:7248-7256.
- Vetter, I.R., and A. Wittinghofer. 2001. The guanine nucleotide-binding switch in three dimensions. *Science.* 294:1299-1304.

- Voelker, D.R. 1989. Reconstitution of phosphatidylserine import into rat liver mitochondria. *J Biol Chem.* 264:8019-8025.
- Voeltz, G.K., W.A. Prinz, Y. Shibata, J.M. Rist, and T.A. Rapoport. 2006. A class of membrane proteins shaping the tubular endoplasmic reticulum. *Cell.* 124:573-586.
- Voigt, J., J.A. Chen, M. Gilchrist, E. Amaya, and N. Papalopulu. 2005. Expression cloning screening of a unique and full-length set of cDNA clones is an efficient method for identifying genes involved in *Xenopus* neurogenesis. *Mech Dev.* 122:289-306.
- Wadhwa, R., K. Taira, and S.C. Kaul. 2002. An Hsp70 family chaperone, mortalin/mthsp70/PBP74/Grp75: what, when, and where? *Cell Stress Chaperones.* 7:309-316.
- Walker, G., R.G. Dorrell, A. Schlacht, and J.B. Dacks. 2011. Eukaryotic systematics: a user's guide for cell biologists and parasitologists. *Parasitology.* 138:1638-1663.
- Wang, C., Z. Liu, and X. Huang. 2012. Rab32 is important for autophagy and lipid storage in *Drosophila*. *PLoS One.* 7:e32086.
- Wang, F., H. Zhang, X. Zhang, Y. Wang, F. Ren, Y. Zhai, and Z. Chang. 2008. Varp interacts with Rab38 and functions as its potential effector. *Biochem Biophys Res Commun.* 372:162-167.
- Wasmeier, C., M. Romao, L. Plowright, D.C. Bennett, G. Raposo, and M.C. Seabra. 2006. Rab38 and Rab32 control post-Golgi trafficking of melanogenic enzymes. *J Cell Biol.* 175:271-281.
- Watson, P., and D.J. Stephens. 2005. ER-to-Golgi transport: form and formation of vesicular and tubular carriers. *Biochim Biophys Acta.* 1744:304-315.
- Whyte, J.R., and S. Munro. 2002. Vesicle tethering complexes in membrane traffic. *J Cell Sci.* 115:2627-2637.
- Wideman, J.G., R.M. Gawryluk, M.W. Gray, and J.B. Dacks. 2013. The Ancient and Widespread Nature of the ER-Mitochondria Encounter Structure. *Mol Biol Evol.* 30:2044-2049.
- Wilson, A.L., R.A. Erdman, and W.A. Maltese. 1996. Association of Rab1B with GDP-dissociation inhibitor (GDI) is required for recycling but not initial membrane targeting of the Rab protein. *J Biol Chem.* 271:10932-10940.
- Wu, Y.W., K.T. Tan, H. Waldmann, R.S. Goody, and K. Alexandrov. 2007. Interaction analysis of prenylated Rab GTPase with Rab escort protein and GDP dissociation inhibitor explains the need for both regulators. *Proc Natl Acad Sci U S A.* 104:12294-12299.
- Yi, M., D. Weaver, and G. Hajnóczky. 2004. Control of mitochondrial motility and distribution by the calcium signal: a homeostatic circuit. *J Cell Biol.* 167:661-672.
- Yoon, Y., E.W. Krueger, B.J. Oswald, and M.A. McNiven. 2003. The mitochondrial protein hFis1 regulates mitochondrial fission in mammalian cells through an interaction with the dynamin-like protein DLP1. *Mol Cell Biol.* 23:5409-5420.
- Yoon, Y., K.R. Pitts, S. Dahan, and M.A. McNiven. 1998. A novel dynamin-like protein associates with cytoplasmic vesicles and tubules of the endoplasmic reticulum in mammalian cells. *J Cell Biol.* 140:779-793.
- Zerial, M., and H. McBride. 2001. Rab proteins as membrane organizers. *Nat Rev Mol Cell Biol.* 2:107-117.
- Zhang, F., H. Liu, S. Chen, H. Low, L. Sun, Y. Cui, T. Chu, Y. Li, X. Fu, Y. Yu, G. Yu, B. Shi, H. Tian, D. Liu, X. Yu, J. Li, N. Lu, F. Bao, C. Yuan, J. Liu, L. Zhang, Y. Sun, M. Chen, Q. Yang, H. Yang, R. Yang, Q. Wang, F. Zuo, H. Zhang, C.C.

- Khor, M.L. Hibberd, S. Yang, and X. Zhang. 2011. Identification of two new loci at IL23R and RAB32 that influence susceptibility to leprosy. *Nat Genet.* 43:1247-1251.
- Zheng, Y.T., S. Shahnazari, A. Brech, T. Lamark, T. Johansen, and J.H. Brumell. 2009. The adaptor protein p62/SQSTM1 targets invading bacteria to the autophagy pathway. *J Immunol.* 183:5909-5916.
- Zhu, P.P., A. Patterson, B. Lavoie, J. Stadler, M. Shoeb, R. Patel, and C. Blackstone. 2003. Cellular localization, oligomerization, and membrane association of the hereditary spastic paraplegia 3A (SPG3A) protein atlastin. *J Biol Chem.* 278:49063-49071.

CHAPTER 7:

Appendix

7. APPENDIX

Table 7.1. List of eukaryotic organisms used in this study. The following table shows the list of organisms used in the comparative genomics studies of this thesis, along with a brief description of each organism and the supergroup and subgroups they belong to.

	Organism			Supergroup	Subgroup		Description
1	<i>H. sapiens</i>	<i>Homo sapiens</i>	Hsa	Opisthokonta	Metazoa	Vertebrates	Human
2	<i>G. gallus</i>	<i>Gallus gallus</i>	Gga	Opisthokonta	Metazoa	Vertebrates	Rooster
3	<i>X. tropicalis</i>	<i>Xenopus tropicalis</i>	Xtr	Opisthokonta	Metazoa	Vertebrates	Frog
4	<i>D. rerio</i>	<i>Danio rerio</i>	Dre	Opisthokonta	Metazoa	Vertebrates	Zebra fish
5	<i>C. milii</i>	<i>Callorhincus milii</i>	Cmi	Opisthokonta	Metazoa	Vertebrates	Elephant shark
6	<i>S. canicula</i>	<i>Scyliorhinus canicula</i>	Sca	Opisthokonta	Metazoa	Vertebrates	Catshark
7	<i>L. erinacea</i>	<i>Leucoraja erinacea</i>	Ler	Opisthokonta	Metazoa	Vertebrates	Little skate fish
8	<i>P. marinus</i>	<i>Petromyzon marinus</i>	Pmi	Opisthokonta	Metazoa	Vertebrates	Sea lamprey
9	<i>B. floridae</i>	<i>Branchiostoma floridae</i>	Bfl	Opisthokonta	Metazoa	Vertebrates	Lancelate
10	<i>C. intestinalis</i>	<i>Ciona intestinalis</i>	Cin	Opisthokonta	Metazoa	Invertebrates	Sea squirt
11	<i>C. teleta</i>	<i>Capitella teleta</i>	Cte	Opisthokonta	Metazoa	Invertebrates	Polychaete worm
12	<i>S. purpuratus</i>	<i>Strongylocentrotus purpuratus</i>	Spu	Opisthokonta	Metazoa	Invertebrates	Purple sea urchin
13	<i>D. melanogaster</i>	<i>Drosophila melanogaster</i>	Dme	Opisthokonta	Metazoa	Invertebrates	Fruit fly
14	<i>C. elegans</i>	<i>Caenorhabditis elegans</i>	Cel	Opisthokonta	Metazoa	Invertebrates	Worm, nematode
15	<i>L. gigantea</i>	<i>Lottia gigantea</i>	Lgi	Opisthokonta	Metazoa	Invertebrates	Sea snail
16	<i>H. magnipapillata</i>	<i>Hydra magnipapillata</i>	Hma	Opisthokonta	Metazoa	Invertebrates	Fresh water polyp ("immortal")
17	<i>N. vectensis</i>	<i>Nematostella vectensis</i>	Nve	Opisthokonta	Metazoa	Invertebrates	Sea anemone
18	<i>T. adhaerens</i>	<i>Trichoplax adhaerens</i>	Tad	Opisthokonta	Metazoa	Invertebrates	Small sea water organism
19	<i>A. queenslandica</i>	<i>Amphimedon queenslandica</i>	Aqu	Opisthokonta	Metazoa	Invertebrates	Sea sponge
20	<i>M. brevicollis</i>	<i>Monosiga brevicollis</i>	Mbr	Opisthokonta	Choanoflagellates	Invertebrates	Choanoflagellate
21	<i>M. ovata</i>	<i>Monosiga ovata</i>	Mov	Opisthokonta	Choanoflagellates	Invertebrates	Choanoflagellate
22	<i>S. rosetta</i>	<i>Salpingoeca rosetta</i>	Sro	Opisthokonta	Choanoflagellates	Invertebrates	Choanoflagellate
23	<i>M. vibrans</i>	<i>Ministeria vibrans</i>	Mvi	Opisthokonta	Filasterea	Invertebrates	Small single-celled eukaryote which feeds on bacteria
24	<i>C. owczarzaki</i>	<i>Capsaspora owczarzaki</i>	Cow	Opisthokonta	Filasterea	Invertebrates	Symbiont of a freshwater snail
25	<i>S. arctica</i>	<i>Sphaeroforma arctica</i>	Sar	Opisthokonta	Ichthyosporea	Invertebrates	Unicellular opisthokont
26	<i>A. parasiticum</i>	<i>Amoebidium parasiticum</i>	Apa	Opisthokonta	Ichthyosporea	Invertebrates	Protozoan

27	<i>S. cerevisiae</i>	<i>Saccharomyces cerevisiae</i>	Scs	Opisthokonta	Ascomycetes	Fungi	Baker's yeast
28	<i>B. dendrobatidis</i>	<i>Batrachochytrium dendrobatidis</i>	Bde	Opisthokonta	Chytridiomycetes	Fungi	Non-filamentous aquatic chytrid fungus
29	<i>M. verticillata</i>	<i>Mortierella verticillata</i>	Mve	Opisthokonta	Zygomycetes	Fungi	Causes the fungal infection zygomycosis in animals
30	<i>A. macrogynus</i>	<i>Allomyces macarogynus</i>	Ama	Opisthokonta	Chytridiomycetes	Fungi	Filamentous chytrid fungus
31	<i>S. punctatus</i>	<i>Spizellomyces punctatus</i>	Spun	Opisthokonta	Chytridiomycetes	Fungi	Uniflagellated zoospores, but swimming amoeboid form
32	<i>T. trahens</i>	<i>Thecamonas trahens</i>	Ttr	Opisthokonta	Apusozoa	Amastigomonas	Biciliate gliding flagellate
33	<i>E. histolytica</i>	<i>Entamoeba histolytica</i>	Ehi	Amoebozoa	Archamoebae	Amoebozoa	Intestinal parasite that causes amoebiasis
34	<i>D. discoideum</i>	<i>Dictyostelium discoideum</i>	Ddi	Amoebozoa	Mycetozoa	Amoebozoa	Soil-living amoeba capable of multicellular development
35	<i>N. gruberi</i>	<i>Naegleria gruberi</i>	Ngr	Excavata	Heterolobosea	Excavata	Free-living amoeba-flagellate
36	<i>T. brucei</i>	<i>Trypanosoma brucei</i>	Tbr	Excavata	Metamonada	Excavata	Unicellular protozoan that causes the sleeping sickness
37	<i>A. thaliana</i>	<i>Arabidopsis thaliana</i>	Ath	Archaeplastida	Chloroplastida	Archaeplastida	Small flowering plant of mustard family
38	<i>V. carteri</i>	<i>Volvox carteri</i>	Vca	Archaeplastida	Chlorophyta	Archaeplastida	Multicellular green algae
39	<i>C. merolae</i>	<i>Cyanidioschyzon merolae</i>	Cme	Archaeplastida	Rhodophyta	Archaeplastida	Unicellular red algae
40	<i>C. paradoxa</i>	<i>Cyanophora paradoxa</i>	Cpa	Archaeplastida	Glaucophytes	Archaeplastida	Microalgae, does both nitrogen fixation and photosynthesis
41	<i>B. natans</i>	<i>Bigeloviella natans</i>	Bna	SAR	Rhizaria	SAR	Amoeboflagellate cercozoan
42	<i>E. siliculosus</i>	<i>Ectocarpus siliculosus</i>	Esi	SAR	Chromalveolata	SAR	Filamentous brown algae
43	<i>N. gaditana</i>	<i>Nannochloropsis gaditana</i>	Nga	SAR	Stramenopiles	SAR	Marine phytoplankton "microalgae"
44	<i>P. sojae</i>	<i>Phytophthora sojae</i>	Pso	SAR	Stramenopiles	SAR	Water mold (oomycetes) that affects agricultural plants
45	<i>T. thermopila</i>	<i>Tetrahymena thermopila</i>	Tth	SAR	Alveolata	SAR	Ciliated unicellular, free swimming, freshwater protist
46	<i>T. gondii</i>	<i>Toxoplasma gondii</i>	Tgo	SAR	Alveolata	SAR	Parasite causing toxoplasmosis
47	<i>E. huxleyi</i>	<i>Emiliania huxleyi</i>	Ehu	CCTH	Haptophyta	CCTH	Coccolithophorid algae (phytoplankton)
48	<i>G. theta</i>	<i>Guillardia theta</i>	Gth	CCTH	Cryptophyta	CCTH	Flagellate, unicellular algae.

Table 7.2. List of protein sequences used for the phylogenetic studies of this thesis, identified through comparative genomics. The following table shows the Rab32 family protein sequences identified through comparative genomics. The Accession number is the identification number at the NCBI, JGI, Broad Institute or individual organism's genome databases, followed by the E-value retrieved for each individual sequence using the human Rab32 family sequence. The Reverse Accession number is the protein sequence obtained as the best hit after validation by reciprocal BLASTp searches. The Order criterion shows the order of magnitude difference from the next best hit of the reciprocal BLASTp search.

Protein		Accession number used				
RAB32		<i>Homo sapiens</i> (Hsa): EAW47833.1 (NP_006825.1)				
Taxon	Proposed name	Accession Number	E value	Reverse BLASTp Accession Number	Order criterion	Database
<i>Gallus gallus</i>	GgaRab32	XP_419654.1	2.00E-130	NP_006825.1	31	NCBI
<i>Danio rerio</i>	DreRab32_A	AAH66502.1	4.00E-122	NP_006825.1	24	NCBI
<i>Danio rerio</i>	DreRab32_B	NP_001076317.1	3.00E-91	NP_006825.1	4	NCBI
<i>Danio rerio</i>	DreRab32_C	XP_690992.3	3.00E-102	XP_638960.1	17	NCBI
<i>Xenopus tropicalis</i>	XtrRab32_A	jgi Xentr4 474919 fgenesh1_Sanger_cdna.C_scaffold_2000033	1.51E-109	NP_006825.1	25	JGI
<i>Xenopus tropicalis</i>	XtrRab32_B	jgi Xentr4 333643 e_gw1.117.92.1	1.24E-60	NP_006825.1	4	JGI
<i>Scyliorhinus canicula</i>	ScaRab32	ctg93297	6.00E-107	NP_006825.1	12	Hydra
<i>Leucoraja erinacea</i>	LerRab32_A	AESE010622919.1	3.00E-40	NP_006825.1	2	NCBI
<i>Leucoraja erinacea</i>	LerRab32_B	AESE010002772.1	5.00E-32	NP_006825.1	1	NCBI
<i>Leucoraja erinacea</i>	LerRab32_C	AESE010216257.1	7.00E-31	NP_006825.1	2	NCBI
<i>Branchiostoma floridae</i>	BflRab32_A	jgi Braf1 204961 e_gw.25.187.1	1.51E-88	NP_006825.1	33	JGI
<i>Branchiostoma floridae</i>	BflRab32_B	jgi Braf1 282223 estExt_gwp.C_2520066	3.78E-60	XP_645950.1	23	JGI
<i>Ciona intestinalis</i>	CinRab32	XP_002130668.1	7.00E-96	NP_006825.1	2	NCBI
<i>Capitella teleta</i>	CteRab32_A	jgi Capca1 64412 gw1.27.150.1	1.31E-87	NP_006825.1	2	JGI
<i>Capitella teleta</i>	CteRab32_B	jgi Capca1 110893 e_gw1.461.17.1	2.10E-61	XP_645950.1	7	JGI
<i>Strongylocentrotus purpuratus</i>	SpuRab32_A	XP_782400.2	3.00E-110	NP_006825.1	10	NCBI
<i>Strongylocentrotus purpuratus</i>	SpuRab32_B	XP_003731406.1	7.00E-74	XP_645950.1	20	NCBI
<i>Drosophila melanogaster</i>	DmeRab32	BAA88238.1	8.00E-103	NP_006825.1	6	NCBI
<i>Caenorhabditis elegans</i>	CelRab32	NP_001024837.1	4.00E-66	NP_006825.1	6	NCBI
<i>Lottia gigantea</i>	LgiRab32_A	>jgi Lotgi1 171871 fgenesh2_pg.C_sca_121000061	8.76E-94	NP_006825.1	6	JGI
<i>Lottia gigantea</i>	LgiRab32_B	>jgi Lotgi1 96617 gw1.7.384.1	3.86E-78	XP_645950.1	17	JGI
<i>Nematostella vectensis</i>	NveRab32_A	>jgi Nemve1 25811 gw.147.46.1	4.23E-85	NP_006825.1	30	JGI

<i>Nematostella vectensis</i>	NveRab32_B	>jgi Nemve1 245354 estExt_fgenesH1_pg.C_1560053	8.51E-70	NP_006825.1	5	JGI
<i>Nematostella vectensis</i>	NveRab32_C	>jgi Nemve1 64028 gw.600.25.1	2.05E-14	NP_006825.1	6	JGI
<i>Trichoplax adhaerens</i>	TadRab32_A	>jgi Triad1 27795 e_gw1.7.291.1	3.08E-76	NP_006825.1	1	JGI
<i>Trichoplax adhaerens</i>	TadRab32_B	>jgi Triad1 58409 fgenesH2A2_pg.C_scaffold_7000627	1.35E-69	NP_006825.1	3	JGI
<i>Trichoplax adhaerens</i>	TadRab32_C	>jgi Triad1 58410 fgenesH2A2_pg.C_scaffold_7000628	5.49E-62	NP_006825.1	8	JGI
<i>Trichoplax adhaerens</i>	TadRab32_D	>jgi Triad1 56305 fgenesH2A2_pg.C_scaffold_5000199	1.21E-06	XP_638960.1	1	JGI
<i>Hydra magnipapillata</i>	HmaRab32_A	XP_004211547.1	2.00E-63	NP_006825.1	1	NCBI
<i>Hydra magnipapillata</i>	HmaRab32_B	XP_002161756.2	1.00E-37	NP_006825.1	1	NCBI
<i>Amphimedon queenslandica</i>	AquRab32_A	>Aqu1.216165 PAC:15714693	2.30E-74	NP_006825.1	4	EnsemblMetazoa
<i>Amphimedon queenslandica</i>	AquRab32_B	>Aqu1.216166 PAC:15714694	1.50E-54	NP_006825.1	4	EnsemblMetazoa
<i>Amphimedon queenslandica</i>	AquRab32_C	>Aqu1.224625 PAC:15723153	1.30E-32	NP_006825.1	3	EnsemblMetazoa
<i>Amphimedon queenslandica</i>	AquRab32_D	>Aqu1.228897 PAC:15727425		XP_638960.1	2	EnsemblMetazoa
<i>Monosiga brevicollis</i>	MbrRab32_A	XP_001743523.1	4.00E-96	NP_006825.1	2	NCBI
<i>Monosiga brevicollis</i>	MbrRab32_B	XP_001749931.1	2.00E-48	NP_006825.1	2	NCBI
<i>Salpingoeca rosetta</i>	SroRab32	PTSG_10710	0.00E+00	NP_006825.1	6	Broad Institute
<i>Capsaspora owczarzaki</i>	CowRab32_A	EFW44888.1	1.00E-91	NP_006825.1	1	NCBI
<i>Capsaspora owczarzaki</i>	CowRab32_B	EFW44898.1	6.00E-64	NP_006825.1	1	NCBI
<i>Mortierella verticillata</i>	MveRab32	MVEG_01772	0.00E+00	NP_006825.1	5	Broad Institute
<i>Thecamonas trahens</i>	TtrRab32_A	AMSG_00251	0.00E+00	NP_006825.1	5	Broad Institute
<i>Thecamonas trahens</i>	TtrRab32_B	AMSG_03639	0.00E+00	NP_006825.1	1	Broad Institute
<i>Thecamonas trahens</i>	TtrRab32_C	AMSG_01707	0.00E+00	NP_006825.1	5	Broad Institute
<i>Thecamonas trahens</i>	TtrRab32_D	AMSG_11142	0.00E+00	NP_006825.1	1	Broad Institute
<i>Entamoeba histolytica</i>	EhiRab32	XP_655922.1	2.00E-45	NP_006825.1	8	NCBI
<i>Dictyostelium discoideum</i>	DdiRab32_A	AAD23450.1	5.00E-86	NP_006825.1	20	NCBI
<i>Dictyostelium discoideum</i>	DdiRab32_B	XP_645950.1	8.00E-68	NP_006825.1	4	NCBI
<i>Dictyostelium discoideum</i>	DdiRab32_C	XP_643480.1	5.00E-49	NP_006825.1	4	NCBI
<i>Naegleria gruberi</i>	NgrRab32_A	XP_002674396.1	3.00E-92	NP_006825.1	5	JGI
<i>Naegleria gruberi</i>	NgrRab32_B	XP_002678585.1	6.00E-67	NP_006825.1	3	JGI
<i>Naegleria gruberi</i>	NgrRab32_C	XP_002683044.1	6.00E-51	NP_006825.1	1	JGI
<i>Ectocarpus siliculosus</i>	EsiRab32_A	CBJ26936.1	5.00E-67	NP_006825.1	4	NCBI
<i>Ectocarpus siliculosus</i>	EsiRab32_B	CBJ31636.1	4.00E-51	NP_071732.1	2	NCBI
<i>Ectocarpus siliculosus</i>	EsiRab32_C	CBN77086.1	3.00E-45	NP_071732.1	3	NCBI
<i>Ectocarpus siliculosus</i>	EsiRab32_D	CBJ29277.1	6.00E-28	NP_006825.1	6	NCBI
<i>Phytophthora sojae</i>	PsoRab32_A	>jgi Physo3 561505 estExt_Genewise1Plus.C_5_t80379	1.00E-66	NP_006825.1	1	JGI
<i>Phytophthora sojae</i>	PsoRab32_B	>jgi Physo3 513477 e_gw1.6.5180.1	1.74E-33	NP_006825.1	2	JGI
<i>Tetrahymena thermopila</i>	TthRab32_A	XP_001026291.1	6.00E-38	NP_006825.1	3	NCBI
<i>Tetrahymena thermopila</i>	TthRab32_B	XP_001033512.1	2.00E-22	NP_006825.1	1	NCBI
<i>Guillardia theta</i>	GthRab32	>jgi GuiTh1 117074 au.104_g18176	1.44E-47	NP_006825.1	3	JGI
<i>Bigelowiella natans</i>	BnaRab32	>jgi Bigna1 54186 estExt_Genewise1Plus.C_290104	1.68E-39	XP_645950.1	5	JGI

Protein
RAB38

Accession number used
Homo sapiens (Hsa): AAH15808.1 (NP_071732.1)

Taxon	Proposed name	Accession Number	E value	Reverse BLASTp Accession Number	Order criterion	Database
<i>Gallus gallus</i>	GgaRab38	XP_425653.2	4.00E-133	NP_071732.1	38	NCBI
<i>Danio rerio</i>	DreRab38_A	XP_001342875.2	2.00E-120	NP_071732.1	30	NCBI
<i>Danio rerio</i>	DreRab38_B	XP_003199402.1	4.00E-118	NP_071732.1	28	NCBI
<i>Xenopus tropicalis</i>	XtrRab38	jgi Xentr4 351109 e_gw1.219.105.1	5.31E-116	NP_071732.1	35	JGI
<i>Scyliorhinus canicula</i>	ScaRab38_A	ctg1333	4.00E-85	NP_071732.1	10	Hydra
<i>Scyliorhinus canicula</i>	ScaRab38_B	ctg52487	9.00E-42	NP_071732.1	1	Hydra
<i>Leucoraja erinacea</i>	LerRab38_A	AESE010974462.1	3.00E-44	NP_071732.1	6	NCBI
<i>Leucoraja erinacea</i>	LerRab38_B	AESE011584444.1	1.00E-42	NP_071732.1	3	NCBI
<i>Leucoraja erinacea</i>	LerRab38_C	AESE010075803.1	3.00E-33	NP_071732.1	4	NCBI
<i>Leucoraja erinacea</i>	LerRab38_D	AESE011998585.1	7.00E-11	NP_071732.1	12	NCBI

Protein
RAB29 (RAB7L1)

Accession number used
Homo sapiens (Hsa): CAG46807.1 (NP_003920.1)

Taxon	Proposed name	Accession Number	E value	Reverse BLASTp Accession Number	Order criterion	Database
<i>Gallus gallus</i>	GgaRab29	XP_417967.2	2.00E-120	NP_003920.1	21	NCBI
<i>Xenopus tropicalis</i>	XtrRab29	NP_001107338.1	7.00E-103	NP_003920.1	36	NCBI
<i>Scyliorhinus canicula</i>	ScaRab29	ctg59616	3.00E-74	NP_003920.1	21	Hydra
<i>Leucoraja erinacea</i>	LerRab29_A	AESE012617907.1	1.00E-24	NP_003920.1	7	NCBI
<i>Leucoraja erinacea</i>	LerRab29_B	AESE010021089.1	3.00E-14	NP_003920.1	6	NCBI
<i>Branchiostoma floridae</i>	BflRab29	jgi Braf11 287780 estExt_gwp.C_5450028	1.83E-65	NP_003920.1	14	JGI
<i>Capitella teleta</i>	CteRab29	jgi Capca1 101663 e_gw1.569.6.1	2.24E-67	NP_003920.1	11	JGI
<i>Strongylocentrotus purpuratus</i>	SpuRab29	XP_786497.2	1.00E-68	NP_003920.1	11	NCBI
<i>Lottia gigantea</i>	LgiRab29	>jgi Lotgi1 138291 e_gw1.124.15.1	2.11E-65	NP_003920.1	12	JGI
<i>Nematostella vectensis</i>	NveRab29_A	>jgi Nemve1 84449 e_gw.9.157.1	7.95E-66	NP_003920.1	11	JGI
<i>Nematostella vectensis</i>	NveRab29_B	>jgi Nemve1 200891 fgenes1_pg.scaffold_24000105	5.08E-56	NP_003920.1	7	JGI
<i>Nematostella vectensis</i>	NveRab29_C	>jgi Nemve1 84100 e_gw.9.194.1	1.40E-35	NP_003920.1	5	JGI
<i>Amphimedon queenslandica</i>	AquRab29	XP_003383085.1	1.00E-62	NP_003920.1	16	NCBI
<i>Monosiga brevicollis</i>	MbrRab29	>jgi Monbr1 8415 fgenes1_pg.scaffold_11000039	2.14E-28	NP_003920.1	2	JGI
<i>Salpingoeca rosetta</i>	SroRab29	PTSG_04403	6.38E-40	NP_003920.1	6	NCBI
<i>Capsaspora owczarzaki</i>	CowRab29	EFW44215.1	5.00E-66	NP_003920.1	4	NCBI